



**Protein kinases as targets for the development of novel drugs against alveolar
echinococcosis**

Proteinkinasen als Angriffspunkte für die Entwicklung neuer Chemotherapeutika
gegen die Alveoläre Echinokokkose

Doctoral thesis for a doctoral degree
at the Graduate School of Life Sciences,
Julius-Maximilians-Universität Würzburg,
Section Infection and Immunity

submitted by

Andreas Schubert

from

Gießen

Würzburg, 2015



Submitted on:

(Office stamp)

Members of the Promotions committee:

Chairperson: Prof. Dr. Markus Engstler

Primary Supervisor: Prof. Dr. Klaus Brehm

Supervisor (Second): Prof. Dr. Caroline Kisker

Supervisor (Third): Prof. Dr. Christoph G. Greveling

Date of Public Defence:

Date of Receipt of Certificates:

Affidavit

I hereby confirm that my thesis entitled "**Protein kinases as targets for the development of novel drugs against alveolar echinococcosis**" is the result of my own work. I did not receive any help or support from commercial consultants. All sources and / or materials applied are listed and specified in the thesis.

Furthermore, I confirm that this thesis has not yet been submitted as part of another examination process neither in identical nor in similar form.

Würzburg, 25.02.2015

Signature.....

Danksagung

Diese Arbeit wurde am 13. Dezember 2011 im zweiten Stock des Instituts für Hygiene und Mikrobiologie in der Josef-Schneider-Straße 2/E1 in 97080 Würzburg geboren. Ich möchte nun die Gelegenheit nutzen allen daran beteiligten Personen zu danken, die zu sehr früher Stunde, sowie an den darauffolgenden Tagen, Wochen und Monaten hinzugekommen sind und Ihre Hilfe angeboten haben.

Herrn Prof. Dr. Klaus Brehm möchte ich für die spontane Aufnahme in sein Labor danken und dafür, dass er mir einen Einblick in die Welt der „parasitären Lebensweise“ ermöglicht hat. Zudem gebührt ihm ein besonderer Dank für die konstruktive Kritik am wissenschaftlichen Verfassen von nicht deutschsprachiger Literatur.

Für die Betreuung und Begutachtung meiner Doktorarbeit möchte ich auch Frau Prof. Dr. Caroline Kisker und Herrn Prof. Dr. Christoph G. Grevelding danken.

Meiner Familie möchte ich dafür danken, dass Sie mir die Möglichkeit gegeben haben, dass ich studieren konnte und dass Sie diese „Ausbildung“ in allen Maßen mitbegleitet haben. Dank geht auch an meinen kleinen -körperlich größeren- Bruder, der ab und zu mal mit Vernunft handelt und „Gott sein Dank“ einen anderen Studienweg einschlug. Ganz besonderer Dank gebührt meiner Frau Franziska Schubert, die mich schon sehr lange begleitet und die ich nicht mehr missen möchte. Grüße gehen auch an meine Schwiegereltern, sowie an meine Schwägerin und Schwager.

Hinsichtlich der praktischen Ausführung ist ganz klar Frau Monika Bergmann in den Vordergrund zu rücken, die mir bei meinen Experimenten, wenn benötigt, immer zu Hilfe stand. Meine Kollegen aus dem Labor und Institut sind natürlich auch nicht zu vernachlässigen; angefangen bei Dr. Uriel Koziol, Dirk Radloff, Raphaël Duvoisin, Ferenc Kiss und Dominik Benke. Nicht zu vergessen ist auch Dr. Wilhelm F. Oosthuysen, Frau Prof. Dr. Alexandra Schubert-Unkmeir, Dr. Florian Sauer (AG-Kisker), Michael Ullrich, Matthias Brandt, Rainer Brandner, Stefan Simon und Günter Troll sowie die Brigitte Schraud und Gabriele Krämer. Vielen lieben Dank für eure Hilfe und für manch freundlichen Plausch zwischendurch.

Wahre Freunde kann man nicht kaufen, daher möchte ich auch Sie nicht vernachlässigen und an dieser Stelle erwähnen: Alexander Wolf, Philipp Bergmann (geb. Rodrigues), Christian Schneider und Johannes Birnbaum. Vielen Dank für die schöne Zeit beim Rudern und gemeinsamen Wandern.

Zu guter Letzt eine persönliche Notiz: Eine Ausbildung in Form einer Promotion ist sinnvoll. Man sollte jedoch währenddessen nicht die Perspektive über das universitäre Schwimmbecken hinaus vergessen. Daher sollte man versuchen, gerade als Naturwissenschaftler, offen zu sein für Neues, dem Bezug zur Realität wahren und den Blick auf Geschehnisse, die im Lauf der Zeit passieren, kritisch zu reflektieren. Für Ihre „Sicht der Dinge“ möchte ich daher folgenden Personen ganz herzlich danken. Beginnen wir mit Jonathan Robin Meese als „Die Ameise der Kunst“, dem Musiker Rainald Grebe und dem Publizisten Henryk Marcin Broder u.a. für seinen BLOG „Die Achse des Guten“. Dem Schriftsteller Timur Vermes für seinen im Grunde genommen gesellschaftskritischen Debütroman „Er ist wieder da“ und den Kabarettisten Hagen Rether und Andreas Rebers.

Content

1 Summary	8-9
2 Zusammenfassung	10-11
3 Introduction	12-28
3.1 <i>Echinococcus</i> Phylogeny	12-15
3.2 The life cycle of the fox tapeworm <i>Echinococcus multilocularis</i>	15-17
3.3 Alveolar echinococcosis - infection risk and clinical therapy.....	17-18
3.4 Protein kinases and their characteristic features for the development of novel chemotherapeutics.....	18-20
3.5 Polo-like kinase 1 and their potential as anti-helminthic drug target.....	20-24
3.6 The invertebrate-specific family of Venus Flytrap kinases.....	25-26
3.7 <i>In vitro</i> culture of <i>Echinococcus multilocularis</i>	26-27
3.8 Objectives.....	28
4 Material and Methods	29-48
4.1 Material	29-35
4.1.1 Equipment.....	29-30
4.1.2 Consumables.....	30
4.1.3 Chemicals, media, commercially available kits and Enzymes.....	30-33
4.1.4 Oligonucleotides.....	34
4.1.5 Plasmids.....	34
4.1.6 Antibodies.....	34
4.1.7 <i>Echinococcus multilocularis</i> isolates.....	35
4.2 Methods	36-48
4.2.1 Working with nucleic acids.....	36
4.2.1.1 Determination of nucleic acid concentrations and purity.....	36
4.2.1.2 Isolation of total RNA from <i>E. multilocularis</i> larval stages.....	36
4.2.1.3 DNase treatment of isolated total RNA.....	36
4.2.1.4 Reverse transcription of RNA into cDNA.....	37
4.2.1.5 Isolation and preparation of DNA from metacestode vesicles of <i>E. multilocularis</i>	37
4.2.1.6 Amplification of DNA by DNA-Polymerase Chain Reaction (PCR).....	37-38
4.2.1.7 Purification of DNA from Agarose gels or enzymatic modifications of <i>in vitro</i> reactions.....	38
4.2.1.8 Isolation of plasmid DNA from <i>Escherichia coli</i>	38
4.2.1.9 Sequencing of plasmids.....	38
4.2.1.10 <i>Semi</i> -quantitative reverse transcribed polymerase chain reaction (RT-PCR).....	38-39
4.2.1.11 Colony PCR.....	39
4.2.1.12 Agarose gel-electrophoresis.....	39
4.2.1.13 Addition of 3' Adenosine overhang on PCR amplified DNA fragments (TOPO TA cloning).....	40
4.2.1.14 Bioinformatical and statistical analysis.....	40
4.2.1.15 Modification/restriction digests of DNA plasmids or amplified DNA fragments.....	40
4.2.1.16 Ligation of DNA fragments into plasmids.....	40
4.2.2 Working with bacteria.....	41
4.2.2.1 Bacteria strains and media used in this study.....	41
4.2.2.2 Media for bacteria culture.....	41
4.2.2.3 Overnight culture of bacterial cultures.....	41
4.2.2.4 Bacterial liquid cultures of <i>E. coli</i>	41

4.2.2.5	Chemical competent bacterial cells (<i>E. coli</i>).....	42
4.2.2.6	Transformation of <i>E. coli</i>	42
4.2.2.7	Dimethyl sulfoxide (DMSO) bacterial stocks (at -80°C).....	42
4.2.3	Working with eukaryotic cell lines.....	43
4.2.3.1	<i>Echinococcus multilocularis</i> media used in the <i>in vivo</i> and <i>in vitro</i> cell culture.....	43
4.2.3.2	Cultivation of feeder cells.....	43
4.2.3.3	Isolation and maintenance of <i>in vivo</i> parasitic material from Mongolian jirds.....	43-44
4.2.3.4	<i>In vitro</i> cultivation of <i>Echinococcus multilocularis</i>	44
4.2.3.5	Axenic culture of metacystode vesicles of <i>E. multilocularis</i>	44
4.2.3.6	Isolation and activation of protoscoleces.....	44-45
4.2.3.7	Cultivation of protoscoleces and live-dead staining.....	45
4.2.3.8	Isolation and cultivation of primary cells from metacystode vesicles.....	45-46
4.2.3.9	Treatment of metacystode vesicles, protoscoleces and primary cells with inhibitors.....	46
4.2.3.10	Resazurin assay for monitoring viability of primary cells.....	46-47
4.2.3.11	Microinjection of metacystode vesicles.....	47
4.2.3.12	Labelling of proliferating cells in whole mount metacystode vesicles by EdU pulse staining.....	47-48
4.2.3.13	<i>In situ</i> hybridisation of metacystode vesicles.....	48
5	Results.....	49-79
5.1	Cloning and characterisation of the Polo-like kinase 1 gene (<i>EmPlk1</i>) of <i>Echinococcus multilocularis</i>	49-51
5.2	Structural analyses concerning binding of the Plk1 inhibitors BI 2536 and BI 6727 to EmPlk1.....	51-52
5.3	Expression of EmPlk1 in <i>E. multilocularis</i> larval stages.....	53-54
5.4	Expression of EmPlk1 in the heterologous <i>Xenopus</i> oocytes system triggers germinal vesicle breakdown (GVBD), and can be blocked by the Plk1 inhibitor BI 2536 and BI 6727.....	55-56
5.5	BI 2536 inhibit the formation of metacystode vesicles from parasite primary cells.....	56-58
5.6	<i>In vitro</i> effects of BI 2536 on <i>E. multilocularis</i> metacystode vesicles.....	58-60
5.7	Stem cells of metacystode vesicles are addressed by treatment of BI 2536, visualised by a Click-iT EdU cell proliferation assay.....	60-62
5.8	Attempts towards elucidating the crystal structure of the Polo-like kinase 1 of <i>E. multilocularis</i> (EmPlk1).....	63
5.9	Expression patterns of <i>E. multilocularis</i> β -tubulin genes.....	63-69
6.0	Injection of isolated primary cells into metacystode vesicles treated with the Polo-like kinase 1 inhibitor BI 2536.....	70-72
6.1	Further inhibitor studies on <i>E. multilocularis</i>	72-73
6.2	Characterisation and cloning of the Venus flytrap kinase receptor in <i>E. multilocularis</i> (<i>emvkr</i>).....	74-77
6.3	AG1024 (Tyrphostin), a potential Venus flytrap kinase inhibitor.....	78-79
6.4	Further work on VKR.....	79

7 Discussion	80-91
7.1 Overview.....	80
7.2 Limitations of the current chemotherapy against alveolar Echinococcosis.....	80-82
7.3 Targeting of parasitic stem cells by inhibition of the Polo-like kinase 1 (<i>emplk1</i>).....	83-86
7.4 Microinjection of primary cells into metacestode vesicles.....	87-88
7.5 The Venus flytrap kinase receptor of <i>E. multilocularis</i>	89-91
References	92-99
Supplement Material	100-111
A Sequences.....	100-104
B Table S1 Primer List.....	105-108
C List of Abbreviations.....	109
D List of Publications.....	110
E Conference Contributions.....	110

1 Summary

The metacestode larval stage of the fox tapeworm *Echinococcus multilocularis* is the causative agent of alveolar echinococcosis (AE), one of the most lethal zoonosis of the northern hemisphere. The development of metacestode vesicles by asexual multiplication and the almost unrestricted infiltrative growth within the host organs is ensured from a population of undifferentiated, proliferative cells, so-called germinative cells. AE treatment options include surgery, if possible, as well as Benzimidazole-based chemotherapy (BZ). Given that the cellular targets of BZs, the β -tubulins, are highly conserved between cestodes and humans, the chemotherapy is associated with considerable side-effects. Therefore, BZ can only be applied in parasitostatic doses and has to be given lifelong. Furthermore, the current anti-AE chemotherapy is ineffective in eliminating the germinative cell population of the parasite, which leads to remission of parasite growth as soon as therapy is discontinued.

This work focuses on protein kinases involved in the proliferation and development of the parasite with the intention of developing novel anti-AE therapies. Polo-like kinases (Plks) are important regulators of the eukaryotic cell cycle and are involved in the regulation and formation of the mitotic spindles during the M-phase of the cell cycle. Plks have already been shown to be associated with deregulated cellular growth in human cancers and have been investigated as novel drug targets in the flatworm parasite *Schistosoma mansoni*. In the first part of this work, the characterisation of a novel and druggable parasite enzyme, EmPlk1, which is homologous to the polo-like kinase 1 (Plk1) of humans and *S. mansoni* (SmPlk1), is presented. Through *in situ* hybridisation, it could be demonstrated that *emplk1* is specifically expressed in the *Echinococcus* germinative cells. Upon heterologous expression in the *Xenopus* oocyte system, EmPlk1 induced germinal vesicle breakdown, thus indicating that it is an active kinase. Furthermore, BI 2536, a compound originally designed to inhibit the human ortholog of EmPlk1, inhibited the EmPlk1 activity at a concentration of 25 nM. *In vitro* treatment of parasite vesicles with similar concentrations of BI 2536 led to the elimination of the germinative cells from *Echinococcus* larvae, thus preventing the growth and further development of the parasite. In *in vitro* cultivation systems for parasite primary cells, BI 2536 effectively inhibited the formation of new metacestode vesicles from germinative cells. Thus, BI 2536 has profound anti-parasitic activities *in vitro* at concentrations well within the range of plasma levels measured after the administration of safe dosages to patients (50 nM after 24 h). This implies that EmPlk1 is a promising new drug target for the development of novel anti-AE drugs that would specifically affect the parasite's stem cell population, namely the only parasite cells capable of proliferation. In addition to the chemotherapeutic aspects of this work, the inhibitor BI 2536 could be further used to study the function of stem cells in this model organism, utilising a method of injection of parasite stem cells into metacestode vesicles, for instance, as has been developed in this work.

In the second part of this work, a novel receptor tyrosine kinase, the Venus flytrap kinase receptor (EmVKR) of *E. multilocularis* has been characterised. Members of this class of single-pass transmembrane receptors have recently been discovered in the related trematode *S. mansoni* and are associated with the growth and differentiation of sporocyst germinal cells and ovocytes. The ortholog receptor in EmVKR is characterised by an unusual domain composition of an extracellular Venus

flytrap module (VFT), which shows significant similarity to GABA receptors, such as the GABA_B receptor (γ-amino butyric acid type B) and is linked through a single transmembrane domain to an intracellular tyrosine kinase domain with similarities to the kinase domains of human insulin receptors. Based upon the size (5112bp) of *emvkr* and nucleotide sequence specificities, efforts have been made to isolate the gene from cell culture samples to study the ligand for the activation of this receptor type in *Xenopus* oocytes. To date, this type of receptor has only been described in invertebrates, thus making it an attractive target for drug screening. In a first trial, the ATP competitive inhibitor AG 1024 was tested in our *in vitro* cell culture.

In conclusion, the EmVKR represents a novel receptor tyrosine kinase in *E. multilocularis*. Further efforts have to be made to identify the activating ligand of the receptor and its cellular function, which might strengthen the case for EmVKR as a potential drug target. The successful depletion of stem cells in the metacystode vesicle by the Plk1 inhibitor BI 2536 gives rise to optimising the chemical component for EmPlk1 as a new potential drug target. Furthermore, this inhibitor opens a new cell culture technique with high potential to study the cellular behaviour and influencing factors of stem cells *in vitro*.

2 Zusammenfassung

Das Verbreitungsgebiet des kleinen Fuchsbandwurms erstreckt sich über die nördliche Hemisphäre und eine Infektion des Menschen verursacht eine meist tödliche verlaufende Parasitose, die alveolaren Echinococcose (AE). Durch infiltratives und asexuelles Wachstum des Larvenstadiums der AE im betroffenen Wirtsorgan kommt es zu einer tödlich verlaufenden Krankheit. Das Wachstum der Metacestoden wird dabei durch undifferenzierte proliferierende Stammzellen, den sog. „germinativen Zellen“ des Fuchsbandwurmes verursacht.

Die derzeitigen Behandlungsmöglichkeiten von AE sehen neben einem chirurgischen Eingriff, der in den meisten Fällen nicht möglich ist, nur eine Chemotherapie mit Benzimidazolen (BZ) vor. Die Chemotherapie mit BZ richtet sich dabei gegen die β -Tubuline des Parasiten und ist überwiegend mit einer lebenslangen Behandlung verbunden. Obwohl sich die Behandlungsmöglichkeiten und die Prognose für Patienten seit der Verwendung von Benzimidazolen bedeutsam verbessert haben, kommt es dennoch zu starken Nebenwirkungen und die angewendete Chemotherapie wirkt nur parasitostatisch. Der Grund dafür liegt an der hohen Homologie zwischen den β -Tubulinen des Parasiten und des Menschen, welche die Zielproteine von Benzimidazolen sind. Um die Nebenwirkungen für den Patienten gering zu halten, werden die Benzimidazole nur in Konzentrationen verabreicht, die parasitostatisch wirken, was zu keiner Abtötung des Parasitengewebes führt. Darüber hinaus sind die gegenwärtigen AE-Medikamente nicht wirksam gegen die germinativen Zellen des Parasiten, was zu einem Wiederauftreten des Wachstums von Parasitengewebe führt, sobald die Chemotherapie unterbrochen wird.

Die hier vorliegende Arbeit konzentriert sich auf die Entwicklung eines neuen chemotherapeutischen Ansatzes gegen AE und befasst sich mit Proteinkinasen, die einen wesentlichen Einfluss auf die Proliferation und die Differenzierung von Zellen des Parasiten haben. Proteinkinasen, die in direkten Zusammenhang mit den Zellzyklus stehen, sind beispielsweise die Polo-like kinasen (Plk), welche die Bildung von mitotischen Spindelfasern während der M-Phase regulieren. Wie bereits in vorhergehenden Studien gezeigt werden konnte, sind Plks auch an der Entstehung von Krebs beteiligt und daher interessante Ansatzpunkte für die Entwicklung von neuen Chemotherapeutika. Darüber hinaus zeigte sich auch, dass Sie zur Chemotherapie von parasitären Krankheiten Verwendung finden könnten, wie zur Behandlung von Schistosomiasis, welche durch *Schistosoma mansoni* ausgelöst wird.

Der erste Teil dieser Arbeit befasst sich mit der Charakterisierung der Polo-like kinase 1 (Plk1) aus *E. multilocularis*, die Homologien zur humanen Plk1 und der aus *S. mansoni* (SmPlk1) aufweist und daher als Ansatzpunkt für eine neuartige chemotherapeutische Behandlung von AE angesehen werden kann. Es konnte gezeigt werden, dass EmPlk1 in germinativen Zellen (Stammzellen) des Parasiten stark exprimiert wird und dass es möglich ist, dieses orthologe Protein mit nanomolekularer Konzentration (25 nM) des Plk1 Inhibitors BI 2536 in seiner zellulären Funktion zu hemmen. Darüber hinaus führt die Behandlung *in vitro* zu einem Verlust von Stammzellen im Larvenstadium von *E. multilocularis*, was zu einer drastischen Verminderung des Wachstums und der Entwicklung des Parasiten führt. Des Weiteren konnte sehr deutlich gezeigt werden, dass bei Verwendung des

Inhibitors BI 2536 in Zellkultursystemen mit „Primärzellen“ (80% Stammzellen) des Parasiten diese nicht mit mehr in der Lage sind in Metacestoden zu regenerieren. Dabei ist entscheidend, dass die verwendeten Konzentrationen des Inhibitors BI 2536 innerhalb der gemessenen Plasmakonzentrationen von Krebspatienten liegen (50 nM nach 48 Stunden). Die Inhibierung der PIK1 wird daher als vielversprechender neuer Ansatzpunkt einer Chemotherapie zur Behandlung der AE angesehen. Die Inhibierung der EmPIK1 hat einen wesentlichen Einfluss auf die Differenzierung von Stammzellen des Parasiten, wodurch das Wachstum und die weitere Entwicklung des Parasiten gehemmt werden. Des Weiteren kann neben der chemotherapeutischen Behandlung der Inhibitor BI2536 auch für das weitere Studium von Stammzellen und deren zelluläre Funktion in *E. multilocularis* genutzt werden. Dafür wurden erste *in vitro* Experimente mittels Injektion in stammzellfreie Metacestoden Vesikel durchgeführt.

Der zweite Teil dieser Arbeit befasst sich mit einem neuen Transmembranrezeptor in *E. multilocularis*, der hier als Venus-Fliegenfallen-Rezeptor charakterisiert wird. Dieser Rezeptortyp wurde erst kürzlich in *S. mansoni* beschrieben und steht im Zusammenhang mit der Entwicklung und dem Wachstum von Keimzellen des Parasiten. Der Rezeptor weist eine ungewöhnliche Zusammensetzung aus einer extrazellulären Venusfliegenfallendomäne (VFT) mit starker Ähnlichkeit zu GABA Rezeptoren auf (γ -amino-Buttersäure Typ B) und ist über eine einzelne Transmembrandomäne mit einer intrazellulären Tyrosinkinasedomäne verbunden, die eine hohe Homologie zu humanen Insulinrezeptoren zeigt. Der lange Genabschnitt (5112bp) von *emvkr* mit sequenzspezifischen Eigenschaften war schwierig zu klonieren, um eine anschließende Expression in *Xenopus* Oozyten durchzuführen. Bisher wurde dieser Rezeptor nur in Invertebraten beschrieben und stellt somit einen interessanten Ansatzpunkt für die Entwicklung von neuen Chemotherapeutika dar. In einem ersten Versuch wurde die Wirkung des ATP-Kompetitive Inhibitors AG 1024 in unserer *in vitro* Zellkultur untersucht.

Zusammenfassend wurde die Relevanz von EmVKR als neuartiger Tyrosinkinaserezeptor in *E. multilocularis* verdeutlicht. In anschließenden Studien sollte die Aktivierung durch Ligandenbindung an den Rezeptor, sowie seine weitere zelluläre Funktion untersucht werden. Diese Erkenntnisse könnten dann eine entscheidende Rolle für die Entwicklung von neuen Medikamenten mit EmVKR spielen. Des Weiteren wurde die erfolgreiche Entfernung von Stammzellen aus Metacestoden Vesikel mit dem PIK1 Inhibitor BI 2536 gezeigt. Dies bietet nun die Option diesen Inhibitor auf das Wirkstoffziel EmPIK1 weiter zu optimieren. Darüber hinaus hat die Verwendung dieses Inhibitors den entscheidenden Zugang für eine neue Zellkulturtechnik ermöglicht, die das Studieren von Stammzellen und deren Einflussfaktoren *in vitro* bietet.

3. Introduction

3.1. *Echinococcus* Phylogeny

The phylogenetic position of *E. multilocularis* and its sister species within the genus *Echinococcus* are outlined in detail in Fig. 3.1.1 [1]. All currently distinguished *Echinococcus* species are part of the class Cestoda (true tapeworms), which - together with the sister classes Monogenea, Trematoda, and Turbellaria - form the phylum Plathelminthes (flatworms). Together with several other phyla such as annelids and molluscs, the flatworms are part of the clade of Lophotrochozoa, which - together with the sister clade Ecdysozoa - are grouped together to the clade of protostomes [2, 3]. After the Cambrian Explosion about 500-600 million years ago, the protostomes evolved out of the last common bilaterian ancestor as a sister group to the deuterostomes with several prominent phyla such as Echinodermata, and Chordata (including vertebrates and eventually humans). As such, *Echinococcus* species share relatively close phylogenetic relationships with the parasitic flukes (trematodes) and the free-living Turbellaria (including planarians as a model system). Of all invertebrate phyla, a relatively close relationship is present between flatworms, molluscs and annelids, whereas less homologies - particularly phylogenetic and developmental homologies - are shared between flatworms and Ecdysozoa. Among the Nematelminthes and arthropods are well-studied model organisms such as *Caenorhabditis elegans* and *Drosophila melanogaster* [4, 5].

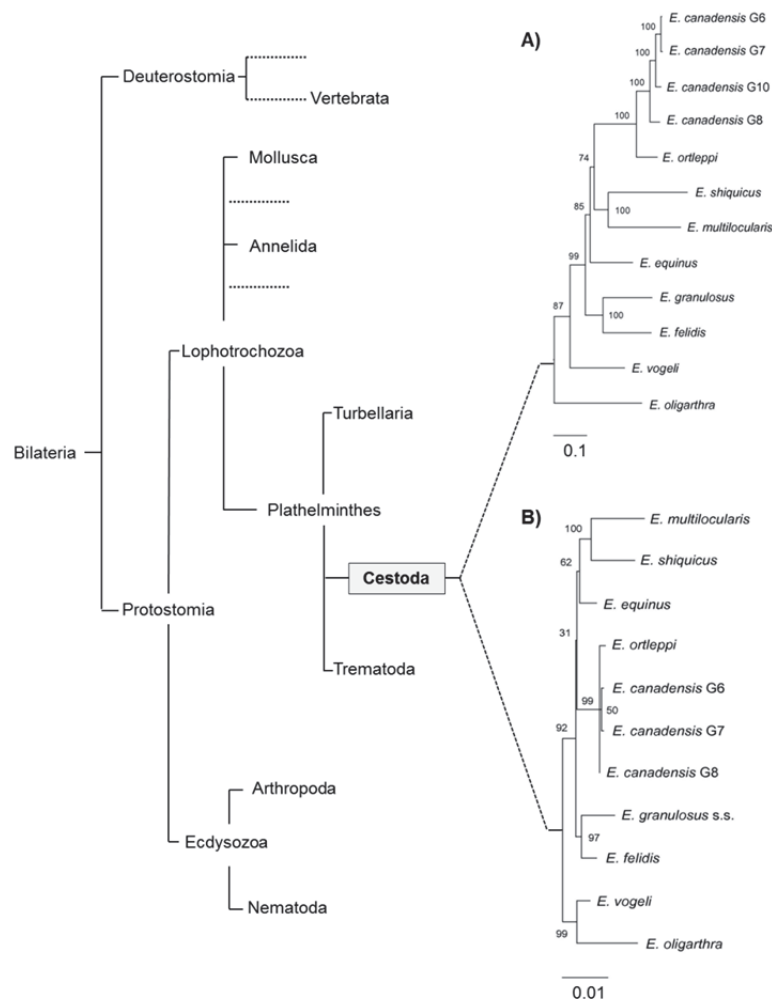


Figure 3.1.1 Phylogenetic tree of bilateral organisms. DNA sequences of mitochondrial (A) and nuclear genes (B) were used for reconstructing the tree. Decay indices are given by values of each node and inserted scale bars represent the number of substitution per nucleotide site. The tree was modified from Nakao *et al.* (2013) [1].

Today, the genus *Echinococcus spp.* comprises nine valid species, shown in a phylogenetic tree in Fig 3.1.1 [1]. Two alternative phylogenies based upon the analyses of mitochondrial and nuclear markers are depicted in Fig. 3.1.1.A and Fig. 3.1.1.B, respectively. Further studies have to clarify the ongoing taxonomic rearrangements of the fox tapeworm regarding its position in the phylogenetic tree.

The fox tapeworm is widely distributed in the northern hemisphere, with high endemic regions in the Republic of China, Turkey, Switzerland, Austria and the southern part of Germany (Fig. 3.1.2) [6, 7]. Unlike the fox tapeworm *E. multilocularis*, its close relative *E. granulosus* (dog tapeworm) is distributed worldwide [8]. These two species, which respectively cause alveolar (AE) and cystic echinococcosis (CE), are highly relevant for animal and human health issues, with somewhat lower importance of the sister species *E. vogeli* and *E. oligarthrus* [9, 10]. The fox tapeworm *E. multilocularis* has a sylvatic life-cycle and its distribution in the northern hemisphere follows that of its natural host, the red-fox (*Vulpus vulpus*) [11]. In direct comparison to some satellite states of the former Soviet Union and the Republic of China, the infection rate of foxes in Europe is comparably high, although the prevalence of human AE is lower [12-14]. In contrast to Europe, the high transfer by domestic animals, predominantly dogs, and the reduced hygiene circumstances/situation are the main reasons behind the higher zoonotic infection rate outside of Europe [7].

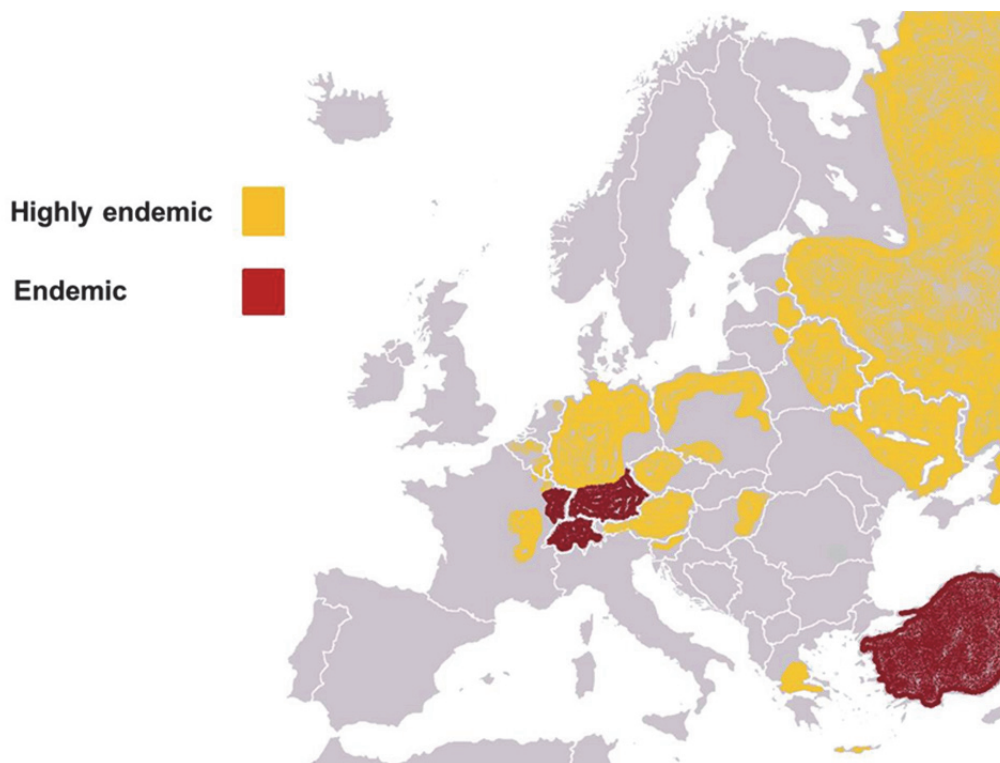


Figure 3.1.2 Distribution of the fox tapeworm *Echinococcus multilocularis* in Europe with endemic regions highlighted. Figure/Data based on Torgerson *et al.* (2010) [7]. Figure was modified from [15].

In high endemic areas in central Europe, the transfer by domestic animals constitutes 10% of the infection rate and can be reasonably controlled through frequent deworming campaigns and higher hygiene standards. [16]. Efforts to conduct regular deworming campaigns of domestic and straying dogs are often not performed in Europe, Asia, Russia and especially in third world countries, due to the high costs of regular treatment [17]. A potential yet hitherto unclear infection risk for AE is also man-made, namely garbage collection. Non-regulated garbage collection in several countries offers new food sources for the red foxes in urban areas, which enables the possibility of contaminating the environment with infected eggs [18]. The lifestyles of humans in urban areas (and valleys) allows for the presence of red foxes, which can have a tendency to influence the rate of this zoonotic infection [19, 20]. An overview of possible preventions to reduce the infection risk is given in Fig. 3.1.3.

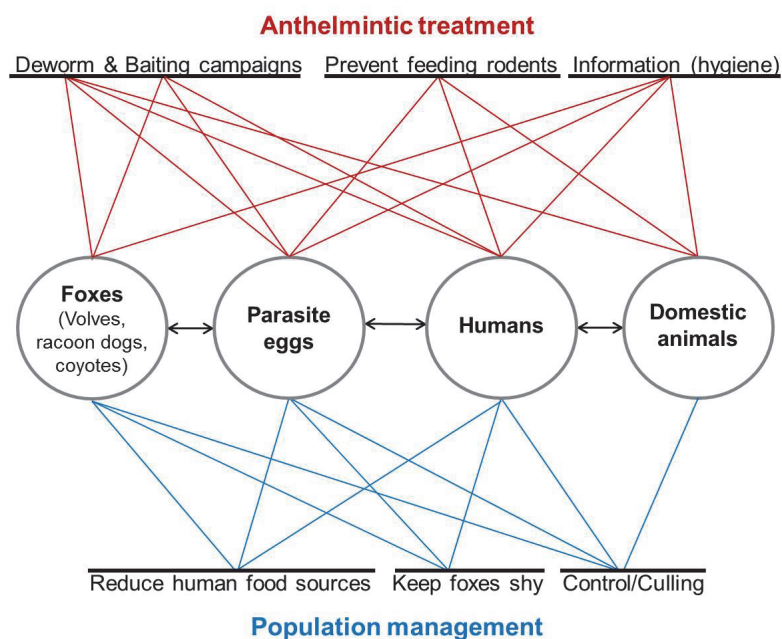


Figure 3.1.3 Infection risks for alveolar echinococcosis and ways of prevention. Actions to prevent the infection with AE are indicated by anthelmintic treatment (red) and population management (blue). Lines (red/blue) are start- and endpoints, showing overall that one action can influence several central spots. Figure was modified from Hegglin *et al.* (2013) [16].

The red-fox population was influenced by the outbreak of rabies until 1990 in Europe, whereby the population gradually increased following a successful vaccination campaign [21]. Together with the recovery of the red-fox population, studies observed an increase in the local distributions of *E. multilocularis* infected red foxes in Central and Eastern Europe [7, 11, 19, 20, 22]. It is assumed that infection rates of humans in Europe will increase in the future due to the increasing rates of infected foxes. Indeed, first indications of a higher infection rate have already been observed in Germany (unpublished results), Switzerland and Austria [23-25]. An observation of new infection rates in Eastern Europe could not be estimate based upon incomplete data from previous decades [26]. Efforts to treat fox populations through baiting campaigns to reduce environmental contamination with *E. multilocularis* eggs are ineffective in the long run and the emergence of resistances are assumed [16, 27]. It has also been observed that the parasite population can recover within 24-36 months

following the end of the cost-intensive baiting campaign [16]. In contrast to the difficult-to-treat fox tapeworm *E. multilocularis*, the dog tapeworm *E. granulosus* is dependent on a man-made life cycle. Historical and cultural issues support the life cycle of the dog tapeworm. Administrative control campaigns have failed with far-reaching consequences, such as the current existence of the zoonotic disease in Europe [22, 24].

3.2 The life cycle of the fox tapeworm *Echinococcus multilocularis*

A common feature of all tapeworms is their complex life cycle, which is associated with two host changes. Species of genus *Echinococcus* are distributed worldwide within a wide spectrum of rodents and ungulates that act as intermediate hosts, whereas carnivores such as foxes, domestic dogs and cats act as definitive hosts [7, 9, 11, 18, 24]. The morphology and localisation of *Echinococcus* larvae in the intermediate host shows a species-dependent characteristic [28].

In the case of the heterogeneous life cycle of the fox tapeworm *E. multilocularis*, two essential mammalian host changes are involved for the development of the intermediate host and the adult tapeworm. An overview of the life cycle of the fox tapeworm is given in Fig. 3.2.1. The adult worm of *E. multilocularis* is present in the intestine of carnivorous definite hosts such as the red fox (*Vulpus vulpus*), the polar-fox (*Alopex lagopus*) and the wolf (*Canis lupus*), among others [11, 29]. The adult tapeworm produces eggs in the intestine of the fox, which contain the first larval stage of the tapeworm, the oncosphere.

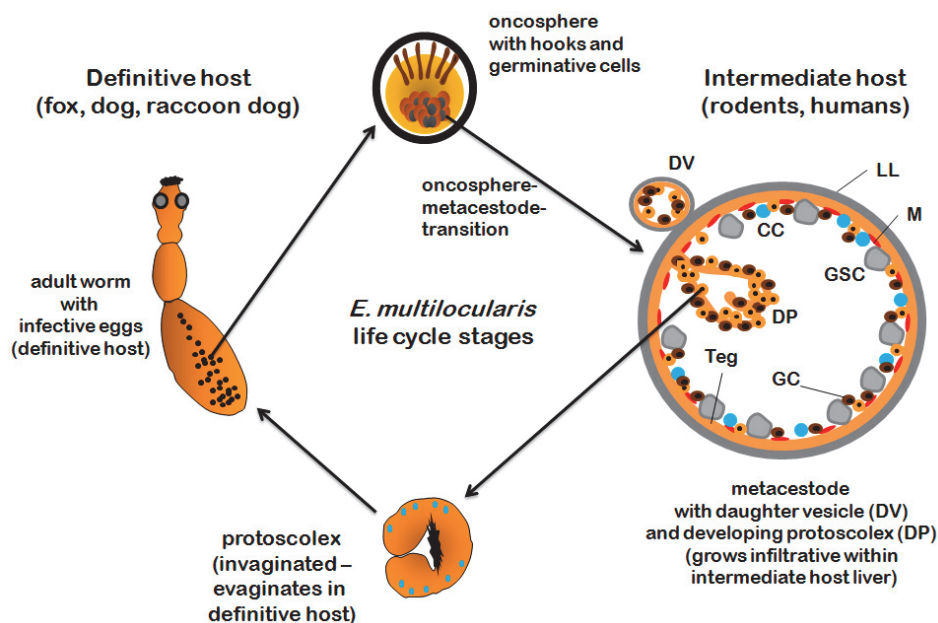


Figure 3.2.1 Life-cycle of the small fox tapeworm *Echinococcus multilocularis*. Figure was kindly provided by Klaus Brehm.

The infective eggs are released into the environment through the posterior segment of the tapeworm, the gravid proglottid. Natural intermediate hosts for *E. multilocularis* are usually rodents (especially *Microtus arvalis* and *Arvicola terrestris*), which acquire the infection through oral uptake of the infective

eggs. In rare cases, humans can become infected after accidental uptake of the infective eggs, and may subsequently develop the disease AE [6, 22]. When the infective eggs reach the stomach and intestine of the intermediate host, the oncosphere becomes activated by acidic pH and bile salts and subsequently hatches from the eggshell. By active penetration of the intestine wall, the oncosphere reaches the venous blood or lymphatic system, followed by passive transport through the body [30, 31]. In most cases (~99%) the oncosphere undergoes a metamorphosis towards the metacestode stage within the liver of the intermediate host, driven by a population of pluripotent stem cells, namely germinative cells [32]. The molecular basis for the prominent organ tropism of *E. multilocularis* towards the liver is currently unknown, although it has recently been shown that host insulin serves as an important stimulus for parasite development *in vitro* [33, 34]. Since the highest insulin concentrations in mammals can be found in the liver, insulin-dependent parasite proliferation could contribute to the organ tropism towards the liver [35].

In both natural intermediate hosts and humans, the metacestode is characterised by an alveolar structure comprising numerous small vesicles [36]. This fluid-filled vesicle is surrounded by an acellular, laminated layer (LL) comprising mucins, to which the cellular so-called germinative layer (GL) is proximally attached [37, 38]. The metacestode vesicle is filled by a protein-rich liquid, the hydatid fluid. The *E. multilocularis* metacestode is capable of producing daughter vesicles in a budding-like mechanism and thus grows infiltrative, like a malignant tumour, into the surrounding liver tissue as a meshwork of interconnected tubes and vesicles [39-41]. The growth of the metacestode vesicle causes a reaction of the immune system in rodents and humans, although it does not cause a strong rejection of the forming tissue. Moreover, it has to be noticed that not all rodents are sensitive for an infection and growth of the metacestode vesicle; rather, several kinds of mice are resistant to infection [42]. Furthermore, humans do not represent a good host for the development of AE overall and it is assumed that the infection also depends upon the human immune status [43].

The inner germinal layer opens towards the outside of the syncytial tegument. The nuclei of this syncytial tegument are localised in tegmental cell bodies connected to the tegument itself by thin cytoplasmic projections. Other cell types of the germinal layer are muscle, nerve, glycogen-storage and undifferentiated cells, like germinative cells [44-47]. At later stages of the infection, the germinal layer forms brood capsules in which the protoscoleces develop [28]. This larval stage already forms the scolex of the adult worm, but does not contain the proglottids as present in the adult worm.

The infiltrative growth of the metacestode tissue in the liver gradually weakens the intermediate host. It is assumed that owing to their reduced fitness, infected rodents can more easily be caught by the definitive host. Upon ingestion of the infected rodent by the fox, the developmental process of the adult tapeworm is triggered in the intestine of the fox. Already in the intermediate host, the germinal layer of the metacestode vesicle forms buds towards the inside of the vesicle cavity into the hydatid fluid. These buds grow and develop vacuoles and stalks, which have been previously described as brood capsules [48]. These brood capsules are covered on the inside by a syncytial tegument, which is similar to the germinal layer. Following the syncytial tegument, the next larval stage proceeds, in which the protoscoleces develops [48]. The protoscolex has the head structure (scolex) of the adult tapeworm, but does not contain the proglottids. The scolex already has the four suckers and the

rostellum (hook ring), including a double ring of hooks, which are present in the scolex region of the adult worm [6]. In the metacestode vesicle, the protoscoleces are invaginated until the metacestode vesicle becomes digested by the fox [11]. This digestion process activates the protoscolex and stimulates the development of the adult worm within a period of 28 to 35 days. The adult worm is attached to the intestine wall of the fox and becomes segmented. The fox tapeworm is small compared to other tapeworms, with an adult size of 1.2 to 4.5 mm. The head region (scolex) of the tapeworm is directly followed by a distal proliferation zone, which produces the adjacent segments, the proglottids of the worm [28]. Given that tapeworms are hermaphrodites, which mean that each proglottid has female and male genitals, self-fertilisation generates the high reproduction rate of eggs in the terminal proglottid of the fox tapeworm. This terminal proglottid is finally released within the faeces of the fox.

3.3 Alveolar echinococcosis - infection risk and clinical therapy

The accidental oral uptake of the oncosphere by humans as a dead-end host interrupts the natural passage between the intermediate host and the definitive host and causes the human endoparasitic zoonotic disease AE. If the infection is not detected through random medical screening, it takes 5 to 15 years until the first symptoms occur [11]. The early symptoms are abdominal pain, weight loss, anaemia, jaundice and hepatomegaly, which culminate in the dysfunction of the affected organ and can result in the patient's death [22]. Beyond that, in later stages of the human infection, metastases can spread to other organs like the lung, bones or the brain. Human AE is often diagnosed in an advanced stage of the disease, when surgical removal of the parasite is no longer possible. After the detection of symptoms, the clinical diagnosis of AE is usually made by imaging (ultrasound, CT, NMR) [44], supported by serological tests. The serological tests allow detection with a sensitivity of 90-95% and a specificity of ~95% [30, 49]. After diagnosis, one option is radical surgery of the infected tissue, although this is only possible in some cases (20 to 40%) [11, 50]. Surgery is often combined with chemotherapy, which includes Benzimidazole carbamate derivatives (BZ) such as Albendazole (ABZ) and mebendazole (MBZ), which often have to be given lifelong [51]. It is not recommended to carry out a complete transplantation of the liver. A preceding radical resection of the parasitic mass before transplantation is difficult to complete and transplantation-associated immune suppression usually leads to massive growth of the residual parasite tissue and metastasised material [30, 52, 53].

According to the recommendations of the WHO informal working group for echinococcosis, surgical treatment should be accompanied by chemotherapy. The current chemotherapeutics were originally used to treat intestinal worm infections in animals and humans [54]. Infection of the liver with AE mirrors a completely differentiated clinical setting. Although the orally-administered drugs reach parasitocidal acting concentrations in the patient's intestine, they do not reach similar concentration in infected organs. The daily-administered dose of Albendazole is between 400-800 mg. It has been shown by *in vivo* studies of patients that the blood serum concentration of Albendazole is 0.65-3 μM

after four hours of treatment, which must be significantly lower than the unknown parasitocidal concentration *in vivo* and thus these drugs only act parasitostatic with drastic consequences and are not even guaranteed to cure the disease [22, 55]. In direct comparison to *in vitro* studies with Benzimidazole derivatives like Mebendazol (MBZ) by Jura *et al.* (1998) and Albendazole Sulfoxide (ABZSO) and Albendazole Sulfone (ABZSN) by Ingold *et al.* (1999), parasitocidal effects ($>0.1 \mu\text{M}$ of MBZ) and changes in the parasite ultrastructure tissue with changes in metabolites in vesicle fluids have been observed ($\geq 0,03 \mu\text{M}$ ABZSO/ABZSN) [56, 57]. Accordingly, it should be theoretically possible to influence the parasite tissue with the given high blood serum concentrations in man after administering the drug. However, the low bioavailability *in vivo* is one essential factor that suppresses the drug's activity. In addition, the protein targets of the current chemotherapy - the beta-tubulins (β -tubulins) - have a high structural homology ($>80\%$ amino acid identity) between humans and the parasite. Albendazol acts on these β -tubulins by inhibiting the polymerisation of microtubuli in the host and the parasite [56, 58]. These circumstances cause side-effects such as urticarial or gastrointestinal disorders and neuronal deficits, often with toxic effects on the bone marrow, followed by reduced numbers of leukocytes and thrombocytes. Adverse events often have a patient-specific pattern and sometimes make it impossible to continue the administration of albendazol [55]. Furthermore, it is estimated that not all cell types of the parasite are affected by the drug, due to low cellular bioavailability. Previous studies have shown that the binding specificity of BZ is dependent on the amino acid sequence of the β -tubulin [58, 59]. It was assumed that a mutation in the amino acid sequence of the β -tubulin at position Phe 200 to Tyr 200 and Phe 167 to Tyr 167 might result in the development of resistance to BZ [58-60].

3.4 Protein kinases and their characteristic features for the development of novel chemotherapeutics

Many outstanding discoveries in science have been found as a side product, whereby their importance for possible future advancements was largely unknown at the time of their discovery. In the 1950s, Krebs and Fischer (Nobel price 1992) researched possible regulatory mechanisms that are dependent on protein phosphorylation and discovered phosphorylating kinases [61]. At the time, they may have underestimated the wide influence of their accidental discovery and the future medical drug developments and applications of phosphorylating kinases on a cellular level as molecular switches [62-65]. Protein kinases are key factors in the regulation of cellular signalling and cell-cell communication and are well conserved among animals. Functionally, kinases carry out similar catalytic process by transferring the γ -phosphate of adenosine triphosphate (ATP) to a hydroxyl group of protein or non-protein targets. Overall, 518 kinases (representing $\sim 2\%$ of the genome) have been identified in the mammalian genome (not including splicing variants) and they show a range of similarities in their protein structure, the so-called sub-domains. A detailed characterisation of protein kinases was undertaken by Hanks and Hunter in 1988 [66, 67]. In their study, they described the conserved sequence motifs, the kinase core and the characteristics of 12 sub-domains that are required for the classification kinases, in a classification that still holds today [66].

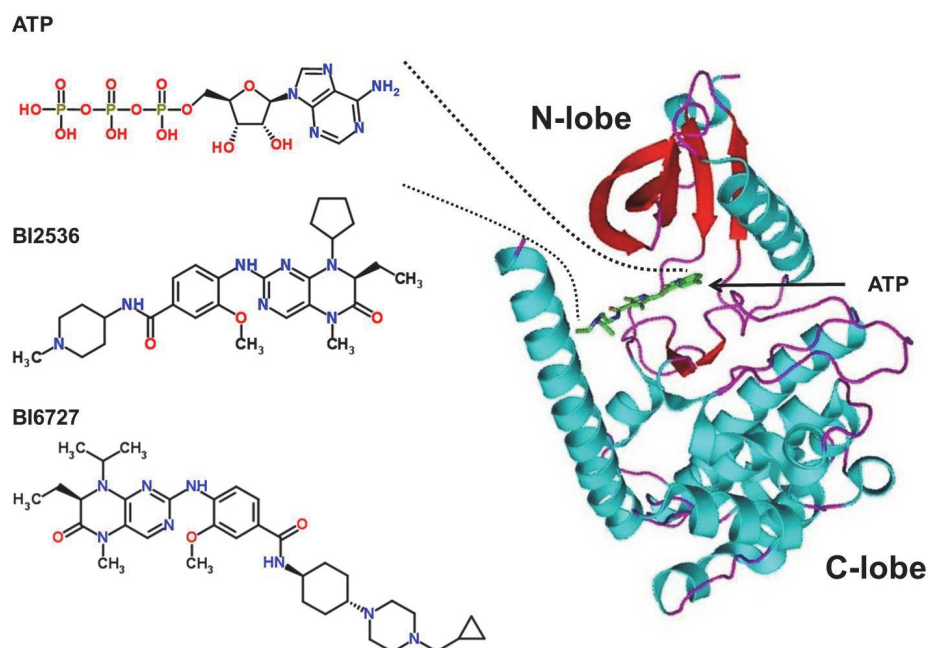


Figure 3.4.1 Crystal structure of protein kinase with bound ATP molecule. The characteristic bilobal folded structure separates the kinase into two main functional domains, N- and C-terminal lobe. The ATP molecule (green) is indicated by an arrow the centre of the kinase domain. α -Helices are indicated in blue, β -Barrels in red. ATP competitive inhibitors (BI2536/BI6727) are drawn to indicate the variability of side chains in functional chemical compounds. Figure of the kinase domain was modified from Curtis Neveu [68]. Chemical structures have been drawn with www.chemspider.com.

According to the classification system of protein kinases by Hanks and Hunter, we are now able to map amino acid sequences of kinases, leading to characteristic sequence motifs for each subdomain [66, 67]. Comparative studies on different types of kinases have shown that these structures are highly conserved over a broad range of eukaryotic organisms. All kinases are bilobal folded in an N-terminal (N-lobe) and C-terminal (C-lobe) part, producing a so-called hinge region in the middle, which is the binding side for the ATP molecule (Fig. 3.4.1). Binding of the ATP molecule and transfer of the phosphate is precisely regulated by elements in the N- and C-lobe in an activating process, including the activation and structural modification of the kinase core. Protein kinases are phosphorylated by other kinases in the core domain, which produces a conformational change to the active form. The phosphorylation takes place at the activation loop, which contains the amino acid threonine. The activation step leads to chemical modification of the central kinase domain and influences the folded structure by the negative charge of the phosphor ion. Depending on the kind of kinase, multiple phosphorylation sites can be present, which are not only located in the core region. In the cases of the mitogen-activated protein kinases (MAPKs) p38 (TGY), ERK (TEY) and JNK (TPY), two phosphorylation sites are present and p38 α is a potential drug target for AE [69, 70]. In close correlation to the phosphorylation site in the activation loop or T-loop, other essential residues are present and relevant, such as the highly flexible region of the Asp-Phe-Gly (DFG) motif. The DFG-loop is necessary to bind an ATP molecule to a transported Mg-ion and plays an important role in the kinases activity. A structural modification in the activation process turns the DFG-motif from the “DFG-motif in” position to the “DFG-motif out” position, which influences the activity state of the kinase and

its catalytic activity. Mutations in the DFG-motif have a negative effect on the kinase activity, leading to a dead kinase (mutant) version. A second important amino acid residue is the “gatekeeper”, which acts as a controlling factor of the chemical structure and size of the incoming ATP molecule. Depending on the size of the gatekeeper residue (large is comprised 77% of Leu, Met, Phe; small is comprised 21% of Thr, Val), variants of the ATP molecule are able to pass and bind in the hydrophobic centre of the core or not. The gatekeeper influences the design of novel chemotherapeutics, whereby many cancer drugs are designed to mimic the ATP molecule and work as a covalently-bound competitive inhibitor with the ability to produce displacing effects and longer resting times in the bound state [71]. Kinases are blocked in their activity by such inhibitors and the transduction of the downstream signal is inhibited. Mutations of the gatekeeper amino acid have significant physiological consequences; for example, the change of a small amino acid to a large amino acid at this position causes drug resistance through the interaction with the chemical structure of the side chains and a non-binding of the drug. For instance, the ATP competitive inhibitor imatinib only acts on the DFG-motif out version in the inactive state of the ABL-kinase. While this situation leads to disadvantages in the development of new drugs due to possible drug resistances, it offers a great target opportunity for therapies with chemical compounds that only need to target one type of kinases with their individual modifications. This individual drug design of ATP competitive inhibitors that bind in the hydrophobic ATP-pocket remains a fruitful approach, but new compounds are often generated in correlation to the activity state (DFG-motif out/in) of the kinase. In addition to the study and design of new drugs, it is important to invest time to understand the cellular functions of kinases and their importance for the regulation in the cellular mechanism. In summary, it can be said that both facts interact with each other and many cellular signal transductions are only discovered through the development of drugs. For instance, the understanding of the cell cycle with its fine-tuned regulatory functions executed and influenced by a battery of kinases is not possible without kinase inhibitors. One of the key players in the regulation of the cell cycle is the family of polo-like kinases, which will be discussed in the following section [72].












3.5 Polo-like kinase 1 and their potential as anti-helminthic drug target

The search of novel therapeutic options to cure AE remains one major challenge of the next ten years in the field of parasitology. A successful implementation of a new drug will also show an impact on the treatment options of other parasitic cestodes and furthermore on the close related parasite *S. mansoni*. Today several drugs against *E. multilocularis* have been evaluated by *in vitro* and *in vivo* studies for their potential use against AE [73, 74]. Together with the comprehensive *Echinococcus* genome information and gene expression data a new area of drug discovery has started. The presents of a broad spectrum of anti-parasitic or anti-cancer drugs that are already marketed or in development, as well as the now much easier *in silico* analysis of ortholog pathways and essential enzymes of the parasite are very useful to identify novel drug targets against AE [60, 75]. One of the essential enzymes is the Plk1, which belongs to the group of serine/threonine kinases (STK) and is part of a larger protein family. The Plk1 was first described in 1988 as a protein kinase

found to be associated with mitotic and meiotic defects in a *D. melanogaster* mutant named *polo* [72, 76]. By genetic screening, orthologs of *polo* gene from *D. melanogaster* have been identified in several eukaryotes, with the exception of plants and apicomplexans. Several isoforms appeared in *D. melanogaster*, including a second polo-like kinase (*sak*), and are associated with a duplication of the genome [77]. In budding and fission yeasts, such as *Saccharomyces cerevisiae* and *Saccharomyces pombe*, the gene *Cdc5* or *plp1* is present and it was shown that both of them carried out similar cellular functions as *polo* in *D. melanogaster* [78]. Yeast strains only have one polo-like kinase gene, whereas higher bilateral eukaryotes have several isoforms, which emerged from the Plk 1 ancestor gene. The polo-like kinases are grouped into subfamilies and an overview of the distribution of polo-like kinases is given in the following Tab. 3.5.1.

Analysis of the function of the Plk1 in several organisms revealed their role as a key regulator of cell cycle progression, acting on the mitotic entry and exit as well as the formation of the spindle poles the activation of cyclin-dependent protein kinases (CDC) [72, 79]. Overall, five Plks of this family have been characterised in humans to date [77, 80]. The human Plks1-3 showed a high similar structure, comprising an N-terminal kinase domain that is relevant for the phosphorylation of the protein substrate and a C-terminal polo-box domain (PBD). The characteristic PBD are involved in the protein-protein-interaction, relevant for phosphorylation of the substrate and furthermore involve in the subcellular localisation of the Plk [81]. A major focus where Plks are involved is the proliferation of eukaryotic cells. The cell cycle is controlled as fine-tuned mechanism, with defined steps and executed by protein kinases as the Plk1.

Table 3.5.1 Evolutionary conservation of Polo-like kinases in eukaryotes. Polo-like kinases are separated into groups of subfamilies. The graphic was taken from Cáceres *et al.* (2011) and modified to include the parasitic helminths *S. mansoni* and *E. multilocularis*. Two orthologs of the Polo-like kinases are present; in the mentioned parasites they are Plk1 and SAK (Plk4) [77].

	YEAST	PLANTS	INVERTEBRATES			VERTEBRATES			Parasitic Helminths			
												
	<i>S. pombe</i>	<i>S. cerevisiae</i>	<i>A. thaliana</i>	<i>C. elegans</i>	<i>Drosophila</i>	<i>S. purpuratus</i>	<i>D. rerio</i>	<i>Xenopus</i>	<i>H. sapiens</i>	<i>S. mansoni</i>	<i>E. multilocularis</i>	
Subfamilies	PLK1	plp1	Cdc5	-	plk-1 plk-2 plk-3	polo	PLK1	plk1	Plx1	PLK1	SmPLK1	predicted
PLK2	-	-	-	-	-	PLK2	plk2b plk3	Plx2 Plx3 Plx5	PLK2 PLK3 PLK5	-	-	
SAK	-	-	-	zyg-1	sak	SAK	plk4	Plx4	PLK4	SmSAK	predicted	

The functions of the Plk-family have been extensively analysed, particularly in mammals. Comparing all five Plks present in the mammalian genome revealed functional differences in their cellular action on the cell cycle as well as their protein sequences and domain structures. The differences in the protein structure arose from genomic duplication during evolution and mutations in the gene sequence [82]. Since this thesis concentrates on the Plk1 subfamily, the cellular functions of this Plk type will be

further outlined below. Plk1 is one of the most studied kinase and its respective inhibitors have been developed and shown promising effects in *in vitro* and clinical *in vivo* studies of cancer [83-85]. Human Plk1 is comprised of 603 amino acids and comprises two highly conserved domains. In the N-terminal part, the 252 amino acid catalytic domain (Fig. 3.5.2, green,) is present. The kinase domain includes all the kinase-specific characteristic features described by Hanks and Hunter [66]. The gatekeeper residue at position 82 (K82) of the amino acid is highlighted, as well as the phosphorylation site at position T210. The kinase domain includes a nuclear localisation signal (NLS), which regulates the nuclear translocation of Plk1 (Fig. 3.5.2, orange) [86, 87]. At the end of mitosis, the Plk1 is ubiquitinated at the D-box side, indicated in red, leading to degradation of the kinase [88].

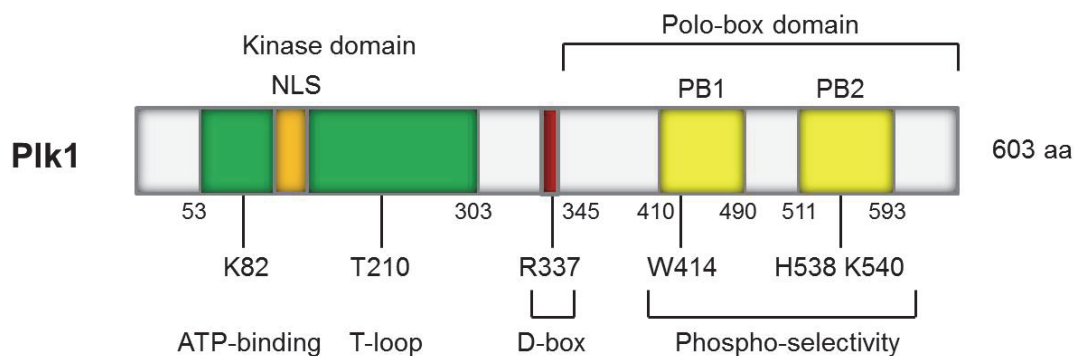


Figure 3.5.2 Schematic representation of the human Polo-like kinase 1 highlighting characteristic protein features for this protein family.

In the C-terminal region of the protein, two protein domains are present, namely the polo boxes (PB1 & PB2). Together, these regions form the PBD. Studies have shown that the PBD-domain is responsible for the binding of the protein substrate by recognising the phosphopeptide-binding motif (Fig. 3.5.2, Phospho-selectivity). The phosphopeptide-binding motif has a strong substrate affinity for either phospho-Serine or phospho-threonine residues located in the consensus peptide Ser-pSer/pThr-Pro [77]. Furthermore, the PBD regulates the subcellular localisation of the polo-like kinases [77, 89]. Both domains act together during the phosphorylation and activation of the Plk1. It is assumed that the PBD without a bound phosphorylated substrate folds back and blocks the kinase domain, leading to a regulation by molecular switching [80, 90].

Activation *via* phosphorylation of the Plk1, during the G2 phase, is mediated by Aurora kinase A, a cellular serine/threonine kinase that binds to the Plk1/Bora protein complex. Aurora A kinase phosphorylates Plk1 at threonine T210 (Thr or T) in the kinase domain, but only in the complex with Bora. Bora serves as a relevant co-factor for the phosphorylation process and is also phosphorylated by the cyclin-dependent kinase 1 (CDK1), which is a downstream signal transduction substrate of the activated Plk1. No further detailed information is present about this Plk1/Bora pre-complex [91]. However, it has been shown by Förster Resonance Energy Transfer (FRET) that Bora is present in a cell cycle-dependent manner in the nucleus and cytoplasm [79]. Where and when the phosphorylation of Bora takes place and whether there is a correlation to the translocation of Plk1 is completely unknown [79]. In the next steps during mitosis are the nuclear envelope breakdown (NEB) and mitotic entry takes place. Bora is subsequently degraded from the Plk1/Bora protein-protein complex directly

after the mitotic entry. Like for the most proteins in the cell cycle also Aurora kinase A is regulated. During mitosis the co-factor Xklp2 (TPX2) takes over the regulation of Aurora kinase A and targets it to the mitotic spindle. Furthermore, it was observed that at later stages of the mitosis Plk1 is no longer Aurora kinase A-dependent. *Drosophila* studies show that Aurora kinase B and the Ste20-like kinase are also regulators of the activation of Plk1. The activation of the Plk1 by these kinases occurs at T182, the equivalent of the human T210. Plk1 subsequently triggers the downstream phosphorylation of the phosphatase CDC25. CDC25 adheres to the kinase complex of WEE1 and MYT1, which is then phosphorylated and inactivates the CDK1/Cyclin B1 complex, which promotes mitotic entry [92]. In addition to the activation of CDC25, Plk1 is also responsible for the inactivation of WEE1 and MYT1 through phosphorylation. Finally, this leads to the onset of mitosis [91, 93].

Moreover, after the activation by phosphorylation of the Plk1, several proteins and cell cycle key factors interact with this kinase. A brief overview of Plk1 interaction partners is given in Fig. 3.5.3. An example of a typical feedback and forward loop in the cell cycle transition is given by the activation of the cyclin B/CDK1 complex. CDK1 is necessary for the activation of Bora *via* phosphorylation, which has a direct consequence of the activation of Plk1, after complex formation. Phosphorylated Plk1 in turn is necessary for the activation of cyclin B, which binds to CDK1. Overall, these kinds of feedback loops are relevant for the establishment of a bistable system that renders cell cycle transitions irreversible [79].

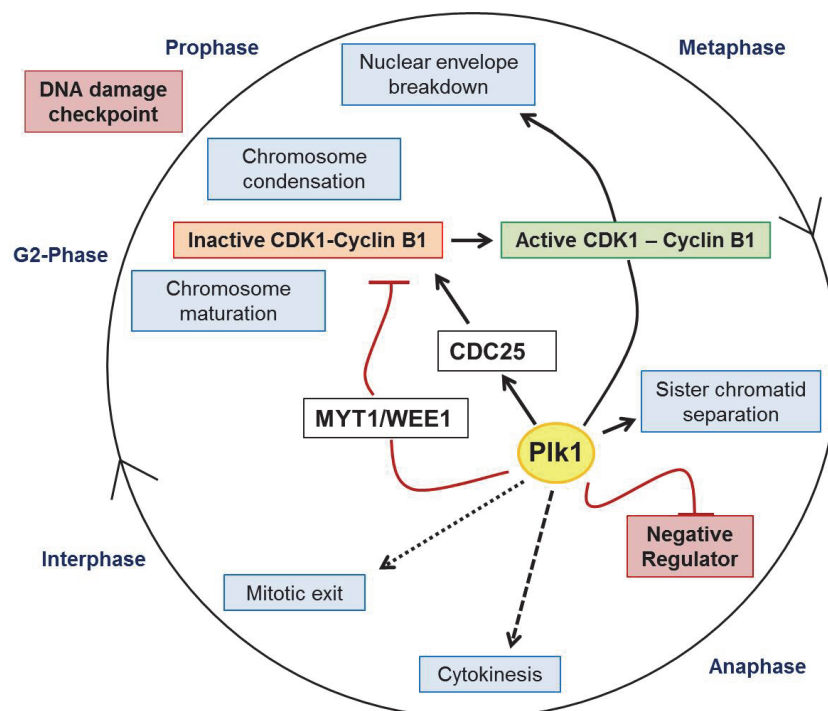


Figure 3.5.3 Schematic representation of some Polo-like kinases 1 protein interacting partners and the transduction of signal cascades during the cell cycle. Plk1 is a central player in the activation and inactivation of several protein factors acting on the transduction of the cellular progression. Figure was modified from Strebhardt *et al.* (2006) [84].

Due to its importance in the cell's entrance into mitosis and thereby cell proliferation, Plk1 is an interesting candidate for possible chemotherapy targets [85]. Several inhibitors for Plk1 have been identified in cancer cells, showing that Plk1 inhibition preferably kills cancer cells compared with normal cells, providing a potential therapeutic window for drug development [71, 83]. Besides the normal cellular proliferation, several cancers show a Plk1 up-regulation on transcriptional and translational level [83]. However, mutations in the Plk1 gene can occur and result in abnormal activation of the protein activity. It has also been shown that the up-regulation of Plk1 can be an indirect consequence of the cellular proliferation in cancers. In addition to this, it has also been reported that mutations in *plk1* trigger a degradation of the protein rather than an increase of its activity [78, 94]. Based upon the fact that Plk1 is a protein kinase, several cancer studies have shown that ATP competitive inhibitors can inhibit its enzymatic activity [71, 83, 95, 96]. These ATP competitive inhibitors act by out-competing the cellular ATP molecule in the ATP binding pocket and thereby block the phosphor transfer of the kinases. The ATP binding pocket in the kinase domain demonstrates only small differences in the amino acid sequence between kinases, indicating a high evolutionary conservation. These small differences of molecular properties can be used to optimise the chemical structure of ATP competitive inhibitors to "personalise" the binding of the ATP binding pocket to the target kinases [65, 95]. Structure-based modelling, high throughput screening and chemical lead optimisation yielded two ATP competitive inhibitors, developed by **B**oehringer **I**ngelheim (Ingelheim, Germany), (**BI** 2536 and **BI** 6727 (second generation)), which belong to the dihydropteridinone substance class and bind to human Plk1 [95, 97, 98]. Both compounds show high selectivity for human Plk1 with more than 10.000 fold higher binding capacity to Plk1 than to other tyrosine or STK [95]. *In vitro* kinase assays for Plk1 showed half maximal inhibitory concentrations (IC_{50}) of 0.83nM for BI 2536 and 0.87nM for BI 6727, underlining the high selectivity for this enzyme [95, 98, 99]. Although revealing a similar IC_{50} for Plk1 as BI 2536, the second-generation inhibitor BI 6727 has an improved half-life *in vivo* and a better accessibility to encapsulated tumour tissues [98]. Within the human polo-like kinase family, BI 2536 shows an IC_{50} of 3,5nM for Plk2 and 9,0nM for Plk3. In the case of BI 6727, the IC_{50} is higher with 5nM to Plk2 and 56nM to Plk3. Several cancer cell lines were used to estimate the half-maximal effective concentration (EC_{50}) *in vitro* for BI 2536, which reaches from 2-25 nM and for BI 6727 from 11-37 nM. Both inhibitors were able to induce mitotic arrest in proliferating cells, followed by apoptosis and significant cytotoxicity for stem cells was observed in the presence of micro-molar concentrations [100, 101].

In addition to the promising effects of this inhibitor in clinical studies, this inhibitor has already been tested in *S. mansoni* and indicated inhibitory effects in the proliferation organs of the parasite [102]. The prediction of a Plk1 ortholog in *E. multilocularis* and the importance of this ortholog in the mechanisms of cellular proliferation prompted us to study the Plk1 of the fox tapeworm.

3.6 The invertebrate-specific family of Venus Flytrap kinases

Investigations on the presence of insulin receptor-like tyrosine kinases (TDKs) in *S. mansoni*, (Vicogne *et al.* 2003) discovered a structurally unusual member of the receptor tyrosine kinase family, SmRTK-1, with certain homologies to insulin receptor tyrosine kinases [103]. Insulin receptor-like tyrosine kinases are typically composed of an extracellular ligand-binding domain, located on the so-called alpha subunit, which is connected to the beta-subunit via disulphide bridges [104]. The beta-subunit of insulin receptors contains a transmembrane domain and an intracellular tyrosine kinase domain, and two typical members of this protein family are indeed present in *S. mansoni* [105]. By contrast, in SmRTK-1, the intracellular, insulin-receptor-like tyrosine kinase domain is connected to an extracellular domain with similarities to the Venus Flytrap module, which is typically found in periplasmic binding proteins (PBP) of bacteria [106, 107]. Molecules employing this unusual combination of an extracellular Venus Flytrap module with homologies to those of GABA(B) receptors, connected to an intracellular RTK domain with homologies to insulin receptors, were later also discovered in insects and other invertebrates and the entire protein family was designated VKRs (Venus Flytrap Kinases) [108].

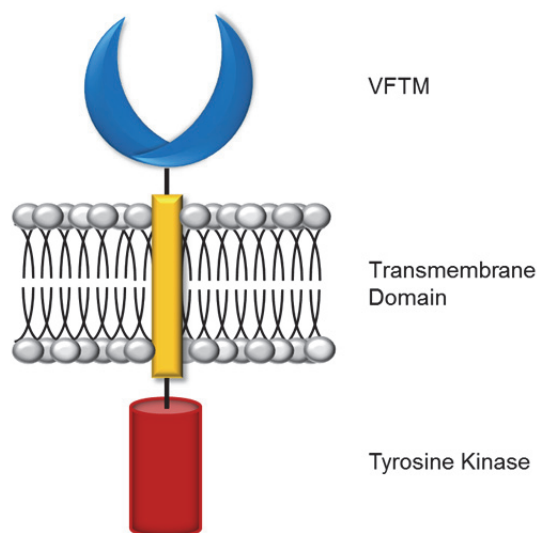


Figure 3.6.1 Schematic representation of the Venus flytrap kinases receptor (VKR). The extracellular Venus flytrap module (VFTM) is connected by a single membrane spanning domain to similar insulin receptor tyrosine kinase domain.

In bacteria, the VFT-containing PBP are involved in sensing sugars and ions as well as in the binding and the transport of amino acids. SmRTK-1 (now designated as SmVKR1) was shown to be activated by L-arginine [106, 108]. In a subsequent study, Vanderstraete *et al.* (2014) described a second *S. mansoni* member of the VKR family, SmVKR2, which was activated by calcium ions [109]. Furthermore, both SmVKR1 and SmVKR2 were shown to control reproduction in *S. mansoni* [109]. Since the tyrosine kinase domains (TKD) of schistosome VKRs share somewhat less homologies with the TKDs of human insulin receptors than the schistosome insulin receptors, the VKR family has

already been suggested as a promising target for drug design against schistosomiasis [103, 108, 110]. Furthermore, since schistosomes employ two members of the insulin receptor family and two VKRs that regulate important processes such as glucose uptake, metabolism, and reproduction, small-molecule compounds that target all these enzymes simultaneously could prove effective in inhibiting several essential functions in these parasites [107]. Interestingly, one such compound, Tyrphostin AG 1024, was shown to be a potent inhibitor of schistosome insulin receptors and the VKRs and affected the viability of both schistosomula and adult worms of *S. mansoni in vitro* [110].

3.7 *In vitro* culture of *Echinococcus multilocularis*

In vitro cultivation techniques are often essential to study parasite biology and host-parasite interaction mechanisms under defined laboratory conditions. For *E. multilocularis* larvae, the first cultivation methods were established by Hemphill and Gottstein in 1995 [111]. These authors introduced a culture system in which parasite material, isolated from infected rodents, was kept as tissue blocks in serum-containing medium. Tissue block-derived metacestode vesicles were morphologically similar to vesicles described in infected livers or other organs of patients [111]. In a second system, Jura *et al.* (1996) co-incubated rat hepatocytes with homogenised parasite material that was isolated from Mongolian jirds and embedded in a collagen matrix [112]. Although both systems were effective in the *in vitro* production of metacestode vesicles and demonstrated that parasite development depends on soluble host factors, they suffered from the fact that host cells were still present in the culture system. Hence, in the case of observed effects of host-derived factors or small-molecule compound inhibitors on parasite survival and development, it was unclear whether this involved direct effects on the parasite vesicles, or indirect effects on the co-cultivated host cells.

To overcome the problems of the parasite-host cell co-cultivation systems, Spiliotis *et al.* (2004) developed the so-called 'axenic' *E. multilocularis* cultivation system [113]. In this system, metacestode vesicles are first generated through co-cultivation with host feeder cells (e.g. hepatoma cells) and are subsequently incubated for one week under a nitrogen atmosphere and with reducing agents in the medium [113]. These culture conditions were found to be important for parasite cultivation in the absence of host feeder cells since these obviously not only produce growth factors for the parasite, but also remove reactive (toxic) oxygen compounds from the medium upon incubation under an oxygen atmosphere [113]. After one week of incubation under 'axenic conditions' such cultures are free of host cells and can be maintained for longer periods of time provided that the reducing conditions are maintained and that host growth factors are constantly supplied, e.g. by adding 'conditioned' culture medium that has previously been incubated with host cells [113]. The authors also found that not only culture supernatant of hepatoma cells but also supernatant of many other cell lines could support *Echinococcus* development. However, hepatocyte-derived growth factors have been demonstrated to be the most effective.

The axenic cultivation system subsequently facilitated the establishment of 'pure' parasite cell cultures. There have been several previous attempts to culture cestode cells *in vitro*, which all suffered from the

fact that parasite material of *in vivo* culture (i.e. from laboratory animals) had been used as a source for parasite cells [114-117]. Consequently, the cultivated parasite cells have always been overgrown *in vitro* by contaminating host cells, mostly fibroblasts [118]. By using axenically cultivated metacestode vesicles as a source for parasite cells (after trypsin digestion), it has been demonstrated that 'primary cell cultures' can be established that exclusively comprise parasite-derived cells [118, 119]. In the presence of suitable culture conditions (reducing environment; 'conditioned' medium), the parasite cells form aggregates within 2-3 days that contain actively proliferating parasite cells [118, 120]. After up to 6 weeks of culture, these aggregates form internal cavities, which later yield completely 'regenerated' metacestode vesicles with a germinal layer surrounded by a LL [118-120]. When injected into laboratory mice, these vesicles resulted in large quantities of metacestode tissue with protoscolexes, indicating that the cultured parasite cells were at least pluripotent [121, 122]. Koziol *et al.* (2014) later showed that after 2 days of incubation the aggregates of 'primary cultures' were strongly enriched in parasite stem cells (the 'germinative cells'; up to 80% of all cells) and that parasite development was exclusively driven by these stem cells [32]. The primary cultivation system has subsequently been extensively used for studies on host-dependent parasite development, on immunomodulatory activities of parasite excretory/secretory molecules, for studies on drug development and as a source for parasite mRNA in the *Echinococcus* genome project [33, 60, 70, 123-126]. Interestingly, the morphology of developing parasite aggregates in the primary culture system closely resembles early stages of parasite development in oncosphere-infected laboratory mice [118]. Furthermore, parasite primary cell cultures show a gene expression profile similar to that of oncospheres [60]. It can thus be assumed that the parasite primary cell culture system closely mimics the oncosphere-metacestode transition as it occurs early during an infection of the intermediate host [59, 124].

3.8 Objectives

A recent publication by Koziol *et al.* (2014) showed that stem cells of the parasite *E. multilocularis* are relevant for proliferation and gave rise to all differentiated cells [32, 127]. This new information has a major impact also for the search of novel drug targets and should now be used together with the recently published genomic and transcriptomic data of the fox tapeworm to help to cure AE [60].

In the last 10 years, efforts have been made to identify important cellular signalling cascades as potential drug targets, such as the mitogen-activated protein kinases (MAPK), the epidermal growth factor (EGF), the fibroblast growth factor (FGF), the transforming growth factor β /Bone morphogenetic protein (TGF β /BMP) and the insulin signalling pathways, which are involved in the proliferation and differentiation of cells, but a cell type specific action of the drug was not possible to show [33, 70, 126].

Together with the current techniques available for the cultivation of *E. multilocularis*, which allow us to study the larval stages of this tapeworm in the laboratory, we want to test new inhibitors. In the first part of this work, the inhibitory action of the Plk1 inhibitor BI 2536, which should act on the cell cycle by suppressing the proliferation of cells, was evaluated [77, 118, 120, 128]. In the second part, we want to show that the specific action of this inhibitor BI 2536 is directly acting on parasite stem cells and try to validate the hypothesis that this cell type is expressing a β -tubulin isoform (*tub-2*), which shows limited affinity to benzimidazoles. Moreover, the study should finally show that the Plk1 is a fruitful target for further optimisations of the inhibitor BI 2536 and furthermore opens up a new approach for the treatment of AE and for the study of the role of stem cells in the larval stages of the metacystode vesicle.

In the third part of this thesis, a novel receptor tyrosine kinase, the Venus flytrap kinase receptor (EmVKR) of *E. multilocularis*, was characterised. Members of this class of single transmembrane receptors were recently discovered in *S. mansoni* with an unusual receptor composition of extracellular and intracellular domains [103]. Moreover, this type of receptor has only been described in invertebrates to date [107]. The structural property - as well as the fact that this receptor type in this composition is not described for vertebrates - provides several interesting aspects for the study of the cellular functions in *E. multilocularis* and potentially as a new drug target for AE.

4 Material and Methods

4.1 Material

4.1.1 Equipment

Bio-Rad Laboratories Universal Hood III for development of western blots RNA/DNA-agarose and protein gels	(Bio-Rad, München)
Developer for radiographic films	(AGFA Graphics Germany, Düsseldorf)
ELISA reader Multiscan Ex Primary EIA V.2.1-0	(Thermo Scientific, Braunschweig)
Eppendorf Research Plus pipette set	(Eppendorf, Hamburg)
Eppendorf Thermomixer Compact	(Eppendorf, Hamburg)
Eppendorf Xplorer 15-300µl (41555AZ) Pipette	(Eppendorf, Hamburg)
Gel documentation system: MidiDoc	(Herolab, Wiesloch)
Gelelectrophoresis camber	(Bio-Rad, München)
Heating Block: DB-3	(Techne, Cambridge, UK),
Heizblock	(Liebisch, Bielefeld)
Heating stirrer: Typ RCT	(Jahnke & Kunkel, Staufen i. Br.)
HERA safe	(Heraeus, Thermo Electron, Langenselbold)
Incubator: Heraeus	(Thermo Electron, Langenselbold)
Leica IRB	(Leica Microsystems, Wetzlar)
Leica TCS SP5 Confocal	(Leica Microsystems, Wetzlar)
Leica Microtom 2065	(Leica Microsystems, Wetzlar)
Mikro 200 table centrifuge	(Hettich, Tuttlingen)
Micro scales: R160P	(Sartorius, Göttingen)
Mini-PROTEAN II System	(Bio-Rad, München)
MSC advantage laminar flow	(Thermo Scientific, Braunschweig)
NanoDrop 1000	(PeqLab Biotechnologie, Erlangen)
Neubauer chamber (0.1 mm, 0.0025 mm ²)	(Hartenstein, Würzburg)
Nuaire laminar flow	(Nuaire)
Power Pack P24 and P25	(Biometra, Göttingen)
Refrigerated Centrifuge 3K30	(Sigma-Aldrich, München)
Scale: 10-1000 g	(Sartorius, Göttingen)
Selectomat S2000 autoclave	(Münchner Medizin Mechanik, München)
G24 shaking incubator	(New Brunswick Scientific, Edison, N.J., USA)
Spectrophotometer U-2000	(Hitachi, NY, USA)
TECAN ELISA reader	(Tecan Group, Crailsheim)
T-Gradient Thermocycler	(Biometra, Göttingen)
TH30 shaking incubator	(Hartensein, Würzburg)
Tricarb scintillation counter	(Packard)

Trio-Thermoblock™ heated lid	(Biometra, Göttingen)
Trio-Thermoblock™ oil	(Biometra, Göttingen)
Vacuum pump	(ILMVAC, Ilmenau)
Vortex mixer: L46	(Gesellschaft für Laborbedarf, Würzburg)
Zeiss microscope Imager Z1 AXIO with AxioCam MRm	(Zeiss, Wetzlar)

4.1.2 Consumables

96-well plates	(Sarstedt, Nuembrecht)
48-well plates	(Greiner Bio-One International AG, Kremsmünster Österreich)
24-well plates	(Nunc, Roskilde, Denmark)
12-well plates	(Nunc, Roskilde, Denmark)
25 cm ²	(Sarstedt, Nümbrecht)
75 cm ²	(Sarstedt, Nümbrecht)
175 cm ²	(Sarstedt, Nümbrecht)
Microtom sample adapter	(Rudens Platinindustri, Hestra, Sweden)
Microinjection cannula, sterile 0.30 x 12mm BL/LB 30G x ½ “	(Braun Melsungen AG, Melsungen)
Nitrocellulose membran	(GE Healthcare, München)
PD-10 column	(GE Healthcare, München)
Radiographic Film	(Fujifilm Europe, Düsseldorf)
Safe-Lock Tubes 0,5, 1,5 and 2 ml	(Eppendorf, Hamburg)
Semi-micro cuvettes	(Sarstedt, Nümbrecht)
Sterilfilter	(Nalgene, New York, USA)
Sterile tubes, 15 and 50 ml	(Greiner, Nürtingen)
Superfrost Plus slides	(Thermo Scientific, Braunschweig)
Syringes and canula, sterile	(Braun Melsungen AG, Melsungen)
Whatman blotting paper	(GE Healthcare, München)
X-Ray film Hyperfilm™ -MP	(Amersham, Braunschweig)

4.1.3 Chemicals, media, commercially available kits and Enzymes

[14C]-D-Glucose	(Hartmann Analytic, Braunschweig)
2',5'-Dideoxyadenosine	(Sigma-Aldrich, München)
3,3 Diaminobenzidine 4 Hydrochloride	(Serva, Heidelberg)
5-Bromo-2-Deoxyuridine	(AppliChem, Darmstadt)
Adenine hemisulfate	(Sigma-Aldrich, München)
Agarose	(Carl Roth, Karlsruhe)

Albumin fraction V (pH 7) Blotting grade (BSA)	(AppliChem, Darmstadt)
Ammonium peroxodisulfate (APS),	(Carl Roth, Karlsruhe)
Artemisinin 98% 361593-100MG	(Sigma-Aldrich, München)
Aqua demin. (VE-water)	
Aqua B. Braun Spüllösung 1 Liter	(B. Braun Melsungen AG, Melsungen)
Ampuwa	(Fresenius, Bad Homburg)
Ampicillin	(Sigma-Aldrich, München)
Antarctic Phosphatase	(New England Biolabs Inc., Schwalbach)
AS601245	(Calbiochem, Merck, Darmstadt)
BA-6; BA-3-33, BA-3-35; BA-3-29;	(University of Siena)
BA 3-61; BA 103; BA -126; BA 3-45	
Bacto agar	(Difco Laboratories, Augsburg)
Bathocuproine disulfonic acid	(Sigma-Aldrich, München)
BI 2536 Catalog No.S1109	(Selleck Chemicals, München)
BI 6727 Volasertib Catalog No.S2235	(Selleck Chemicals, München)
BIRB 796 Doramapimod Catalog No.S1574	(Selleck Chemicals, München)
CIP	(New England Biolabs Inc., Schwalbach)
Chloroform	(Merck, Darmstadt)
CloneJET PCR Cloning Kit pJET 1.2	(Thermo Scientific, Braunschweig)
Color Plus Prestained Protein Marker (10- 230 kDa)	(NEB, Schwalbach)
Colorimetric Cell Proliferation ELISA BrdU	(Roche, Grenzach)
Complete Mini phosphatase inhibitor Mix	(Roche, Grenzach)
Ciprofloxacin Kabi 2mg/ml- Infusionslösung	(Fresenius KABI Austria GmbH, Graz)
Dimethyl sulfoxide (DMSO)	(Sigma-Aldrich, München)
Dimethyl sulfoxide,	(Sigma Life Science, München)
for inhibitors in cell culture (D8418-50ml)	
dNTP lyophilised	(Carl Roth, Heidelberg)
DMEM- glucose free	(Biochrom, Berlin)
DMEM- GlutaMAX TM (DMEM)	(Invitrogen, Darmstadt)
DMEM no phenolred	(Invitrogen, Darmstadt)
DO Supplement –Ade/–His/–Leu/–Trp	(Clontech, Heidelberg)
DO Supplement –Leu/–Trp	(Clontech, Heidelberg)
Entellan	(Merck, Darmstadt)
Eosine	(Roche, Mannheim)
Fetal Calf Serum (FCS)	(Invitrogen, Darmstadt)
GW843682X 98% G2171-1MG	(Sigma-Aldrich, München)
Haemalaun	(Roche, Mannheim)
Hystidine HCL mono-hydrate	(Sigma-Aldrich, München)
Imatinib-mesyate	(Enzo Life Sciences, Lörrach)
Insulin, recombinant human	(Sigma-Aldrich, München)

K11777	(By courtesy of Caffrey Conor, UCSF, USA)
KOD Hot Start DNA Polymerase (71086-3)	(Merck KGaA, Darmstadt)
L-Cystein	(Sigma-Aldrich, München)
Lufenuron PESTANAL® 31662-100MG	(Sigma-Aldrich, München)
Matchmaker Two Hybrid System 3	(Clontech, Heidelberg)
β-Mercaptoethanol	(Sigma-Aldrich, München)
2-Methoxyestradiol (2-MeOE2) Catalog No.S1233	(Selleck Chemicals, München)
Mycophenolic acid M3536-50MG	(Sigma-Aldrich, München)
NucleoSpinR Extract II	(Macherey-Nagel, Düren)
NucleoSpinR PC100	(Macherey-Nagel, Düren)
NucleoSpinR Plasmid Kit	(Macherey-Nagel, Düren)
Oligonucleotides	(Sigma-Aldrich, München)
OmniscriptR RT Kit	(Qiagen, Hilden)
Oridonin Catalog No.S2335	(Selleck Chemicals, München)
pBAD/TOPOR ThioFusion™ Expression Kit	(Invitrogen, Darmstadt)
PCR Cloning Kits	(Qiagen, Hilden)
Penicillin/Streptomycin	(Invitrogen, Darmstadt)
Pepsin	(Sigma-Aldrich, München)
PierceR BCA Protein Assay Kit	(Thermo Scientific, Braunschweig)
PierceR ECL western blot substrate	(Thermo Scientific, Braunschweig)
Pierce ReactBindR	(Thermo Scientific, Braunschweig)
ProBond™ Nickel-Chelating Resin	(Invitrogen, Darmstadt)
Proteinase K	(AppliChem, Darmstadt)
Phenytoin Zentropil®	(Sandoz Pharmaceuticals GmbH, Ismaning)
RNAse A	(Roche, Grenzach)
RNAseOut	(Invitrogen, Darmstadt)
Peptone	(Difco Laboratories, Augsburg)
Phospho Detect™ Phosphoserine Detection kit	(Calbiochem, Merck, Darmstadt)
PhosStop	(Roche, Grenzach)
Polyethylene glycol	(PEG 3350, Sigma-Aldrich, München)
PrimeScript RNA Polymerase	(Takara, Verviers, Belgium)
Rapamycin	(Cell Signalling, NEB, Schwalbach)
Resazurin	(Sigma-Aldrich, München)
Restriction enzymes	(New England Biolabs Inc., Schwalbach)
RotiphoreseR Gel 30 (37,5:1)	(Carl Roth, Karlsruhe)
RotiphoreseR Gel 40	(Carl Roth, Karlsruhe)
RQ1 RNase-Free DNase	(Promega, Mannheim)
SmartLadder	(Eurogentec, Köln)
SMART™ RACE cDNA Amplification kit	(Clontech, Heidelberg)
SOC	(Invitrogen, Darmstadt)

Sodium taurocholat	(Sigma-Aldrich, München)
Sodium hydroxide 306576-25G	(Sigma-Aldrich, München)
SuperSignal West Femto Chemiluminescent Sub.	(Thermo Scientific, Braunschweig)
T4 DNA Ligase	(New England Biolabs Inc., Schwalbach)
Taq-Polymerase	(New England Biolabs Inc., Schwalbach)
TAK-715 Catalog No.S2928	(Selleck Chemicals, München)
TavanicR (Tava, active component levofloxacin, 5mg/ml)	(Aventis)
Technovit 8100	(Heraeus Kulzer, Wehrheim)
TEMED (N,N,N',N'-Tetramethylethylendiamin)	(Merck, Darmstadt)
TritonR X-100	(Sigma-Aldrich, München)
TrizolR Reagent	(Invitrogen, Darmstadt)
TOPO-TA CloningR KIT	(Invitrogen, Darmstadt)
Trypsin/EDTA (0,05%/0,02% (w/v)/	(Biochrom, Berlin)
PBS w/o Ca ²⁺ , Mg ²⁺)	
TweenR 20	(Merck, Darmstadt)
UlitraGoldTM	(Perkin Elmer, Rodgau)
Yeast extracts	(Difco Laboratories, Augsburg)
Yeast nitrogen base w/o amino acids	(Difco Laboratories, Augsburg)
Zeiss Immersol 518F Immersionsöl	(Zeiss, Wetzlar)

All inhibitors were dissolved in Dimethyl sulfoxide (usable for cell culture, D8418, Sigma Aldrich), aliquoted into 0.5 ml tubes at concentrations for treatment (1000x fold higher) and stored at -80°C until usage.

All buffers and solutions were made with commercial Aqua B. Braun sterile water. For RNA, either DEPC-treated or RNase-free water was used. For enzymatic reactions, double distilled and autoclaved water was used.

4.1.4 Oligonucleotides

A list of all genes specific Primers (AKO-Number/ASO-Number) used within this thesis is given in Tab. S1 in the supplement material.

4.1.5 Plasmids

Plasmid	Sequencing Primer	Sequence
pDrive	T7 (T7-Primer)	GTAATACGACTCACTATAG
	SP6	CATTTAGGTGACACTATAG
pBad/Thio-Topo [®]	pBad fw (AKO-11)	GCTATGCCATAGCATTITTTATCC
	pBad rev (AKO-12)	GACTAAATTAGACATAGTCCG
pJET1.2 CloneJET	pJetfw (AKO-95)	CGACTCACTATAGGGAGAGCGGC
	pJetrev (AKO-96)	AAGAACATCGATTTTCCATGGCA
pSec-HygroA	psecfw or T7	CTAGTTATTGCTCAGCGGTGG
	psecrev or	TAATACGACTCACTATAGGG
pcDNA3.1	pcDNA3.1rev	CTAGAAGGCACAGTCGAGGC
	T7 (T7-Primer)	GTAATACGACTCACTATAG

4.1.6 Antibodies

Primary antibodies:

Antibody	Dilution	Source	Company
Elp	1:1000 5 % skim milk TBST	Mouse	Cell Signalling
β -Actin	1:1000 5 % BSA TBST	Rabbit	Cell Signalling
anti-Plk1 (phosphor T210)	1:500 5 % skim milk TBST	Rabbit	Abcam (ab12157)
anti-Polo-like Kinase (Plk1) pT210	1:1000 5 % skim milk TBST	Rabbit	Antibodies-online.com (ABIN129581)
anti-PLK-1	1:500 5 % skim milk TBST	Rabbit	BioLegend (Catalog #/ 618501; Clone Poly6185)

Secondary antibodies:

Antibody	Dilution	Company
anti-mouse IgG–HRP	1:10.000 5 % skim milk TBST	Jackson, ImmunoResearch
anti-rabbit IgG–HRP	1:5.000 5 % skim milk TBST	Jackson, ImmunoResearch

4.1.7 *Echinococcus multilocularis* isolates

Isolate (Sample accession number)	Origin of Isolate	Year of infection	Used for experiments
H95 (ERS097684)	Oral infection of jirds (<i>Meriones unguiculatus</i>) by oncospheres of from the intestine of a fox.	1995	Co-culture of metacestode vesicles, isolations of primary cells.
GH09 (ERS097686)	Javaner Affe (<i>Macaca fascicularis</i>) intermediat host	2009	Co-culture, isolation of protoscoleces and primary cells
Ingrid (G-Nr. 8292)	Javaner Affe (<i>Macaca fascicularis</i>) intermediat host (female *19.06.1988 †14.09.2010)	2010	Co-culture, isolation of protoscoleces and primary cells. The production of protoscoleces is reduced.
J2012 (G-Nr. 8604)	Javaner Affe (<i>Macaca fascicularis</i>) intermediat host (male *26.12.2003 †16.02.2012)	2012	Co- culture, isolation of protoscoleces and primary cells.
DPZ 13 (G-Nr. 8785)	Javaner Affe (<i>Macaca fascicularis</i>) intermediat host (female *13.07.2008 †30.01.2013)	2013	

4.2 Methods

4.2.1 Working with nucleic acids

4.2.1.1 Determination of nucleic acid concentrations and purity

Nucleic acid concentrations of RNA/DNA were determined photometrically at a wavelength of 260nm with the spectrometer NanoDrop 1000. The protein, organic compounds and salt impurities of nucleic acids were analysed based upon the ratio of 260nm/280nm (protein; pure DNA, $A_{260/280}$ is 1.8; pure RNA $A_{260/280}$ is 2.0) and 260nm/230nm (salt; expected values for $A_{260/230}$ are in the range of 2.0-2.2). Concentrations of DNA fragments/bands were also estimated by comparison of the band intensity to the known DNA standard concentration given by the marker (e.g. SmartLadder, Eurogentec) in agarose gels.

4.2.1.2 Isolation of total RNA from *E. multilocularis* larval stages

Parasite material (metacystode vesicles, primary cells and protoscoleces) were washed intensively with cold 1x PBS and centrifuged at 600g for 2 minutes (') at room temperature (RT). The supernatant was removed and 1ml of TRIzol[®] reagent was added. (The volume of parasite material should not be more than 10% of the total volume.) Parasite material was disrupted by re-suspension with a 1ml pipette and vortexed for 20 seconds (''), followed by 5' of lysis at RT. Chloroform (200 μ l) was added followed by vortexing for 20'' and incubated for 5' at RT. The sample was centrifuged at 12000g for 15min at 4°C and the upper water phase was transferred to a new tube. For precipitation of the RNA, 0.7 Vol% Isopropanol was added and the tube was placed at -20°C for at least 2 hours (h) or overnight (O/N). Additional salts like the frequently used 10 Vol% of 2M sodium acetate 5.2 pH were not utilised based upon the already high salt concentration of TRIzol[®]. Nucleic acids were pelleted by centrifugation at 12000g for 10min at 4°C, the supernatant was removed and the pellet was washed with ice-cold 70% ethanol. An additional centrifugation step at 12000g for 5min at 4°C followed, whereby the supernatant was removed and the pellet was air-dried. The pellet was dissolved in DMPC treated water and the concentration was determined photometrically at the NanoDrop 1000. The quality of the RNA was analysed by an RNA-agarose gel. RNA was stored at -80°C or subsequently reverse transcribed into cDNA.

4.2.1.3 DNase treatment of isolated total RNA

To remove co-precipitated genomic DNA from isolated total RNA samples, RNA was treated according to the commercial available protocol of RQ1 RNase-Free DNase (Cat.# M6101) from Promega. RQ1 DNase was heat inactivated for 10' at 65°C. A second phenol-chloroform extraction was not carried out.

4.2.1.4 Reverse transcription of RNA into cDNA

Reverse transcription of RNA was carried out using PrimeScript™ Reverse Transcriptase from Takara (2680A, Clontech) or SuperScript® III Reverse Transcriptase from Life-technologies (18080044, Invitrogen). In both cases, the manufactures recommendation formula was used to reverse transcribe 1-2µg of total RNA. In addition to the reverse transcription protocol, 1µl of a recombinant ribonuclease inhibitor (10777-019, RNaseOUT™) from Life-technologies was added to the reaction. For all cDNA synthesis, the same oligo-dT-primer was used (AKO-cDNA) for 1h at 42°C of reverse transcription.

4.2.1.5 Isolation and preparation of DNA from metacestode vesicles of *E. multilocularis*

Genomic DNA was isolated from metacestode vesicles (isolate H95). Metacestode vesicles were disrupted by pipetting and intensively washed with 1x PBS to remove the hydatid fluid. The metacestode vesicles were pelleted by centrifugation for 10' at 5000g at RT. The supernatant was removed and the pellet was re-suspended in lysis buffer (100mM NaCl, 10mM Tris-HCL, pH 8.0, 50mM EDTA pH 8.0, 0.5 % SDS, 20 µg/ml RNase A; 1.2 ml/100mg pellet) supplemented with 0.1 mg/ml Proteinases K. To ensure a complete digestion of the metacestode vesicles an O/N incubation at 50°C was completed. On the following day, a phenol-chloroform extraction was performed followed by ethanol precipitation to concentrate the DNA (the exact protocol was established by Markus Spiliotis and includes the following steps), Briefly, an equal amount of phenol-chloroform-isoamyl-alcohol (25:24:1) was added to the O/N treated sample solution. After centrifugation for 25' at 2000g at RT, the upper aqueous phase was transferred into a new tube. This step was executed two times to ensure the remove of protein digestion products. The DNA was precipitated by adding of 0.1 Vol% of LiCl (stock 5M; pH 4.5) and 2 Vol% of 96% ethanol followed by incubation O/N at -20°C. On the following day, a centrifugation step for 30' at 20000g at 4°C was carried out. The supernatant was removed and the pellet was washed with 70% ethanol followed by a second centrifugation step, the supernatant was removed and air-dried. The pellet was re-suspended in 1x TE buffer (10mM Tris, 1mM EDTA pH 8.0).

For concentration of DNA solutions (water based) 0.1 Vol% of the 3M sodium acetate pH 5.2 and 0.7 VOL% of isopropanol (98%) or 2.5 Vol% of ethanol (96%) were added. After mixing the samples were incubated O/N at -20°C. The DNA was pelleted by centrifugation at 12000g for 30min at 4°C. The supernatant was removed and the pellet washed with 70% of ice-cold ethanol. After a second centrifugation step for 5' at 12000g at 4°C, the supernatant was removed and the pellet was re-suspended in water or 1x TE buffer (10mM Tris, 1mM EDTA pH 8.0).

4.2.1.6 Amplification of DNA by DNA-Polymerase Chain Reaction (PCR)

All polymerase chain reactions were carried out with custom-made oligonucleotides from Sigma Aldrich (DNA oligos, PCR concentration 10µM) and included in the primer list (Tab. S1) in the supplemented material. The annealing temperature was estimated by the online software program

“Tm Calculator” on the New England Biolabs (NEB) webpage (<https://www.neb.com/tools-and-resources/interactive-tools/tm-calculator>). A calculation of the annealing temperature with the equation according to the Wallace rule $T_a [^{\circ}\text{C}] = 4x (\text{G+C}) + 2x (\text{A+T})$ was not undertaken. The elongation time (E_{time}) was calculated with 1kb/min for the *Taq* DNA-Polymerase (NEB) with an elongation temperature (E_{temp}) of 72°C. For the proof reading KOD Hot Start DNA-Polymerase (Novagen) an E_{time} of 3kb/min with an E_{temp} of 70°C was used. PCR amplification was carried out to the manufacture protocol for both DNA-Polymerases (initial denaturation = ID; primer annealing time = AT; elongation time = E_{time} ; final elongation = FE). To increase the primer specificity to a total PCR volume (50µl) 1µl MgCl₂ (25mM) or MgSO₄ (25mM) was added additionally to the reaction in the case of the *Taq* DNA-Polymerase (NEB).

4.2.1.7 Purification of DNA from Agarose gels or enzymatic modifications of *in vitro* reactions

Agarose gels were used to separate enzymatic digested plasmids or PCR amplified DNA fragments by size under usage of electrophoresis. DNA bands of interested were excised and purified with the commercial available NucleoSpin[®] Gel and PCR Clean-up kit (Macherey-Nagel; REF 740609.250). DNA samples that were enzymatic modified (e.g. restriction digest, poly-A-tailing, alkaline phosphatases treatment) *in vitro* have been purified with the same kit. In both cases, the manufacturer’s instruction were followed.

4.2.1.8 Isolation of plasmid DNA from *Escherichia coli*

The isolation of plasmid DNA from *E.coli* stains was performed with the NucleoSpin[®] Plasmid Kit (Macherey–Nagel; REF 740588.250). A 5 ml O/N bacterial (LB Media, with antibiotic resistance) culture was inoculated with the bacterial stain of interest and 4ml of the O/N culture was used for DNA-plasmid isolation.

4.2.1.9 Sequencing of plasmids

Isolated plasmids were sequenced by the company “Gesellschaft für Analyse-Technik und Consulting” (GATC in Konstanz, Germany). According to the company protocol for isolated DNA (plasmid 300ng-500ng; PCR product 200ng-300ng), 1µl of sequencing-primer (10µM) was added to the DNA in a final volume of 10µl.

4.2.1.10 Semi-quantitative reverse transcribed polymerase chain reaction (RT-PCR)

Total RNA was isolated from parasite material according to the isolation protocol for total RNA. Metacestode vesicles, primary cells of day 2, day 5 and day 11 isolated from metacestode vesicles as well as non-activated and *in vitro* activated protoscoleces obtained from gerbil material was used. Isolated RNA was DNase treated (RQ1 RNase-free DNase, Promega) followed by phenol-chloroform extraction. RNA concentration was quantified spectrophotometrically and 750 ng of each

stage were used for reverse transcription (RT) and used as a template for gene-specific PCR. Intron-flanking, gene-specific primers were used to estimate the *semi*-quantitative expression profile by PCR employing a protocol of 32 cycles. The constitutively expressed gene *elp* (Primer AKO-36, AKO-037) served as a quantitative control.

4.2.1.11 Colony PCR

To prove the integration of amplified DNA fragment into the multiple cloning sites (MCS) of corresponding target plasmids, a colony PCR was carried out. A gene and a plasmid specific primer was selected and used for PCR with *Taq* DNA-Polymerase (NEB). A bacterial colony was picked from a PCR-tip and suspended in 30µl of sterile water. For PCR, 3µl of this bacteria-suspension were used under standard conditions for *Taq* DNA-Polymerase. The initial denaturation step of the PCR cycle programme was extended for 5' to disrupt the bacterial cells. Bacterial colonies showing the right amplified PCR fragment size were used for a bacterial O/N culture followed by plasmid isolation.

4.2.1.12 Agarose gel electrophoresis

Separation of PCR amplified DNA products were carried out by agarose gel electrophoresis. Depending on the size of the DNA fragments, different concentrations of agarose were dissolved in 1x TAE Buffer (40mM Tris, 1mM EDTA, pH 8.0, 0.11% glacial acetic acid in 1liter of H₂O, pH 8.5) and stored until use at 55°C. For the separation of DNA fragments larger than 4 kilo bases (kb), an agarose concentration of 0.7% was chosen. For DNA fragments in size of 0.2 to 7kb an agarose concentration of 1% was used. DNA fragments shorter than 0.5kb have been separated in 1.5% or 2% agarose gels. The overlapping DNA fragment size to the chosen agarose concentration is not strict and also depends on the biological question to be addressed. Agarose gels have been poured into a horizontal gel sleigh with loading wells left by a fitting comb. The DNA samples were mixed with 6x loading buffer, for agarose gels (0.25% bromophenol blue, 0.25% xylene cyanol, 40% saccharose and 30% glycerol) and separated at a voltage of 80-140 volts for 20 to 45min. Visual observation of the electrophoretic separation was recognised by the two dyes bromophenol blue and xylene cyanol of the loading buffer. In a 1% agarose gel, the bromophenol blue band and the xylene cyanol dye correspond to a 0.3 kb and a 3kb DNA fragment. Ethidium bromid (EtBr) was used to stain separated DNA fragments; therefore, EtBr (0.2 mg/ml in 1xTAE) was dissolved and the agarose gel was incubated for 15min at RT. For visualisation of DNA fragments, UV light was used. In all agarose gels, a size marker was used to determine the size of the separated DNA fragment (SmartLadder, Eurogentec). In case of the electrophoretic separation of RNA in agarose gels, all materials used were treated with 2% peroxide solution (H₂O₂, 32% VOL) for at least 30', followed by intensive washing with sterile water.

4.2.1.13 Addition of 3' Adenosine overhang on PCR amplified DNA fragments (TOPO TA cloning)

The *Taq* DNA-Polymerase automatically adds at the 3'-end of a PCR product an additional adenosine. This property can be used to clone the amplified DNA fragment into a plasmid supporting this so-called TA cloning. The plasmid "pDrive" (Qiagen) is a linearised plasmid with a tyrosine at its 5'-end. The insert (DNA) and linearised plasmid were incubated following the manufactures instruction. Ligated plasmid was transformed into competent bacterial cells (*E.coli* TOP10). Selection of bacterial colonies was conducted by blue-white screen (X-Gal) and colony PCR.

4.2.1.14 Bioinformatical and statistical analysis

The *E. multilocularis* genome sequence assembly was used as available in GeneDB (<http://www.genedb.org/Homepage/Emultilocularis>). In addition to the basic local alignment search tool (BLAST) of GeneDB, the National Center for Biotechnology Information (NCBI) BLAST programme was used for amino acid comparisons (<http://blast.ncbi.nlm.nih.gov/Blast.cgi>). Amino acid sequence and domain predictions were carried out using UniProt (<http://www.uniprot.org/>) and SMART (<http://smart.embl-heidelberg.de/>) software. Based upon the genomic sequence information, primers were designed to amplify the full coding sequence. Amino acid alignments were constructed with the programmes CLUSTA W(2) and MUSCEL, integrated in the software BioEdit (Version 7.1.11). Modification of the alignments - if needed - were carried out manually.

All experiments were performed with at least three technical and biological replicates. Linear regression analysis was carried out using Microsoft Excel-2007. Error bars in figures represent standard deviation. Differences were considered significant for p-values below 0.05 (indicated by (*)), for p-values between 0.001 and 0.01 (**), and for $p < 0.001$ (***). For $p > 0.5$, differences were considered non-significant.

4.2.1.15 Modification/restriction digests of DNA plasmids or amplified DNA fragments

Restriction digest and modifications of purified or amplified DNA fragments was carried out with enzymes purchased from NEB. Re-ligation of plasmids was avoided by dephosphorylation of the plasmid by CIP- or antarctic phosphatase from NEB. All enzymes were used according to the manufactures recommendations. Restriction digests were carried out for 2h and CIP or antarctic phosphatase treatment for 45' at 37°C.

4.2.1.16 Ligation of DNA fragments into plasmids

DNA fragments from plasmid or PCR amplification with or without restriction digest were ligated with T4 DNA-Ligase (NEB). The ligation reaction was incubated O/N at 16°C. In case of blunt-end ligation of DNA fragments, the pJET1.2 CloneJET (Thermo Scientific) was used according to the manufactures instructions (20' at RT). The (molar) concentration of the DNA was calculated as follow

(ngInsert = [(ngVector x kbInsert)/(kb Vector) x Ratio]. For all ligations, a ratio of 3:1 - 5:1 of DNA insert to vector was used.

4.2.2 Working with bacteria

4.2.2.1 Bacteria strains and media used in this study

<i>E. coli</i> DH5 α	Invitrogen	F- Φ 80 <i>lacZ</i> Δ M15 Δ (<i>lacIZY-argF</i>) U169 <i>recA1 endA1 hsdR17</i> (<i>r_K, m_K</i>) <i>phoA supE44 thi-1λ gyrA96 relA1 tonA</i>
<i>E. coli</i> TOP10	Invitrogen	F- <i>mcrA</i> Δ (<i>mrr-hsdRMS-mcrBC</i>) Φ 80 <i>lacZ</i> Δ M15 Δ <i>lacX74 recA1 araD139</i> Δ (<i>ara-leu</i>)7697 <i>galU galK rpsL</i> (Str _R) <i>endAI nupG</i>
<i>E. coli</i> BL21	Amersham	B F ⁻ , <i>ompT, hsdS</i> (<i>r_B, m_B</i>), <i>gal, dcm</i>

4.2.2.2 Media for bacteria culture

Luria-Broth (LB)	Invitrogen	
LB agar plates	Invitrogen	LB medium with 1.5% Bacto-Agar
SOC Media	Invitrogen	

All bacterial strains were grown on LB agar plates or in liquid culture under shaking conditions (225rpm) at 37°C. Bacterial culture media or agar plates were supplemented with antibiotics dependent on the transformed plasmid resistance (Ampicillin Amp^R (Amp^R 100 μ g/ml) Kanamycin Km^R (Km^R 50 μ g/ml) or Chloramphenicol Cm^R (Cm^R 50 μ g/ml)).

4.2.2.3 Overnight culture of bacterial cultures

Bacterial strains were on LB agar plates plated O/N and incubated at 37°C supplemented with antibiotics. A single bacterial colony was picked with a sterile plastic tip and a 5ml LB-liquid culture supplemented with antibiotic was inoculated and grown O/N under shaking conditions (225rpm) at 37°C.

4.2.2.4 Bacterial liquid cultures of *E. coli*

All bacterial liquid cultures were incubated at 37°C under shaking conditions of 225rpm. The culturing flask was chosen whereby one-fifth of the total volume was filled with LB media. Bacterial cultures were inoculated from O/N culture. For expression of proteins, a special flask "Schikanekolben" (DURAN^R) was chosen, namely an Erlenmeyer flask with four baffles on the bottom to interrupt the laminar flow to create a turbulent flow.

4.2.2.5 Chemical competent bacterial cells (*E. coli*)

Uptake of extracellular DNA is a natural property of bacterial strains. An increase of DNA uptake could be observed by treatment of bacteria with calcium chloride (CaCl₂) generating competent cells. Bacterial strains TOP10 or BL21 were treated as follows to make them chemically competent. A bacterial O/N culture of 1ml was inoculated and grown at 37°C and 225rpm. The O/N culture was transferred into 50ml of fresh LB media and further grown at 37°C and 225rpm until the OD₆₀₀ of 0.5 - 0.7 was reached (~ 2-3 h). The bacteria were pelleted by centrifugation for 10' at 500g at 4°C. The supernatant was discarded and the pellet was re-suspended in 12ml of ice cold 100mM CaCl₂ and centrifuged. The supernatant was discarded and the pellet was carefully re-suspended in 1ml of fresh 100mM CaCl₂ and incubated on ice for up to one hour. Glycerol (86%) was added in a final concentration of 20%. The bacteria were frozen on dry ice in aliquots of 50µl and stored at -80°C until use.

4.2.2.6 Transformation of *E. coli*

An aliquot of competent bacterial cells were thawed on ice and 5-10µl of ligated plasmid was added. The transformation reactions were incubated for 45' on ice, followed by a heat shock of 90'' at 42°C and additional cooling on ice for 2'. In case of plasmid born antibiotic resistance with Cm^R or Km^R to 250µl of SOC or LB media was added to the transformation suspension and the reaction was incubated at 37°C under shaking (225rpm) conditions for 2h. During this incubation time, the antibiotic resistance develops. Incubation in SOC or LB Media for by Amp^R resistance is not necessary based upon the fact that Amp^R only acts bacteriostatic and not bactericidal like Km^R or Cm^R. The bacteria were centrifuged at 500g for 3' at RT. 150µl of the supernatant was discarded, the bacterial pellet was re-suspended and the suspension was plated on LB agar plates supplemented with the antibiotic resistance. LB agar plates were incubated over night at 37°C. In case of the vector pDrive (Qiagen) 40µl of X-Gal (40mg/ml) in DMSF) was plated additionally before plating the bacterial suspension.

4.2.2.7 Dimethyl sulfoxide (DMSO) bacterial stocks (at -80°C)

Bacterial strains with proofed sequences of plasmids were stored in DMSO-stocks at -80°C in cryo-caps. DMSO-stocks were made by 90%Vol (0.9 ml) of a bacterial O/N culture and 10%Vol (0.1 ml) of DMSO. The DMSO stock was frozen immediately at -80°C. For inoculation of a bacterial culture of a strain or for streaking on a LB agar plate, a small portion was scraped of the frozen culture.

4.2.3 Working with eukaryotic cell lines

4.2.3.1 *Echinococcus multilocularis* media used in the *in vivo* and *in vitro* cell culture

Media and solutions	Preparation
Culture medium	DMEM, 10% FCS, 1% PST, 4µl Levofloxacin (Tavanic) or Ciprofloxacin.
A4 media	Pre-incubation of 100ml culture medium for 7 days with 10^6 Rh ⁻ cells, sterile filtration and stored at -20°C until use.
B2 media	Pre-incubation of 100ml culture medium for 3 days with 2×10^7 Rh ⁻ cells, sterile filtration and stored at -20°C until use.
cMEM	Undefined conditioned medium (sterile filtered supernatant of Rh ⁻ cells from co-culture.
Reducing agents	100µM L-Cysteine, 10µM Bathocuproine disulfonic acid, 0.01% β-mercaptoethanol.

4.2.3.2 Cultivation of feeder cells

For *in vitro* cultivation of metacestode vesicles, feeder cells are necessary. Based upon several tests with different cell lines, the cell line of Reuber hepatoma cells (Rh⁻; ATCC No.: CRL-1600) was selected. The cells were cultivated in 50ml of culture media in a 75cm² cell culture flasks and trypsinised once a week. After trypsinisation, the cells were counted with a Neubauer camber and 10^6 cells were seeded in fresh media. Cells were cultivated at 37°C and 5% CO₂ atmosphere with saturated humidity.

4.2.3.3 Isolation and maintenance of *in vivo* parasitic material from Mongolian jirds

The long-term maintenance of *E. multilocularis* metacestode is ensured by the repeated passages in the peritoneum of laboratory animals. Therefore, Mongolian jirds (*Meriones unguiculatus*) were infected with homogenised larval material of a single isolate by intraperitoneal injection to develop, secondary AE. Animals selected for this procedure were about three months old. By successful infection of *E. multilocularis* into the jirds secondary AE developed after approximately two-to-three months. Isolate-specific characteristics of parasite material concerning the growth time and tissue material features could be drawn. Animals were scarified with CO₂ and the parasite material was isolated under sterile conditions. Jirds were intensively washed with 70%Vol ethanol before parasite material was isolated. The isolated parasite tissue was cut into small pieces (0.5-1cm slices) and subsequently strained through a metallic tea sieve. The ground material was subsequently washed at least three times with sterile 1x PBS to remove host cells (blood cells). (At this point, different ways depending of the following experiments were able to choose.) The isolation of protoscolecocytes from smashed parasite material is described in chapter 4.2.3.6. For reinfection of jirds with parasitic material, the isolated material was incubated O/N at 4°C supplemented with Ciprofloxacin (5µl/ml) and Penicillin G/Streptomycin (10µl/ml). Parasitic material was washed with 1x

PBS the following day and syringes for reinfection of jirds were prepared (0.3-0.5ml/jird). Furthermore, the treated parasite material was used to set up new *in vitro* cell culture of metacestode larvae described in chapter 4.2.3.4.

4.2.3.4 *In vitro* cultivation of *Echinococcus multilocularis*

Isolated homogenised parasitic material was treated O/N with antibiotic as described in chapter 4.2.3.3. After intensive washing (3x) with 1x PBS, 1ml of parasitic material was used to set up a new 50ml co-culture. As previous described, no additional passing through a plastic tea sieve was carried out. The co-culture was supplemented with freshly trypsinised Rh⁻ feeder cells (10⁷). Media was changed weekly and new Rh⁻ cells were added during each change. The parasitic material was passaged after reaching a certain number as per “reference” [113]. Parasite cells were cultivated at 37°C and 5% CO₂ atmosphere with saturated humidity.

4.2.3.5 Axenic culture of metacestode vesicles of *E. multilocularis*

Study cell type specific effects require the independence of possible side-effects reaching from other cell types. Rh⁻ cell of the co-culture have to be removed by incubation under axenic conditions. Co-cultured metacestode vesicles were removed from supernatant and intensive washed with 1x PBS and carefully transferred into a new culture flask (75cm²). Pre-conditioned media (cMEM, A4, B2) with reducing agents was added and the atmosphere was changed to a nitrogen atmosphere. The lid of the bottle was always closed for cultivation under axenic conditions. Parasitic cells were incubated for 2-3 days at 37°C until use.

4.2.3.6 Isolation and activation of protoscoleces

Parasitic material was isolated from jirds as described in chapter 4.2.3.3. The material was transferred into a 50ml tube and diluted with 1x PBS to obtain a 1:4 suspensions and vigorously shaken for 10' to release the protoscoleces from the metacestode material. To isolate the protoscoleces from the rest of the parasitic material, the suspension was filtered by sieving through polyester gauze (pore size 150µm). The flow through was filtered by a second finer polyester gauze (pore size 30µm). The protoscoleces were collected on the top of the filter and transferred into a Petri dish (10cm). By horizontal-circular-rotation, of the Petri dish the protoscoleces were gathered in the middle. Protoscoleces were transferred into a 2ml tube for further applications. The residual white shadow on the ground of the Petri dish a calcium bodies with are separated from the protoscoleces by this method.

For activation of the protoscoleces (1ml) the gastrointestinal passage was mimicked by adding of 0.05% pepsin in DMEM (30ml) without FCS at pH 2 (200µl of 25% HCl). The tube was incubated for 30' at 37°C under shaking conditions (125rpm). The protoscoleces were washed with 1x PBS to remove the acid condition and stop the treatment with pepsin. The supernatant was decanted from the sediment protoscoleces and 30ml of 0.2% sodium taurocholate in DMEM without FCS was added. The

protoscoleces were further incubated for 3h at 37°C under shaking conditions (125rpm). Finally the protoscoleces were washed with 1x PBS and subsequently used for further experiments, like isolation of total RNA or setting up an *in vitro* culture.

4.2.3.7 Cultivation of protoscoleces and live-dead staining

Protoscoleces isolated from jirds were cultivated in A4-media under axenic conditions independent of an activation treatment. In a 12-well plate, approximately 200-400 protoscoleces were seeded. To observe the viability of protoscoleces especially after inhibitor treatment, a live-dead staining was carried out. Protoscoleces of one well were transferred into a 1.5ml tube washed with 1x PBS and stained with 0.03% of methylene blue (in 1x PBS). After 1' of incubation at RT, the staining was stopped by three washing steps with 1x PBS. The protoscoleces were diluted 1:10 with 1x PBS and 100µl of the suspension was transferred on a cover side. Microscopic pictures of the protoscoleces were taken randomly and the live-to-dead ratio was counted by eye. Dead protoscoleces appeared blue, while healthy protoscoleces were not stained.

4.2.3.8 Isolation and cultivation of primary cells from metacestode vesicles

Metacestode vesicles that were co-cultivated for more than three months and showed a milky-white appearance with a thick laminar layer were transferred into a fresh culture flask and axenised for three days. After intensive washing with 1x PBS the metacestode vesicles were transferred into a 50ml tube and destroyed by pipetting with a 10ml pipette. To remove the hydatid fluid the destroyed metacestode vesicles were sediment by gravity and the supernatant was decanted. Metacestode vesicles were pelleted by centrifugation for 3' at 600g at 4°C. The supernatant was removed and four volumes of trypsin (0.05% trypsin, 0.02% EDTA in PBS) were added. An incubation time of 25' at 37°C followed with a harsh shaking after 15min. After trypsinisation, the majority of metacestode vesicles were floating at the surface of the liquid (so-called "ghosts"). The suspensions was shaken vigorously again for 2min and directly filtered over a polyester gauze (pore size 150µm) on top of a glass breaker. The flow through was filtered by a second finer polyester gauze (pore size 30µm). The flow through was collected in a 50ml tube and centrifuged for 2' at 100g to remove the calcium bodies. The supernatant was transferred by decanting into a new 50ml tube. Primary cells were pelleted by centrifugation for 6' at 600g at 4°C. The pellet was re-suspended in a total volume of 2ml of pre-warmed A4 media. Subsequently, the cell density was measured at OD₆₀₀, whereby 12.5 µl of the isolated primary cells were diluted in 1ml 1x PBS. An OD₆₀₀ of 0.2 corresponds to 1Unit of primary cells [118, 119]. Ideal grow conditions were noticed with the following combinations of primary cells to chosen size of well and volume of A4-media. Primary cells were always cultivated under axenic conditions.

Plate (wells)	Units	A4-media (ml)
6	500	2-2.5
24	80-100	1.5-1.9
48	30-50	1-1.4
96	10-20	0.200-0.280

4.2.3.9 Treatment of metacystode vesicles, protoscoleces and primary cells with inhibitors

All experiments were performed using the isolate H95, Ingrid and GHO9 of *E. multilocularis*. Mongolian jirds (*Meriones unguiculatus*) were used for *in vivo* propagating of the parasite in the peritoneum as previously described by Siles-Lucas *et al.* 2002 [122]. Co-cultivation of parasite material *in vitro*, including metacystode vesicles and isolation of primary cells (stem cells), was carried out according to the protocol from Spiliotis *et al.* 2004 and 2008 [113, 118]. Metacystode vesicles than 4mm were axenised and protoscoleces and primary cells were isolated as described before. All experiments were performed under axenic conditions. In case of inhibitor treatment with metacystode vesicles, a 6-well plate was used and 5-10 vesicles were transferred by pipetting and 5ml of A4-media was added. All inhibitors were dissolved in DMSO in a 1000 fold higher concentrated as the final used concentration, e.g. to a 5ml culture volume, 5µl of inhibitor was added. The A4-media was changed every second day by pipetting and fresh pre-warmed media with the final concentration of inhibitor was added. In case of inhibitors test in non-activated protoscoleces a 24-well plate with 2ml of A4 media was used and an amount of 80% confluence in the well covered with protoscoleces was used. Inhibitors were added according the final concentration and media was changed every second day. Primary cells were isolated as described before and 50 Units (15000 cells /Units, *unpublished*) of isolated primary cells were seeded in a 48-well plate with 1.0-1.3 ml of conditioned A4-media. The A4-media was changed every second day and fresh inhibitor was added. All experiments were performed with technical and at least three biological replicates. In the case of protoscoleces and primary cells not the complete media could be removed, only 80%, based upon the biological fact that primary cells and protoscoleces are not adhered.

4.2.3.10 Resazurin assay for monitoring viability of primary cells

Resazurin (7-Hydroxy-3H-phenoxazin-3-one-10-oxide sodium salt) is a redox-sensitive dye that can be used for measuring the viability of living cells by absorbance or fluorescence of the cell culture media, without having a cell-toxic effect. We optimised the Resazurin assay for our cellular requirements based upon free online available protocols. Isolation of primary cells from metacystode vesicles was carried out according to the protocol described in detail in chapter 4.2.3.8. Overall, 10 units of primary cells were seeded per well in a 96-well plate and pre-conditioned media (DMEM with phenol red) with rat hepatoma cells (A4-media) was added to a final volume of 200µl. After 24 hours of pre-incubation under axenic conditions the formation of cellular aggregation was controlled by light microscopy and inhibitors of interest were added to the wells with a 1/1000 dilution (generating their final concentration). 1% Triton (X-100) was used as a cytotoxic control. After 48h of further incubation,

20 μ l (1/10 of Vol/%) of Resazurin (Stock solution 20mg/ml in 1xPBS at -20°C; Diluted in 1:100 with 1xPBS) was added with a final concentration of 0,018mg/ml to each well. The absorbance was measured at 570nm with a reference wavelength of 600nm (TECAN 2000 ELISA plate reader). The first measurement was directly taken after addition of the Resazurin solution (first measurement; zero hours) and after three hours of further incubation (final measurement).

4.2.3.11 Injection of metacestode vesicles

Metacestode vesicles were incubated under axenic conditions in A4-Media pre-conditioned media A4. All metacestode vesicles had a size of more than >0.5cm. After three days of axenic co-culture, metacestode vesicles were wash intensively with 1x PBS transferred to a 25cm² cell culture flask and further in A4-media in the presents of BI 2536 (50nM). Treatment of metacestode vesicles was stopped and vesicles were further incubated for five more days to remove the releasing inhibitor BI 2536. Metacestode vesicles were transferred into a 24 well plate (1MC/well) at day five of recovery. The metacestode vesicles were totally covered by A4-media. Primary cells were isolated according to the primary cell isolation protocol chapter 4.2.3.8. Primary cells were re-suspended in 2 ml of pre-warmed A4-media. For injection of primary cells into stem cell depleted metacestode vesicles, a 1ml tuberculin syringe with a fine cannula (Injection cannula, sterile 0.30 x 12mm BL/LB 30G x ½ “, Braun) was used. Injection was carried out in a 24 well plate including intact metacestode vesicle with covering media. Cannula was injected into metacestode vesicle with high sensitivity and with a soft tipping on the syringe. A volume of primary cells with A4 media that was injected into the metacestode vesicle could not be estimated. After injection, the cannula was removed with high sensitivity. Metacestode vesicles were further co-cultivated under axenic conditions. After five days of co-cultivation, an EdU pulse experiment was carried out (50 μ M) for five hours to invest the integration into the germinal layer and proliferation of stem cells. As a negative control, metacestode vesicles were treated with BI 2536 (50nM) for 21 days. Metacestode vesicles were injected with A4-media without primary cells, non- injected and/or primary cells were added to the A4-media without destroying the vesicle integrity. EdU staining was carried out according to the previous described protocol [32].

4.2.3.12 Labelling of proliferating cells in whole mount metacestode vesicles by EdU pulse staining

Proliferation of stem cells was investigated by staining of newly-synthesised DNA using the Click-iT[®] EdU cell proliferation assay (Invitrogen, C10337). Metacestode vesicles from hepatocyte co-culture were washed once with 1x PBS and carefully transferred into a 15 ml tube containing 3 ml A4-medium. A final concentration of 50 μ M EdU (Component A) was added and the metacestode vesicles and incubated for 5 h at 37°C (with gentle agitation every 20 min). For fixation, metacestode vesicles were transferred to a Petri dish and carefully opened with a syringe tip to remove hydatid fluid. After intense washing with 1x PBS, fixative (4% paraformaldehyde (PFA) in 1x PBS) was added and samples were incubated for 1 h at RT under shaking conditions. The samples were washed again (1x PBS) to remove the fixative, before being transferred to a 1.5 ml tube. The EdU labelling procedure

was carried out according to the manufacturer's instructions (Invitrogen, C10337), but with extended incubation times. Metacestode vesicles were finally analysed by fluorescence microscopy. For long-term treatment (21 days) with BI 2536, metacestode vesicles were cultivated in A4-medium for 21 days with inhibitor (medium and inhibitor changed every second day), followed by three days recovery without treatment. As a control, a medium with an identical amount of DMSO (without inhibitor) was used. Randomly chosen metacestode vesicles ($t = 4$) were isolated and EdU stained as outlined above. For each metacestode vesicle, three randomly chosen sections of the GL were analysed by microscopy and EdU positive cells were counted. The number of EdU positive cells was calculated to cells per mm^2 of the GL. For short-time inhibitor experiments, metacestode vesicles were treated *in vitro* for 24, 48 and 72 hours with 50 nM or 100 nM BI 2536, followed by 24 h regeneration without inhibitor. EdU staining and the calculation of Edu positive cells per mm^2 of GL were subsequently performed as described above.

4.2.3.13 *In situ* hybridisation of metacestode vesicles

Metacestode vesicles of GH09 with brood chambers were used for *in situ* hybridisation according to Koziol *et al.* (2013) [47]. A 1.3 kb long sequence of EmPlk1 was sub-cloned into pDrive cloning vector (Qiagen) using AKO-55 (CTCTCATGGAACTGCATAAGAG) and AKO-60 (CGATCTATCATATCGTAGGCG). Digoxigenin-labelled antisense and sense RNA was *in vitro* transcribed using T7 or SP6 promotor of the linearised vector.

5. Results

5.1. Cloning and characterisation of the Polo-like kinase 1 gene (*EmPlk1*) of *Echinococcus multilocularis*

In silico analysis by BLASTP genome sequence mining of the available genome data for *E. multilocularis* (<http://www.genedb.org/Homepage/Emultilocularis>), using the full-length amino acid sequence of the human Polo-like kinase 1 as a query, identified a single orthologous gene, *emplk1*, (EmuJ_000471700.1; *Echinococcus multilocularis* **P**olo-**l**ike **k**inase **1**, *EmPlk1*) encoding the protein EmPlk1 (e-value: $3.5e^{-161}$). A second hit in this BLASTP analyses, with much lower homologies (e-value: $6.2e^{-52}$) identified an ortholog of the human Polo-like kinase 4 encoding gene, *emplk4*, (EmuJ_000104700.1; *Echinococcus multilocularis* **P**olo-**l**ike **k**inase **4**, *emPlk4*) with, as in the case of human Plk4, only one predicted PBD. In both cases, iterative BLASP analyses using the deduced EmPlk1 and EmPlk4 amino acid sequences against the SWISSPROT database were carried out and confirmed highest homologies and similar domain structures of both proteins to human Plk1 and Plk4, respectively. Since currently available Polo-like kinase inhibitors are highly specific for Plk1, but not for Plk4, the *E. multilocularis* EmPlk4-encoding cDNA was cloned (ASS-057) and sequenced, but not further analysed in this thesis. The gene *emplk1* spans a genomic region of 3174bp and is located on chromosome 3 (supercontig pathogen_EMU_scaffold_007614: 4512575-4515749). Analyses of the *emplk1* exon-intron structure identified seven exons and six introns, which all displayed the canonical GT-AG dinucleotide sequences at the splice donor and splice acceptor sites, respectively (Fig. 5.3.1A) [129]. *Trans*-splicing or alternative splicing of *emplk1* transcripts were not observed by analysing available RNA-deep sequencing transcriptome data [60]. The full-length *emplk1* and *emplk4* cDNAs were cloned from isolated total RNA of metacestode vesicles (isolate H95) using an RT-PCR strategy. The total length of the *emplk1* open reading frame is 1833bp (cDNA; excluding poly-A tail), encoding a protein, EmPlk1, of 610 amino acids (aa) and a calculated molecular mass of 69.5 kDa. Analysis of the protein sequence by SMART software (<http://smart.embl-heidelberg.de/>) identified an N-terminal Ser/Thr protein kinase catalytic domain and a C-terminal protein binding domain (PBD), including two Polo boxes (PB), as shown in Fig. 3.5.2 and Fig. 5.1.2. The kinase domain of EmPlk1, spanning from aa-residue Tyr22 to Phe274, includes all invariable residues for protein kinases (Fig. 5.1.2) [66]. The amino acid sequence was further aligned using the Software MUSCLE (**M**U**l**tiple **S**equence **C**omparison by **L**og- **E**xpectation) and a phylogenetic tree was constructed following the instructions of Phylogeny.fr “One click” (<http://www.phylogeny.fr>) [130].

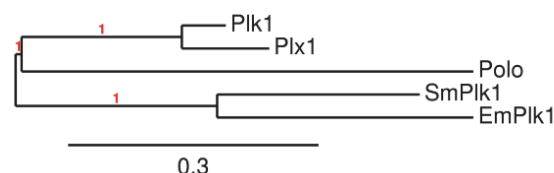


Figure 5.1.1 **Phylogenetic tree for Polo-like kinase 1 orthologs from different taxa.** Amino acid sequences of *Homo sapiens* Plk1, *Xenopus laevis* Plx1, *Drosophila melanogaster* Polo, *Schistosoma mansoni* Plk1 (SmPlk1) and the Polo-like kinase 1 of *Echinococcus multilocularis* (EmPlk1) were aligned and graphically represented in a phylogenetic tree, constructed by Phylogeny.fr. Correlations are indicated by numbers (1 = highly correlated, red) and the size of the line [131].

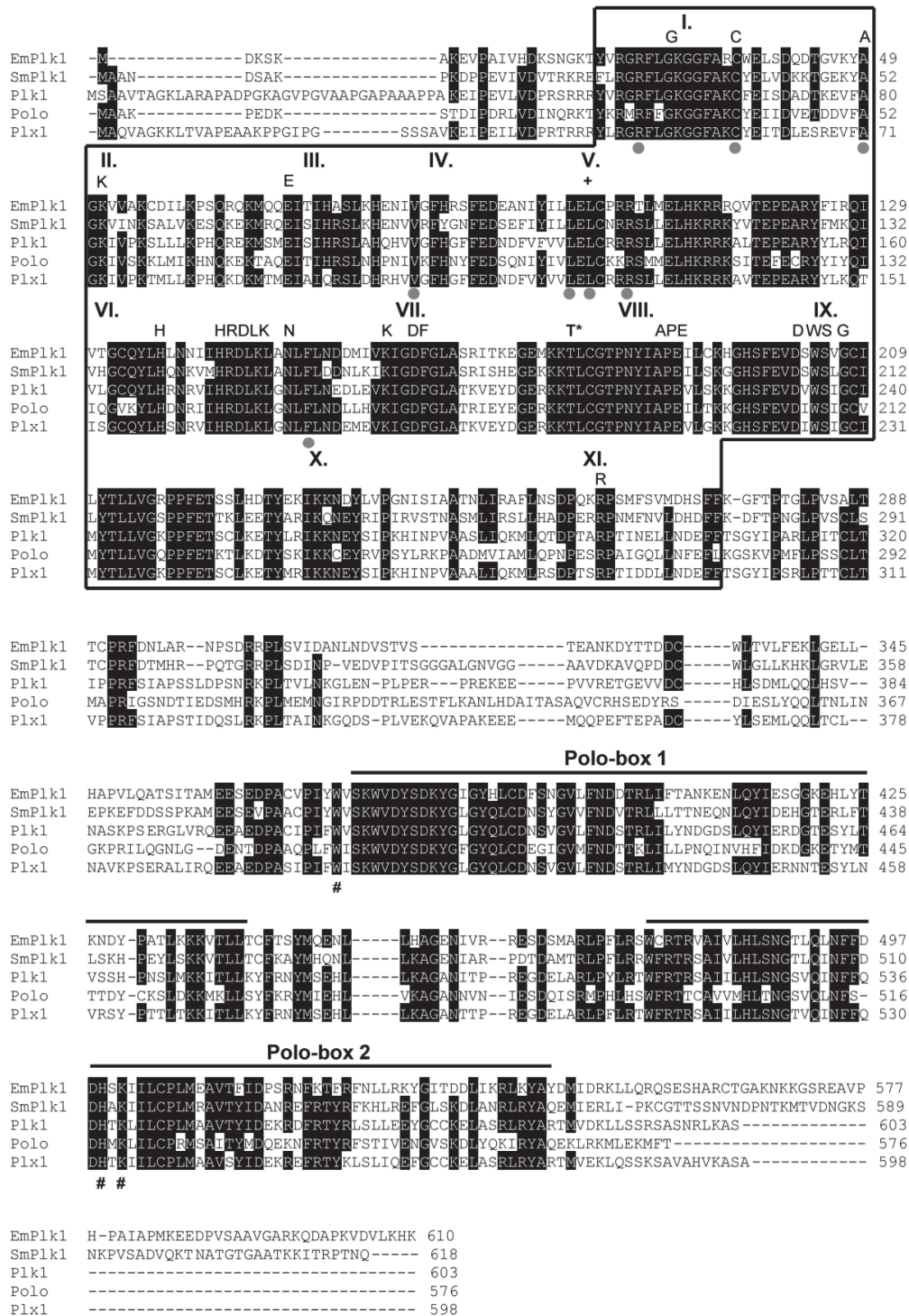


Figure 5.1.2 Structural features of EmPlk1. Multiple sequence alignment of Polo-like kinase 1 orthologs from different taxa, highlighting similarities in conserved protein regions. The orthologous kinases of *E. multilocularis* (EmPlk1; GenBank accession number: HG931729), *S. mansoni* (SmPlk1; AY747306), *Homo sapiens* (Plk1; P53350), *D. melanogaster* (Polo; P52304) and *X. laevis* (Plx1; P70032) are aligned. Identical aa residues are shown in white on black background and. Kinase domains including the 11 sub-domains of the kinases as defined by Hanks and Hunter (I-XI) [66] are boxed. The conserved threonine residue for activation of the kinase domain is marked by (T*) above the alignment. Residues for binding of phosphosubstrates in the PBD are marked by (#). BI 2536 interacting residues are indicated by grey dots.

A multiple sequence alignment of Plk1 like kinases of different organisms is shown in Fig. 5.1.2. The EmPlk1 kinase domain contains all 11 sub-domains (I-XI) that are characteristic of STKs as described by Hanks and Hunter [66]. Strong indicators for a STK kinase domain are particularly the amino acid sequence motifs HRDLKxxN and GTPNYIAPE, present in sub-domains VI and VIII. A third important and highly conserved motif in the kinase domain is the canonical GxGxxGxV motif for ATP binding. A characteristic variation of this motif is present in the Polo-like kinase family with the motif sequence GxGGFAXC (Fig 5.1.1). In mammals, activation of Plk1 during the cell cycle occurs in the activation loop (T-loop) with the major phosphorylation site at Threonine 210 (Thr²¹⁰) [80, 90]. A similar phosphorylation site was found in *S. mansoni* at the corresponding Threonine residue 182 (Thr¹⁸²) [102] and in *E. multilocularis* at Threonine 179 (Thr¹⁷⁹) of the kinase domain (Fig. 5.1.2.) [132]. Within the kinase domain, EmPlk1 displayed 68% amino acid sequence identity to *S. mansoni* SmPlk1, 62% to human Plk1, 60% to *D. melanogaster* Polo and 60% to *X. laevis* Plx1. Plk1 protein-protein interactions and cellular localisation during the cell cycle is regulated by the C-terminal domain of the enzyme and involves a non-conserved linker region between the kinase domain and the PBDs. The two C-terminal Polo boxes (PB1 & PB2) of all Plk1-like enzymes that form the so-called PBD are also present in EmPlk1 and cover the region from Tyr³⁷⁸-Thr⁴⁴¹ for PB1 and Cys⁴⁷⁶-Tyr⁵⁴⁵ for PB2. The three residues Trp³⁸⁸, His⁵¹² and Lys⁵¹⁴, which are involved in Plk1-binding to the phosphorylated substrate [81], are also highly conserved in EmPlk1 (Fig. 5.1.2) [67]. Overall, EmPlk1 displayed significant homologies of 57% to *S. mansoni* SmPlk1, 47% to human Plk1, 43% to *D. melanogaster* Polo and 46% to *X. laevis* Plx1. Taken together, these structural analyses identified EmPlk1 as a typical member of the Plk1 protein family.

5.2. Structural analyses concerning binding of the Plk1 inhibitors BI 2536 and BI 6727 to EmPlk1

In a previous study by Kothe *et al.* (2007) the crystal structure of the human Plk1 kinase domain together with bound inhibitor BI 2536 was analysed [95]. In this study, several important amino acid residues were identified that are essential for the binding of the drug. In addition to interacting amino acid residues involved in the binding process of the inhibitor, one essential determinant for inhibition of the kinase domain is the gatekeeper residue. The gatekeeper is often quite large and prevents large molecules from entering the site binding site in the kinase domain. In the human Plk1 enzyme, the gatekeeper is present at position 132 in the amino acid sequence and represented by Leucin (Leu¹³²). In direct comparison to other kinases of this protein family, this gatekeeper amino acid has a small amino acid side chain, which ensures the binding of BI 2536. The putative gatekeeper residue in EmPlk1 is also Leucine, at position 101 (Leu¹³²). Interacting residues for the binding of the drug, according to the previous study by Kothe *et al.* (2007), are marked by grey dots in the alignment in Fig. 5.2.1 [95]. Based upon the amino acid alignment in Fig. 5.1.2, a comparison of the interacting amino acid residues with Plk1 inhibitors BI 2536 and BI 6727 are summarised in Fig. 5.2.1.

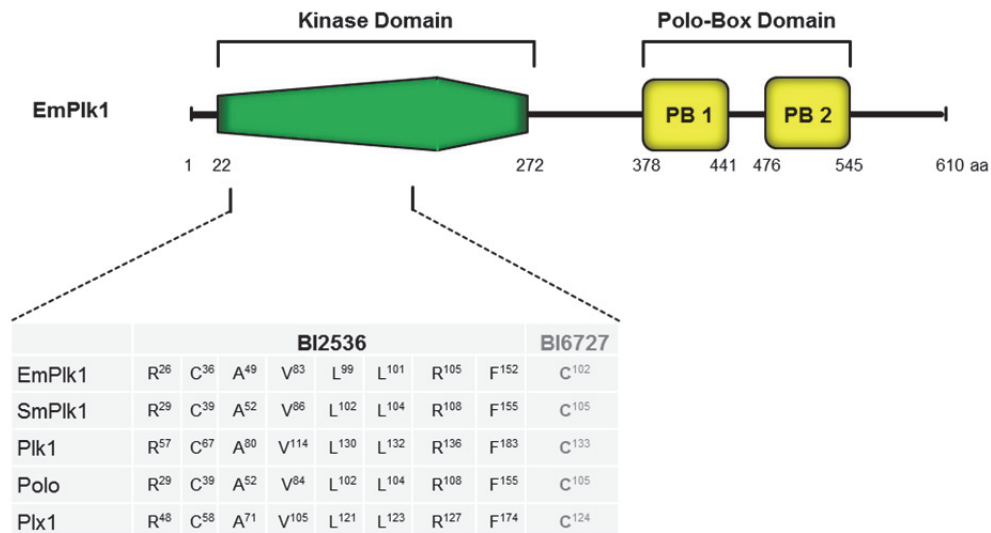


Figure 5.2.1 Schematic representation of the domain structure of EmPlk1 and amino acid residues for binding of the ATP competitive inhibitors BI 2536 and BI 6727. Amino acid sequences of Plk1-like enzymes were aligned from different taxa including *E. multilocularis* (EmPlk1; GenBank accession number: HG931729), *S. mansoni* (SmPlk1; AY747306), *Homo sapiens* (Plk1; P53350), *D. melanogaster* (Polo; P52304) and *X. laevis* (Plx1; P70032). Residues relevant for binding of the inhibitors BI 2536 and BI 6727 [95, 97] were identified and outlined in an extra table.

All amino acid residues important for binding of BI 2536 and BI 6727 to human Plk1 are highly conserved in EmPlk1 and in SmPlk1 of the related organism *S. mansoni*, for which a previous study has shown effective in vitro inhibition at micro-molar concentrations [102]. Based upon these results it was expected that BI 2536 and BI 6727 also exhibit inhibitory activities against EmPlk1.

5.3 Expression of EmPlk1 in *E. multilocularis* larval stages

After the identification of a Plk1-like enzyme in the kinome of *E. multilocularis*, the expression profile of *emplk1* in *Echinococcus* larvae was investigated. To this end, RNA-deep sequencing transcriptome data, obtained through the recently published *E. multilocularis* genome sequencing project [60] were used. The *emplk1* expression profiles for primary cells after 2 and 11 days of development, as well as protoscoleces before and after activation by pepsin/low pH and metacystode vesicles from *in vitro* cell culture are shown in Fig. 5.3.1C. Relatively high expression in primary cell culture after day 2 and day 11, and a basal expression pattern in the activated/dormant protoscoleces and metacystode vesicles were observed. Since primary cell cultures are strongly enriched in parasite germinative (stem) cells when compared to metacystode vesicles and protoscoleces [32], these data indicated a stem cell-specific expression of *emplk1*.

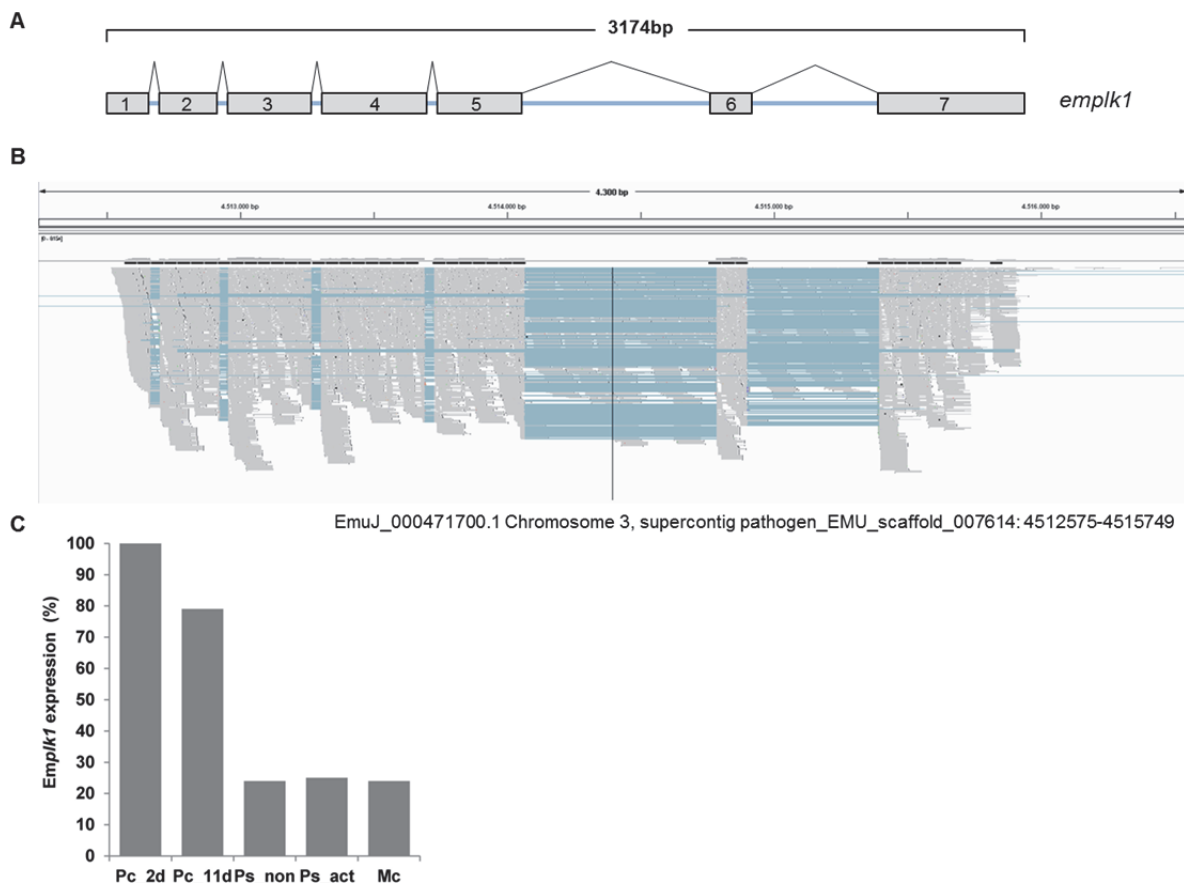


Figure 5.3.1 Expression of *EmPlk1* in *E. multilocularis* larval stages as assessed by RNA-Seq. (A) Exon- intron structure of *emplk1*, spanning a genomic region of 3174bp. The exons (grey) and introns (blue) are matched to the RNA-deep sequencing transcriptome data according to the colours (B). Illumina read profile for *emplk1* (merge of all libraries analysed). (C) Larval stage expression profile for primary cells of day 2 (Pc_2d) and day 11 (Pc_11d), activated and dormant protoscoleces (Ps_non and Ps_act) and metacystode vesicles (Mc). Note that Illumina sequencing has been performed only once for each sample.

Based upon the fact that the Illumina sequencing results shown above are based upon only one dataset, the results were validated by semi-quantitative reverse transcription polymerase chain reaction (RT-PCR). Total RNA was isolated from primary cells from cultures after day 2, day 5, and day 11 of development, as well as from activated and dormant protoscoleces and metacystode vesicles. Serial 10-fold dilutions of reverse transcribed RNA (cDNA) were subjected to *emplk1* gene-specific PCR. All larval stages clearly expressed *emplk1*, which was higher expressed in primary cells, in accordance with the expression profile obtained by RNA-Sequencing (Fig. 5.3.2).

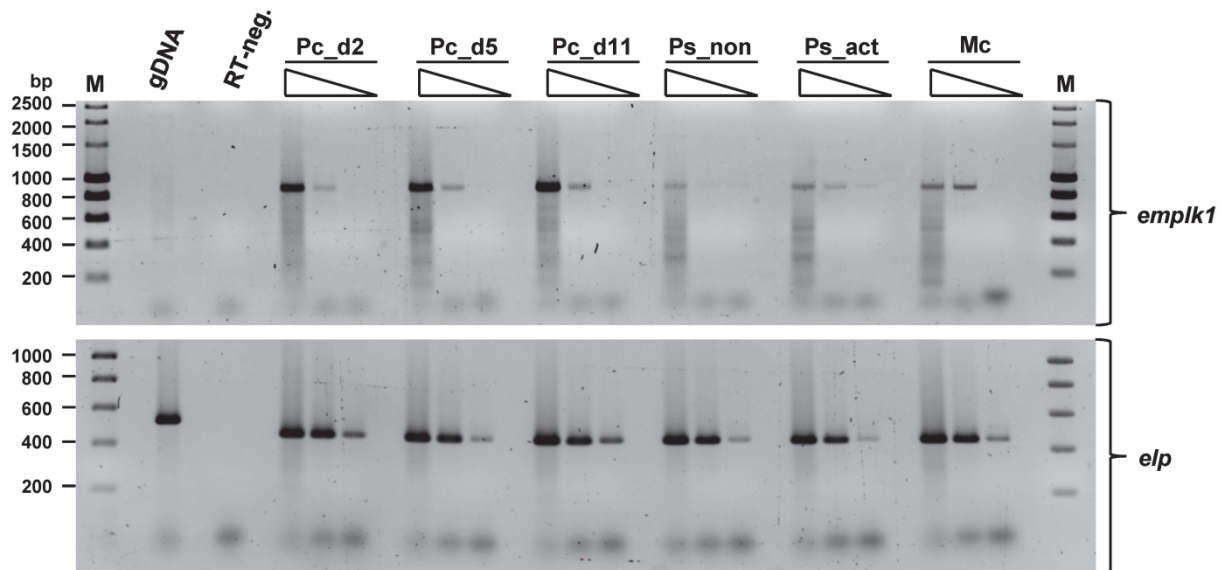


Figure 5.3.2 Expression profile of *emplk1* in *E. multilocularis* larval stages. Total RNA was isolated from primary cell cultures (Pc) from day 2, 5 and 11 (d2, d5, d11), dormant (Ps_non), and activated protoscoleces (Ps_act), as well as *in vitro* cultivated metacystode vesicles (Mc). Equal amounts of isolated RNA were reverse transcribed to cDNA and subjected to gene-specific (RT)-PCR for *emplk1*. The house keeping gene *elp* [133] was used for normalisation. The generated cDNA was 10-fold diluted in 1, 1:10 and 1:100 for PCR. Genomic DNA (gDNA) served as a positive control and purity of DNA contamination during RNA isolation. Non-reverse transcribed RNA was used as a purity control for DNA contamination during RNA isolation. Marker sizes are indicated on the left. (1,5% Agarose; EtBr stained).

Taken together, the RT-PCR experiments verified the prominent expression of *emplk1* in *in vitro* cultivated primary cells, which again indicated the possibility of a stem cell-specific expression pattern of *emplk1*.

5.4. Expression of EmPlk1 in the heterologous *Xenopus* oocytes system triggers germinal vesicle breakdown (GVBD), which can be blocked by the Plk1 inhibitor BI 2536 and BI 6727

The *Xenopus* oocyte system has frequently been used for studying enzymatic activities of heterologously expressed protein kinases [102]. In a previous study, Long *et al.* (2010) analysed the functions of the Plk1-like enzyme of *S. mansoni* with this system, using active, inactivated and dead kinase mutant forms of SmPlk1 [102]. In the present work, similar studies were carried out with EmPlk1. In addition to wild type EmPlk1 (EmPlk1^{WT}), an activated (mutant) version (EmPlk1^{T179D}) was generated by replacing Thr-179 through phosphomimetic Asp. An inactivated version was created by replacing Thr-179 by Val (EmPlk1^{T179V}) and two “kinase dead” versions of EmPlk1^{WT} and EmPlk1^{T179D} were generated by replacing the D₁₆₃FG motif of the active loop through D₁₆₃SV₁₆₅, yielding versions wt^{KD} and T₁₇₉D^{KD}, respectively. As shown in Tab. 5.4.1, expression of EmPlk1^{WT} and the inactive version EmPlk1^{T179V} in *Xenopus* oocytes did not induce GVBD, which was only observed with the activated form EmPlk1^{T179D} in a similar way as through the natural stimulating factor progesterone (PG). The kinase dead versions of the enzyme, wt^{KD} and T₁₇₉D^{KD} only induced a low basal activation.

Table 5.4.1 *Xenopus* oocytes serving as a heterologous system for the expression of EmPlk1. Microinjection of *in vitro* transcribed RNA constructs of wild type (EmPlk1^{WT}) and mutant forms (EmPlk1^{T179D}, constitutively active; EmPlk1^{T179V}, non-active; wt^{KD}, T₁₇₉D^{KD}, kinase dead mutants) of EmPlk1 were expressed in *Xenopus* oocytes. Progesterone (PG) served as a natural inducer (positive control) for G2/M transition and induction of germinal vesicle breakdown (GVBD). Overall, 20 oocytes per setting were used. Germinal vesicle breakdown (GVBD) assays were performed in the presence of different concentrations of BI 2536 as indicated to the left. Listed are the percentages of *Xenopus* oocytes that underwent GVBD in the different experimental settings (mean of three independent experiments). ‘-’ indicates that this condition has not been tested.

BI 2536	PG	EmPlk1 (wt)	T ₁₇₉ D	T ₁₇₉ V	EmPlk1 (wt ^{KD})	T ₁₇₉ D ^{KD}
0nM	90	0	90	0	0	10
1nM	-	-	90	-	-	-
5nM	-	-	80	-	-	0
10nM	90	-	20	-	-	-
20nM	-	-	10	-	-	0
50nM	-	-	0	-	-	-
100nM	80	-	0	-	-	0

As revealed in the *Xenopus* oocyte experiments, the active version of EmPlk1^{T179D} was able to induce the G2/M transition in the *Xenopus* system, which resulted in germinal vesicle breakdown (GVBD). Furthermore, an effective inhibition of EmPlk1 at 20 nM concentrations of the inhibitor BI 2536 and the second-generation inhibitor BI 6727 (data not shown in Tab 5.4.1) was observed. Regarding the first generation inhibitor BI 2536 (20 nM) this concentration lead to a 90% reduction of GVBD and 80% reduction in the case of the second generation inhibitor BI 6727. Overall, it was noticed that BI 6727 inhibited the EmPlk1 kinase activity about 50% less than BI 2536 at similar molar concentrations. No

change in GVBD was observed with and without inhibitor for the wild type version EmPlk1^{T179D}, the inactive kinase domain version EmPlk1^{T179V} and “kinase dead” version of the enzyme wt^{KD}. The observed basal activity of the double mutated version of T₁₇₉D^{KD} was blocked at the lowest concentration of 5 nM with BI 2536. Unaffected by even high concentrations of BI 2536 and BI 6727 was GVBD induced by the natural stimulating factor progesterone. Taken together, these data indicated that EmPlk1 is a functional kinase with binding affinity to the inhibitors BI 2536 and BI 6727 at a low nanomolar range.

5.5. BI 2536 inhibits the formation of metacystode vesicles from parasite primary cells

As already shown above, the Plk1 inhibitors BI 2536 and BI 6727 affected the activity of EmPlk1 when expressed in the *Xenopus* system. Furthermore, *emplk1* showed highest expression levels in parasite primary cell cultures and displayed an expression pattern in WMISH that is typical for stem cell-specifically expressed genes [32, 132]. To test effects of Plk1 inhibitors on parasite germinative cells, the primary cell culture system was used, which - as recently shown - is highly enriched in germinative cells and leads to the formation of mature metacystode vesicles within 2-3 weeks [32]. As shown in Figs. 5.5.1 and 5.5.2., BI 2536 treatment showed a statistically significant and concentration dependent inhibition of the formation of metacystode vesicles within two weeks of treatment. At concentrations of 25, 50 and 100 nM, vesicle formation was almost completely abolished, parasite cells were only loosely aggregated and central cavities, which eventually should result in vesicles, were not observed [118, 123, 132]. Even at concentrations as low as 5 and 10 nM, only about 50% and 25%, respectively, of mature vesicles were formed when compared to the control. Taken together, these data indicated that parasite stem cell proliferation and/or differentiation, which eventually results in the formation of mature metacystode vesicles in the culture system employed, can be effectively inhibited by BI 2536 [118].

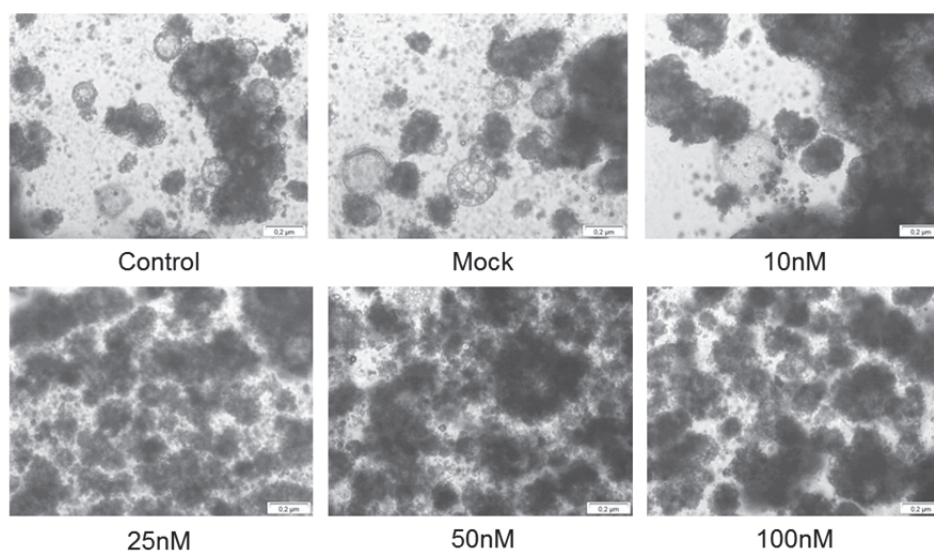


Figure 5.5.1 BI 2536 affects the formation of metacestode vesicles from primary cell culture. Primary cells were isolated from intact metacestode vesicles and seeded in a 48-well plate format. Metacestode vesicle formation was observed by light microscope in non-treated and treated wells with different concentrations (10 nM, 25 nM, 50 nM, 100 nM) of the Plk1 inhibitor BI 2536. 'Mock' indicates cultures with DMSO (without inhibitor). Experiments with primary cells were performed in A4-media. A4-Media with freshly added inhibitor was changed every second day. Pictures were taken on day 14. Size is indicated by a white bar on the bottom right corner of each picture.

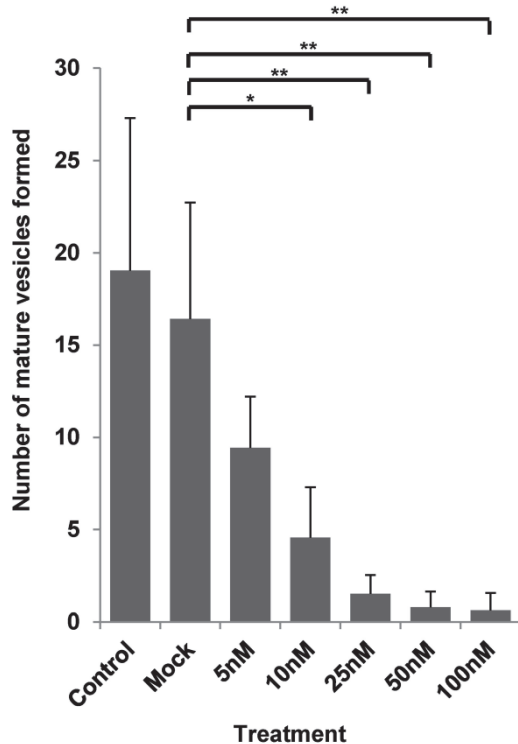


Figure 5.5.2 Formation of *E. multilocularis* metacestode vesicles from primary cells are inhibited by BI 2536. Primary cell cultures were established from intact metacestode vesicles and incubated under ideal growth conditions (A4 medium) treated with different concentrations (5 nM, 10 nM, 25 nM, 50 nM and 100 nM) of BI 2536 or non-treated Control and 'Mock' indicating cultures with DMSO (without inhibitor). The formation of mature metacestode vesicles (with laminated layer) was observed by light microscopy and counted on day 14. All conditions were assessed at least in three different biological replicates with at least three technical replicates. *(p,0.05); **(p = 0.001–0.01) (Student's t-test).

In addition to the two inhibitors BI 2536 and BI 6727, belonging to the chemical substance class of Dihydropteridinone, a third Plk1 inhibitor GW843682X was tested on metacestode vesicles and in the primary cell culture system. GW843682X is a thiophene benzimidazole ATP competitive inhibitor for human Plk1 and Plk3 with nanomolar acting concentration of IC_{50} of 2.2 nM and 9.1 nM, respectively. Several studies on cancer tissues showed that this inhibitor is acting in a micro-molar concentration and it was also tested in *S. mansoni* acting on SmPlk1 [85, 102, 134].

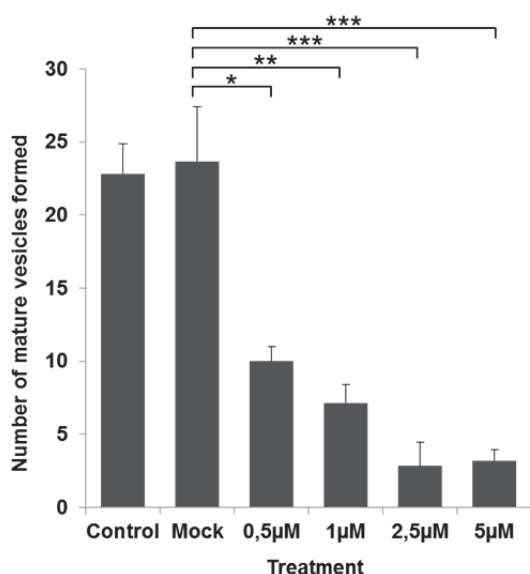


Figure 5.5.3 Formation of *E. multilocularis* metacestode vesicles from primary cells are inhibited by GX843682X. (B) Primary cell cultures were established from intact metacestode vesicles and incubated under ideal growth conditions (A4 medium) treated with different concentrations (0.5 µM, 1 µM, 2.5 µM, 5 µM) of GW843682X or non-treated Control and Mock indicating cultures with DMSO (without inhibitor). Formation of new metacestode vesicles was observed by light microscopy and counted on day 14. (A, B) All conditions were assessed at least in three different biological replicates with at least three technical replicates. *(p,0.05); **(p = 0.001–0.01) (Student's t-test). (A, B) 'Mock' indicating cultures with DMSO (without inhibitor).

Similar to the previous experiment with the BI 2536 inhibitor, primary cells were treated with GW843682X. A concentration dependent inhibition in the formation of metacestode vesicles from primary cells was observed, statistically significant at an inhibitor concentration of 0.5 µM. Taken together, these data indicated that several different PIK1 inhibitors are able to inhibit the formation of metacestode vesicles from parasite primary cells in a concentration dependent manner.

5.6 *In vitro* effects of BI 2536 on *E. multilocularis* metacestode vesicles

Parasite material was isolated from Mongolian jirds (*Meriones unguiculatus*) and grown in the *in vitro* cultivation system for at least three months in the presence of rat Rheuber hepatoma (Rh-) feeder cells. Feeder cells were subsequently removed and mature vesicles were incubated for up to three weeks in conditioned medium (A4-Media) in the presence of different concentrations of BI 2536 (5 nM, 10 nM, 25 nM, 50 nM and 100 nM). Subsequently, structurally intact vesicles were counted by visual inspection. Interestingly, even after three weeks of incubation at a concentration of 100 nM BI 2536, no significant reduction in structurally integer vesicles were observed (Fig. 5.6.1A). However, as shown in Fig. 5.6.1B, BI 2536 treated vesicles were consistently smaller than control vesicles, indicating that inhibitor treatment had impaired growth and proliferation capacity of the metacestode vesicles.

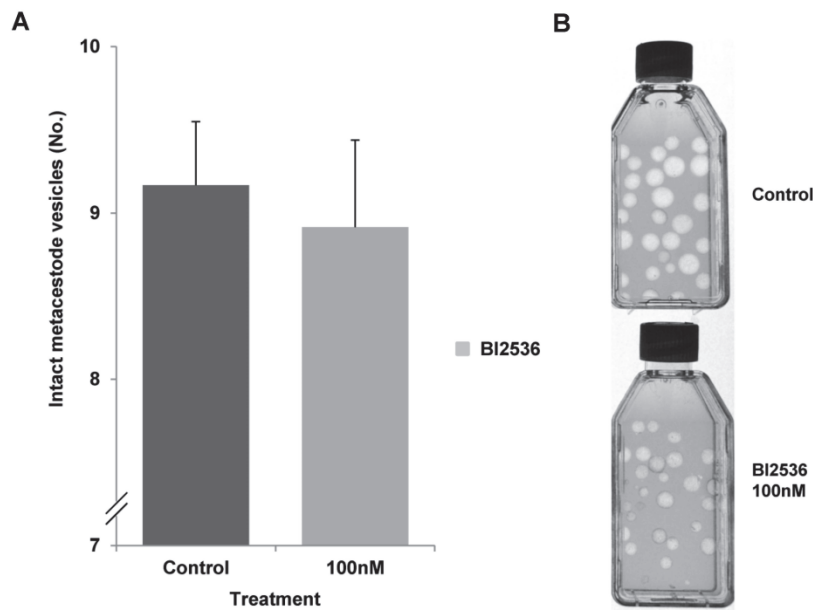


Figure 5.6.1 *In vitro* effects of BI 2536 on *E. multilocularis* metacystode vesicles. (A) Cultivated metacystode vesicles under axenic conditions were treated *in vitro* over 21 days in the absence (Control) and presence of the Plk1 inhibitor (BI 2536, 100 nM). A4-Media with fresh added inhibitor was changed every second day. (B) Co-culture flasks after 21 days of treatment with Control and treated metacystode vesicles with BI 2536 (100 nM). (A) The experiment was performed in three independent biological replicates (n=3).

Furthermore, a second inhibitor, GX843682X was tested in micro-molar concentrations on metacystode vesicles over 10 days. An effect on the vesicle integrity or a particular phenotype, showing abnormalities in the laminated or germinal layer by light microscopy was not observed (Fig 5.6.2).

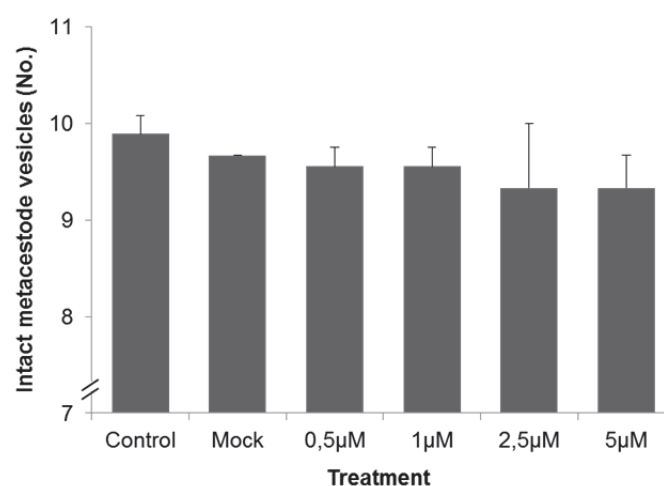


Figure 5.6.2 *In vitro* effects of GX843682X on *E. multilocularis* metacystode vesicles. Metacystode vesicles were cultivated over 10 days in the absence (Control, Mock) and in the presence of increasing concentrations of the Plk1 inhibitor GX843682X (0.5 μM, 1 μM, 2.5 μM, 5 μM). Metacystode vesicle integrity was observed by light microscope. A4-Media with fresh added inhibitor was changed every second day. The experiment was performed in three independent biological replicates (n=3).

To address the question whether parasite stem cells were affected in the structurally intact metacystode vesicle after treatment with the inhibitor BI 2536, a Click-iT EdU cell proliferation assay (EdU (5-ethynyl-2'-deoxyuridine; Invitrogen, C10337) pulse experiment was carried out. This assay provided an overview of whether proliferating cells remained present after a defined time of treatment with this inhibitor (Chapter 5.7).

5.7. Stem cells of metacystode vesicles are affected by treatment with BI 2536, visualised by a Click-iT EdU cell proliferation assay

The experiments outlined above highlighted that BI 2636 inhibited the growth of metacystode vesicles and the formation of mature metacystode vesicles from primary cells. Metacystode vesicles are the chemotherapeutic target in infected patients and thus the main focus for the development of new lead compounds in drug development.

As shown above, the treatment mature metacystode vesicles with 100 nM BI 2536 over 21 days did not lead to structural disintegration or vesicle collapse. Interestingly, in a recent study carried out by Koziol *et al.* (2014), hydroxyurea (HU) at high concentrations was used to successfully eliminate germinative (stem) cells in metacystode vesicles, which remained structurally intact for several weeks in culture. Hence, in the present study it was indeed possible that BI 2536 had similar effects as HU. To test this hypothesis, a Click-iT EdU cell proliferation assay on BI 2536 treated vesicles was carried out. Labelling of proliferating cells in treated and untreated metacystode vesicles was performed as previously described by Koziol *et al.* (2013) [47]. Metacystode vesicles were cultivated under axenic conditions in A4-medium and treated with increasing concentrations (from 10 nM to 100 nM) of BI 2536 for 21 days. After 21 days, treatment was stopped and followed by three days of recovery, (without further inhibitor treatment) to allow surviving stem cells to re-enter the cell cycle. Proliferating cells were subsequently labelled using an EdU pulse approach. All metacystode vesicles were intact and did not show any phenotypic variation after these 21 days of treatment and three days of recovery. Microscopic analysis of inhibitor-treated metacystode vesicles vs untreated samples showed significant differences in the number of proliferating EdU positive cells (Fig. 5.7.1). In particular, the treated samples showed a drastically reduced number of EdU positive cells (Fig. 5.7.1A). A statistical analysis by counting EdU positive cells (cells/mm²) demonstrated that the remaining proliferating cells in the treated metacystode were highly significantly reduced by treatment with concentrations of 25 nM BI 2536 and higher (Fig. 5.7.1B). Overall, only two EdU positive cells/mm² were found in the sample treated with 100 nM BI 2536. The observation of less proliferating cells was in line with the suppression of growth in metacystode vesicles and the suppressed regeneration capacity of *in vitro* cultivated primary cells.

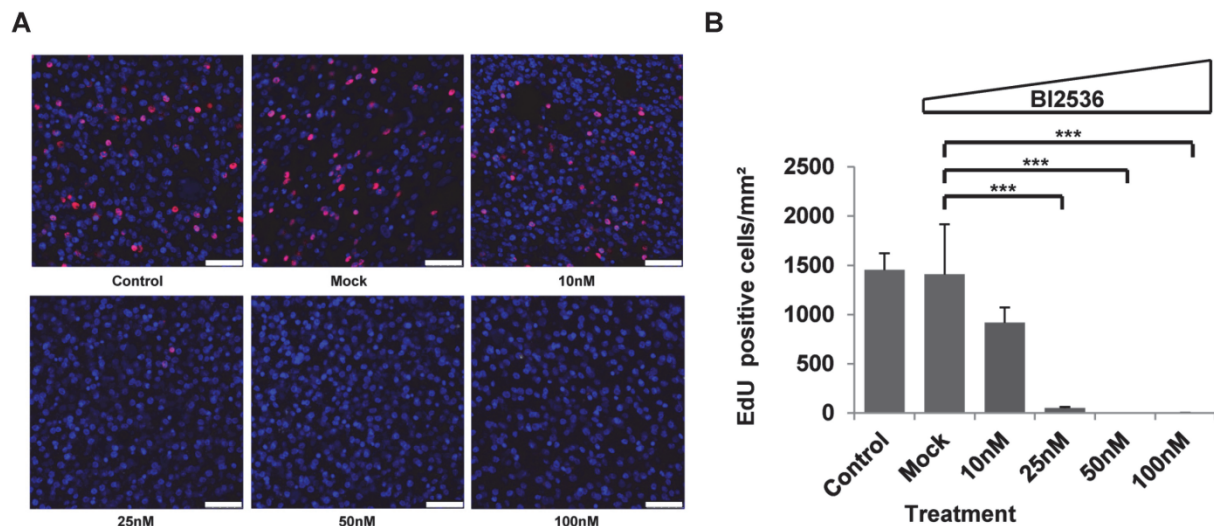


Figure 5.7.1 Elimination of proliferating germinative cells in metacestode vesicles after treatment with BI 2536. Metacestode vesicles were cultivated under axenic conditions over 21 days with different concentrations (10 nM, 25 nM, 50 nM and 100 nM) of the Polo-like kinase 1 inhibitor BI 2536 and without (Control, Mock (DMSO)), followed by three days of recovery without inhibitor. On day three of recovery, an EdU pulse [EdU (5-ethynyl-2'-deoxyuridine)] experiment was performed. Three out of ten labelled metacestode vesicles were randomly chosen for the EdU staining and microscopically counting of EdU positive cells. (A) Microscopic pictures of the germinal and LL (GL) of BI 2536 treated (10 nM, 25 nM, 50 nM, 100 nM) and non-treated *E. multilocularis* metacestode vesicles after staining with EdU (red; proliferating cells) and DAPI (blue; nuclei). Scale bar (white, bottom right corner) represents 25 μ m. (B) EdU positive cell counts per mm^2 of GL. 'Control' indicates vesicles cultivated in A4 medium alone. 'Mock' indicates the DMSO control. ***(p , 0.001) (Student's t-test). Please note that the specific examples shown in (A) display slightly different total cell numbers but that the overall cell numbers in metacestode vesicles were not altered by drug treatment.

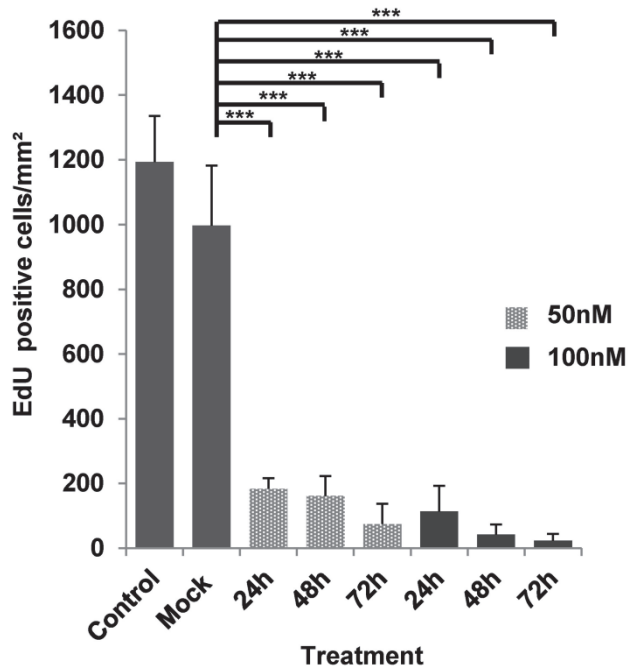


Figure 5.7.2 Short-term treatment of *E. multilocularis* metacestode vesicles with the Polo like kinases 1 inhibitor BI 2536 reduced proliferating stem cells. Metacestode vesicles were treated for 24, 48 or 72 hours (h, as indicated) with 50 nM (light grey) or 100 nM (darker grey) of BI 2536, followed by one day of recovery without inhibitor treatment. EdU labelling for 5 hours with 50 μ M EdU reagent was carried out and labelled cells were microscopically counted. Identified EdU-positive cell were counted per mm^2 of germinal and laminated layer (GL). 'Control' indicates vesicles cultivated in A4-medium alone. 'Mock' indicates the DMSO control. ***(p ,0.001) (Student's t-test).

Besides the long-term treatment over 21 days with the inhibitor BI 2536, the question of the effectivity of short-term treatment with the same inhibitor was addressed. To this end, a short-time treatment over 24, 48 and 72 hours with concentrations of 50 nM and 100 nM of BI 2536, followed by one day of recovery and EdU pulse approach, was carried out. EdU stained positive cells were counted as before (cells/mm²) and graphically represented in Fig. 5.7.1. After 24 hours and particularly 48 hours of treatment with the lowest concentration of 50 nM, the number of proliferating cells in the metacestode vesicles was drastically reduced. Even higher reduction was observed upon incubation with 100 nM BI 2536. Hence, short-term incubation of metacestode vesicles with high concentrations of BI 2536 was effective in eliminating large parts of the stem cell population, which could prove valuable for future studies on stem cell dynamics or stem cell-specific gene expression in *E. multilocularis*.

5.8 Attempts towards elucidating the crystal structure of the Polo-like kinase 1 of *E. multilocularis* (EmPlk1)

The design of new lead compounds in drug development takes into account several factors such as the accessibility of the inhibitor to an organism, direct interactions between drug and protein target, as well as the acting drug concentration, which is relevant concerning adverse side-effects. Based upon these facts and that the two tested Polo-like kinase 1 inhibitors BI 2536 and BI 6727 passed phase II of the clinical trials [98, 99] we decided to go one step further and tried to optimise these inhibitors for the inhibition of EmPlk1. Our *in vitro* experiments on metacestode vesicles, primary cells and in the heterologous expression in *Xenopus* oocytes clearly showed that the inhibitors act on EmPlk1 and inhibit the proliferation of these cells. Targeted drug design is greatly facilitated by the availability of crystal structures of the respective protein target. In collaboration with the Kisker group at the Rudolf-Virchow-Centre for experimental Biomedicine, the crystallisation of EmPlk1 (with and without inhibitors) was thus attempted. For this purpose, and similar to such previous approaches for the crystallisation of human Plk1, the EmPlk1 regions encoding amino acids 8 to 296 of the EmPlk1 kinase domain were chosen for cloning, expression, and purification [95]. Respective clones were generated for wild type EmPlk1^{WT}, for the mutated, active form EmPlk1^{T179D} and an inactive version, EmPlk1^{T179V}. As a vector system for cloning and bacterial expression, pETM-14 was used. Several crystallisation conditions were tested, which remains an ongoing process for optimisation with and without inhibitors. To date, small crystals have only been seen in the wild type form of EmPlk1^{WT} without inhibitor (data not shown). The questions that we want to address from this approach concern (I.) whether there is a binding correlation of the inhibitors compared to the human Plk1, (II.) what are the differences in the binding of BI 2536 and BI 6727 to EmPlk1 and do they correlate with the better inhibition as seen in experiments with BI 2536, and (III.) whether it is possible to optimise the chemical structure of BI 2536 or BI 6727 for binding to EmPlk1 [135].

5.9. Expression patterns of *E. multilocularis* β -tubulin genes.

The current chemotherapy of AE is based upon benzimidazoles, such as mebendazole or albendazole (Chapter 3.3), which target the cellular β -tubulins of *E. multilocularis*. β -tubulins are usually highly conserved between helminths and mammals and only a few amino acid sequence differences account for a higher affinity of benzimidazoles to helminth β -tubulins than to mammalian β -tubulins. The most important amino acid in this context is residue 200, which in helminth β -tubulins is usually Phe, whereas in mammalian isoforms it is typically Tyr [59]. In a previous study, three different β -tubulin isoforms (*tub-1*, *tub-2*, *tub-3*) that are expressed by *E. multilocularis* had been identified and of these, Tub-2, was shown to contain Tyr at position 200, indicating that it might represent an isoform with diminished affinity to benzimidazoles [58]. Since it was unclear whether Tub-1, Tub-2 and Tub-3 represented the entire set of *Echinococcus* β -tubulins, the available *E. multilocularis* genome sequence was utilised in the present study for BLASTP analyses using the already-characterised *Echinococcus* β -tubulin sequences as queries [60].

```

EmuJ_001126150 MREILVLMIGQCGNQIGAKFWEVIADEHGIGPDGTYRGSDDLQTERIHVYEMEAAGGRMV 60
EmuJ_001081200 MREILVLIQVQCGNHTGKFWETISGEHGVSNGSEHGSEIQLERMNVYYTEAMGGRFV 60
EmuJ_000041100 MREIVHIIQIGQCGNQIGAKFWEVVSDEHGLSADCLYNGSDQLQERIGVYNEAIGGKIV 60
EmuJ_000202500 MREILVHMQAGQCGNQIGSKFWEVTSQEHGIDEMGSYHGSDQLQERINVYVNEGCGGKYV 60
EmuJ_000617000 MREIVHIIQAGQCGNQIGAKFWEVVSDEHGIDPTGTYHGSDQLQERISVYVNEGSGTKYV 60
EmuJ_000955100 MREIVHIIQAGQCGNQIGAKFWEVVSDEHGIDPTGTYHGSDQLQERINVYVNEAIGGKYV 60
EmuJ_000569000 MREIVHIIQAGQCGNQIGAKFWEVVSDEHGIDPTGTYHGSDQLQERINVYVNEAIGGKYV 60
EmuJ_000672200 MREIVHIIQAGQCGNQIGAKFWEVVSDEHGIDPTGTYHGSDQLQERINVYVNEAIGGKYV 60
EmuJ_000069900 MREIVHIIQAGQCGNQIGAKFWEVVSDEHGIDPTGTYHGSDQLQERINVYVNEAIGGKYV 60
EmuJ_000202600 MREIVHIIQAGQCGNQIGSKFWEVVSDEHGIDPTGTYHGSDQLQERINVYVSEASGGKYV 60

EmuJ_001126150 PRTVLADLEPGTLDIVRSGEYGCIFRPDNEAFGNA GAGNNWAKGHYTEGAEMIESIMEIV 120
EmuJ_001081200 PRCVLIIDLDPGIQNTVRSPPFGRIFRPENFIAGRAGSGNNWAKGRYTDGLEMMDAVLDVV 120
EmuJ_000041100 PRAIITDLEPGTMDAIRSGPVGNLFRPDNIVFGTIGAGNNWAKGHYTEGAELIDNIDVV 120
EmuJ_000202500 PRALLIDLEPGTMDSVRSGLPKLFRPDNFI FGQSGAGNNWAKGHYTEGAELIEEVLDDVV 120
EmuJ_000617000 PRSILVDLEPGTMDSVRAGPFGQLFRPDNFVFGQSGAGNNWAKGHYTEGAELIDAVLDVV 120
EmuJ_000955100 PRAVLVDLEPGTMDSVRAGPFGQLFRPDNFVFGQSGAGNNWAKGHYTEGAELVDSVLDVV 120
EmuJ_000569000 PRAVLVDLEPGTMDSVRAGPFGQLFRPDNFVFGQSGAGNNWAKGHYTEGAELVDAVLDVV 120
EmuJ_000672200 PRAIIVDLEPGTMDSVRAGPFGQIFRPDNFVFGQSGAGNNWAKGHYTEGAELVDSVLDVV 120
EmuJ_000069900 PRAIIVDLEPGTMDSVRAGPFGQIFRPDNFVFGQSGAGNNWAKGHYTEGAELVDSVLDVV 120
EmuJ_000202600 PRCVLIIDLEPGTMDSVRAGPFGQLFRPDNFVFGQSGAGNNWAKGHYTEGAELVESVLDVV 120

EmuJ_001126150 HRECEACDCLQGFQVHSMGGGTGAGMGTLISKIREEYYPDRIMCTFSCYPSPKVSDVVV 180
EmuJ_001081200 RKEAEGCDHLQGFQIHSIGGGCGSGMGSATMDQIRDEWSDRIFNNFTVLPSPKVSDVVV 180
EmuJ_000041100 RKEAEBSECLQGFQVHSLGGGTGAGLGTLLVTKIREEYYPDRITCCFSTVPSPKVSDVVV 180
EmuJ_000202500 RKECEACDCLQGFQIHSIGGGGTGSGMGTLLIAKIREEYYPDRIMTFSVVPSPKVSDVVV 180
EmuJ_000617000 RKEAECDCDCLQGFQIHSISGGGTGSGMGTLLISKIREEYYPDRIMTFSVVPSPKVSDVVV 180
EmuJ_000955100 RKEAESCDCLQGFQIHSISGGGTGSGMGTLLISKVREEYADRIMNTFSVVPSPKVSDVVV 180
EmuJ_000569000 RKEAESCDCLQGFQIHSISGGGTGSGMGTLLISKVREEYYPDRIMNTFSVVPSPKVSDVVV 180
EmuJ_000672200 RKEAESCDCLQGFQIHSISGGGTGSGMGTLLISKIREEYYPDRIMVTVSVVPSPKVSDVVV 180
EmuJ_000069900 RKEAESCDCLQGFQIHSISGGGTGSGMGTLLISKIREEYYPDRIMSTFSTVPSPKVSDVVV 180
EmuJ_000202600 RKECESCDCLQGFQIHSISGGGTGSGMGTLLISKVREEYYPDRIMNTFSVVPSPKVSDVVV 180

EmuJ_001126150 EPYNATLSSEHLETEYSDSEFTLDNEALEDCIFRTLKIQHPTLGDNLHLSVATMSGVTTCL 240
EmuJ_001081200 EPYNSIEFSLDHLIETSDLTVIDNEALYD ICNHVLRKTFCS-FADLNHLISSTAICGITTCF 239
EmuJ_000041100 EPYNATLSSEHLETEYSDSEFTLDNEALYD ICNRTLKIVTPTYGDNLHLSVATMSGVTTCL 240
EmuJ_000202500 EPYNATLSVHQLVSTDETECIDNEALYD ICFRTLKLPNPNYSQDLNHLVSTTMSGVTTSL 240
EmuJ_000617000 EPYNATLSVHQLIDNIDQTECIDNEALYD ICFRTLKLTNPTYGDNLHLSVATMSGVTTCL 240
EmuJ_000955100 EPYNATLSVHQLVENIDETETCIDNEALYD ICFRTLKLTPTYGDNLHLSVATMSGVTTCL 240
EmuJ_000569000 EPYNATLSVHQLVENIDETETCIDNEALYD ICFRTLKLTPTYGDNLHLSVATMSGVTTCL 240
EmuJ_000672200 EPYNATLSVHQLVENIDETETCIDNEALYD ICFRTLKLTNPTYGDNLHLSVATMSGVTTCL 240
EmuJ_000069900 EPYNATLSVHQLVENIDETETCIDNEALYD ICFRTLKLTPTYGDNLHLSVATMSGVTTCL 240
EmuJ_000202600 EPYNATLSVHQLVENIDETETCIDNEALYD ICFRTLKLTNPTYGDNLHLSVATMSGVTTCL 240

EmuJ_001126150 RFPQQLNADLRKLGTLNIPFPRLHFFVPGFAPLTSRYGQAVHTYNVHDLTSQMFARNMM 300
EmuJ_001081200 RFPQQLNSDLRKLAVNIVPFPRIHFFVAFCFVPLTSRDNQTYKAITVPNLVQQMFDAKVM 299
EmuJ_000041100 RFPQQLNADLRKLATNMPFPRLHFFMPGFSPLTSRHSQAYRSYSVQDLTLQMFDSKNMM 300
EmuJ_000202500 RFPQQLNSDLRKLAVNMVFPFRLHFFVPGFAPLASRYSQSYQSCITILELTRQMFDAKNMM 300
EmuJ_000617000 RFPQQLNADLRKLSVNMVFPFRLHFFMPGFAPLTSRGSQQYRALTVPELTQQMFDAKNMM 300
EmuJ_000955100 RFPQQLNADLRKLAVMVFPFRLHFFMPGFAPLTSRGSQQYRALTVPELTQQMFDAKNMM 300
EmuJ_000569000 RFPQQLNADLRKLAVMVFPFRLHFFMPGFAPLTSRGSQQYRALTVPELTQQMFDAKNMM 300
EmuJ_000672200 RFPQQLNADLRKLAVMVFPFRLHFFMPGFAPLTSRGSQQYRALTVPELTQQMFDAKNMM 300
EmuJ_000069900 RFPQQLNADLRKLAVMVFPFRLHFFMPGFAPLTSRGSQQYRALTVPELTQQMFDAKNMM 300
EmuJ_000202600 RFPQQLNADLRKLAVMVFPFRLHFFMPGFAPLTSRGSQQYRVLTVAEALTQQMFDAKNMM 300

EmuJ_001126150 SACDPRHGKYLTVAGMFRGRISVKEVEEVIDVQNKNSAYFVEWIPNNIKTALICDVPK 360
EmuJ_001081200 AACNPLKGRYLTCAAVFRGRISVAEEVEEMMLNQTQKNSAHFVEWIPNNCOTALCDIPPR 359
EmuJ_000041100 AACDPRHGKYLTVAAVFRGRISMKQVDENMLNVQNKNSAYFVEWIPNNVKTAVCDIPPR 360
EmuJ_000202500 AACDPHSHGRYLTVAAVFRGRISMKEVEDRILETQTRNSYFVEWIPNNVKTAVCDIPPR 360
EmuJ_000617000 AACDPRHGKYLTVAAVFRGRISMKEVDEQMLNVQNKNSYFVEWIPNNVKTAVCDIPPR 360
EmuJ_000955100 AACDPRHGKYLTVAAVFRGRISMKEVDEQMLNVQNKNSYFVEWIPNNVKTAVCDIPPR 360
EmuJ_000569000 AACDPRHGKYLTVAAVFRGRISMKEVDEQMLNVQNKNSYFVEWIPNNVKTAVCDIPPR 360

```



```

EmuJ_000672200 AACDPRHGRLTVAALFRGRMSMKEVDEQMLNVQNKNSSYFVEWI PNNVKTAVCDI PPRG 360
EmuJ_000069900 AACDPRHGRLTVAAMFRGRMSMKEVDEQMLNVQNKNSSYFVEWI PNNVKTAVCDI PPRG 360
EmuJ_000202600 AACDPRHGRLTVAAMFRGRMSMKEVDDQMLNAQNKNSSYFVEWI PNNVKTAVCDI PPRG 360

EmuJ_001126150 MSMSATFVGNITAVQELFKRVCDQFAVMLKKRAFLHWYLTGMDAEAEFDEAFINVDLIG 420
EmuJ_001081200 MKMSATEMGNSTAIQAVEGRVQSAYSSMLKRKAFLHWYTGEMEESEFLSTESNVLDLIS 419
EmuJ_000041100 LKMAVTFI GNNTAIQELFKRVREQFMAMFRRRAFLHWYTGEMDEIEFQEAQINMDDLNS 420
EmuJ_000202500 EKVAGTFI GNNTAIQELFKRVSDQFSAMFRRRAFLHFFTSSEGMDEMEFSEAESNMNDLIS 420
EmuJ_000617000 LKMAVTFI GNSTAIQQLFRRVSEQFTAMFRRKAFLHWYTGEMDEMEFTEAESNMNDLVS 420
EmuJ_000955100 LKMAATFVGNSTAIQELFRRVSEQFTAMFRRKAFLHWYTGEMDEMEFTEAESNMNDLVS 420
EmuJ_000569000 LKMAATFVGNSTAIQELFKRVSEQFTAMFRRKAFLHWYTGEMDEMEFTEAESNMNDLVS 420
EmuJ_000672200 LKMSATFVGNSTAIQELFRRVSEQFTAMFRRKAFLHWYTGEMDEMEFTEAESNMNDLVS 420
EmuJ_000069900 LKMSVTFI GNSTAIQELFKRVSEQFTAMFRRKAFLHWYTGEMDEMEFTEAESNMNDLVS 420
EmuJ_000202600 LKMSVTFMGNITAIQELFKRVSEQFTVMFRRKAFLHWYTGEMDEMEFTEAESNMNDLVS 420

EmuJ_001126150 EYQQYQSD----- 428
EmuJ_001081200 EYQQYQEPAPA----- 429
EmuJ_000041100 EYQQYQDAAMDDEVQMEAPAVSCG---- 444
EmuJ_000202500 EYQQYQEVGIDDD--YGEIEAAPEE--- 443
EmuJ_000617000 EYQQYQDATAADDEGEFDEDEDAIQDNE- 447
EmuJ_000955100 EYQQYQEPATAEEEGEFDEEEEEE----- 443
EmuJ_000569000 EYQQYQDACAEDEGEFEEEGEEG---- 444
EmuJ_000672200 EYQQYQDATAEDEGEFDEDEVEVEA--- 445
EmuJ_000069900 EYQQYQDATAEEEGEFEEEGEEA--- 445
EmuJ_000202600 EYQQYQEPAGIGDDEEEDGEGVMGEEIDA 448

```

Figure 5.9.1 β -tubulins from *E. multilocularis*. Multiple sequence alignment of the β -tubulins from *E. multilocularis*. Identical aa residues are shown in white on black background and captioned by upper-case letters. Similar amino acid residues are shown and in black on grey background. Position 200 of the proteins is indicated by a red star. Gene designations according to GeneDB are indicated to the left.

As shown in Fig. 5.9.1, a total of ten β -tubulin encoding genes were thus identified, of which four encoded a protein with Tyr at position 200. During the *E. multilocularis* sequencing project extensive RNA-Seq. data have been obtained for several parasite developmental stages, and as listed in Table 5.9.1, *tub-1*(EmuJ_000202600), *tub-2*(EmuJ_000672200), and *tub-3*(EmuJ_000202500) were indeed the highest expressed β -tubulin genes of the parasite, at least in the larval stages [60].

Table 5.9.1 Expression of *E. multilocularis* β -tubulin genes in different developmental stages

Gene designation*	aa200[§]	PC2 [†]	PC11	MV-	MV+	PS-	PS+	AW	gAW	name [‡]
EmuJ_000041100	DETFCID	3	4	1	0	4	3	71	124	
EmuJ_000069900	DETYCID	6	5	3	80	2	2	306	207	
EmuJ_000202500	DETFCID	57	53	343	661	56	53	108	191	<i>tub-3</i>
EmuJ_000202600	DETFCID	380	411	388	395	189	166	126	409	<i>tub-1</i>
EmuJ_000569000	DETYCID	6	2	2	4	1	0	33	49	
EmuJ_000617000	DQTFCID	3	6	1	7	4	5	11	18	
EmuJ_000672200	DETYCID	1161	1157	806	1641	745	842	1055	1614	<i>tub-2</i>
EmuJ_000955100	DETYCID	1	247	0	6	88	82	29	95	
EmuJ_001081200	DLTVILD	1	4	1	0	7	2	9	21	
EmuJ_001126150	DESFTLD	15	15	17	6	20	15	13	16	

*Gene designation according to Tsai *et al.*, (2013) as available through GeneDB (<http://www.genedb.org/Homepage/Emultilocularis>)

[§]Sequence context around amino acid 200 (in bold)

[†]Expression strength in fpkm (fragments per kilobase of exon per million fragments mapped) according to Illumina RNASeq (Tsai *et al.*, 2013) for primary cells after 2 (PC2) and 11 (PC11) days of development, metacystode vesicles without (MV-) and with (MV+) brood capsules, dormant (PS-) and low pH/pepsin-activated protoscoleces (PS+), pre-gravid adult worms (AW) and gravid adult worms (gAW).

[‡]Gene name according to Brehm *et al.*, (2000).

Interestingly, and as depicted in Fig. 5.9.2., *tub-2* showed an expression profile that is highly reminiscent of genes specifically expressed in the parasite's germinative cell population. According to the analyses made by Koziol *et al.* (2014), such genes should show highest expression in primary cells after 2 days of incubation, somewhat lower expression levels in primary cells after 11 days, and the lowest levels in metacystode vesicles and protoscoleces. Of all three highly expressed β -tubulin genes of the parasite, this could only be observed for *tub-2*, indicating that it might be specifically expressed in germinative cells (Table 5.9.1, Fig. 5.9.2.).

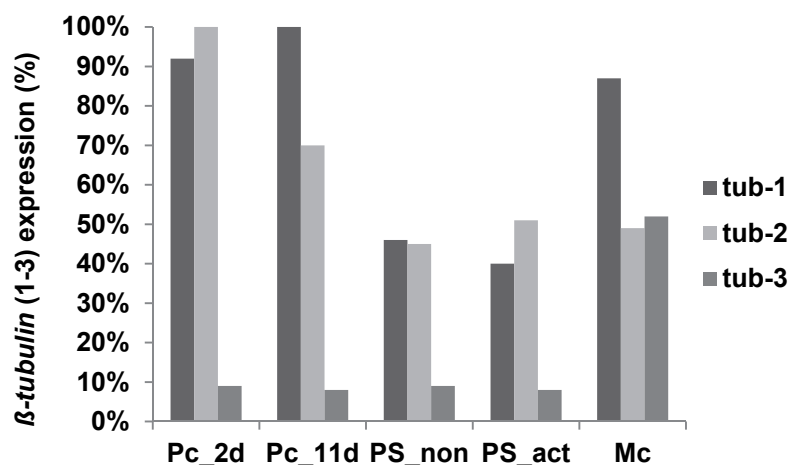


Figure 5.9.2 Expression of β -tubulin genes in *E. multilocularis* larval stages as assessed by RNA-Seq. Larval stage expression profile for primary cells of day 2 (Pc_2d) and day 11 (Pc_11d), dormant and activated protoscoleces (Ps_non and Ps_act) and metacystode vesicles (Mc). Note that Illumina sequencing has been performed only once for each sample.

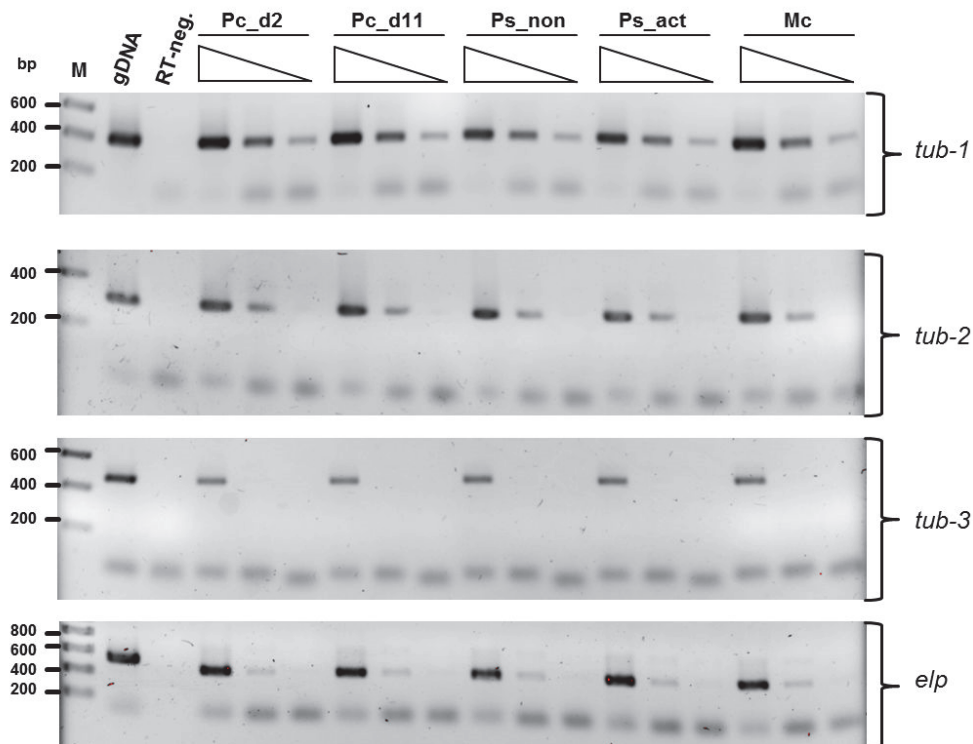


Figure 5.9.3 Expression of *tub-1*, *tub-2* and *tub-3* in *E. multilocularis* larval stages. Total RNA was isolated from primary cell cultures (Pc) after day 2, and 11 (d2, d11) of incubation, dormant (Ps_non) and activated protoscoleces (Ps_act), as well as *in vitro* cultivated metacestode vesicles (Mc). Equal amounts of isolated RNA were reverse transcribed to cDNA and subjected to gene-specific (RT)-PCR for *tub-1*, *tub-2* and *tub-3*. The house keeping gene *elp* was used for normalisation. The generated cDNA was 10-fold diluted in 1, 1:10 and 1:100 for PCR. Genomic DNA (gDNA) served as a positive control and purity of DNA contamination during RNA isolation. Non-reverse transcribed RNA was used as a purity control for DNA contamination during RNA isolation. Marker sizes are indicated on the left. (2% Agarose; EtBr stained).

To verify the results obtained through RNA-Seq. RT-PCR analyses for *tub-1*, *tub-2*, and *tub-3* were carried out in the present study. As shown in Fig. 5.9.3., an expression of all three genes was indeed found in primary cells (2 and 11 days of incubation), in metacestode vesicles and in protoscoleces. The results again indicated that *tub-2* is highest expressed in primary cells after 2 days of incubation, although due to the method used (RT-PCR), expression differences could not be determined to an extent comparable to RNA-Seq. data.

To further investigate possible stem cell-specific expression patterns of Echinococcus β -tubulins, RT-PCR experiments were carried out on metacestode vesicles after treatment with BI 2536, which - as outlined above - leads to a specific elimination of the germinative cell population. To this end, metacestode vesicles were treated with BI 2536 (50 nM) for 21 days, followed by 5 days of recovery without further treatment, to ensure that the inhibitor is dissociated. Total RNA was isolated from treated and untreated metacestode vesicles and used for a *semi*-quantitative RT-PCR. As shown in Fig. 5.9.4., no change in the expression of *tub-1* was observed for treated and untreated vesicles and in the case of *tub-3*, expression levels were even higher after BI 2536 treatment. By contrast, the expression levels of *tub-2* were greatly reduced after BI 2536 treatment, indicating that it is indeed specifically expressed in the germinative cell population. Hence, the most important cell type for

parasite proliferation and development, the germinative cells, most probably express a β -tubulin isoform with diminished affinity for benzimidazoles.

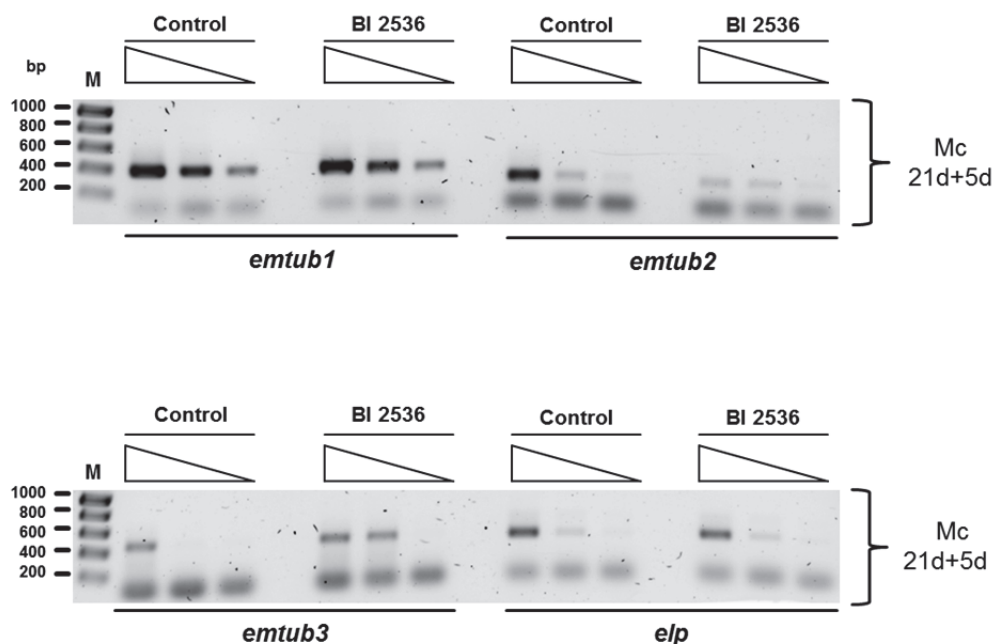


Figure 5.9.4 Expression of *tub-1*, *tub-2* and *tub-3* in BI 2536 treated *E. multilocularis* metacystode vesicles. Total RNA was isolated from *in vitro* cultivated metacystode vesicles (Mc) treated or non-treated with the Polo-like kinase 1 inhibitor BI 2536 (50nM) for 21 days followed by 5 days of recovery without treatment. Equal amounts of isolated RNA were reverse transcribed to cDNA and subjected to gene-specific (RT)-PCR for *tub-1*, *tub-2* and *tub-3*. The house keeping gene *elp* was used for normalisation. The generated cDNA was 10-fold diluted in 1, 1:10 and 1:100 for PCR. Genomic DNA (gDNA) served as a positive control and purity of DNA contamination during RNA isolation. Non-reverse transcribed RNA was used as a purity control for DNA contamination during RNA isolation. Marker sizes are indicated on the left. (2% Agarose; EtBr stained).

Previous unpublished experiments had shown that primary cells were insensitive to even very high concentrations of Albendazole (50 μ M, 100 μ M) (Sarah Hemer, Doctoral thesis, 2012), indicating that parasite stem cells could indeed be insensitive to benzimidazoles. To further investigate these effects, experiments were carried out in this work to verify that albendazole-treated metacystode vesicles indeed still contain viable stem cells. To this end, metacystode vesicles have been treated for one week with high albendazole concentrations (50 μ M, 100 μ M) leading to structural disintegration and collapse of the vesicle (Fig. 5.9.5). Primary cells were subsequently isolated and the formation of metacystode vesicles was measured.

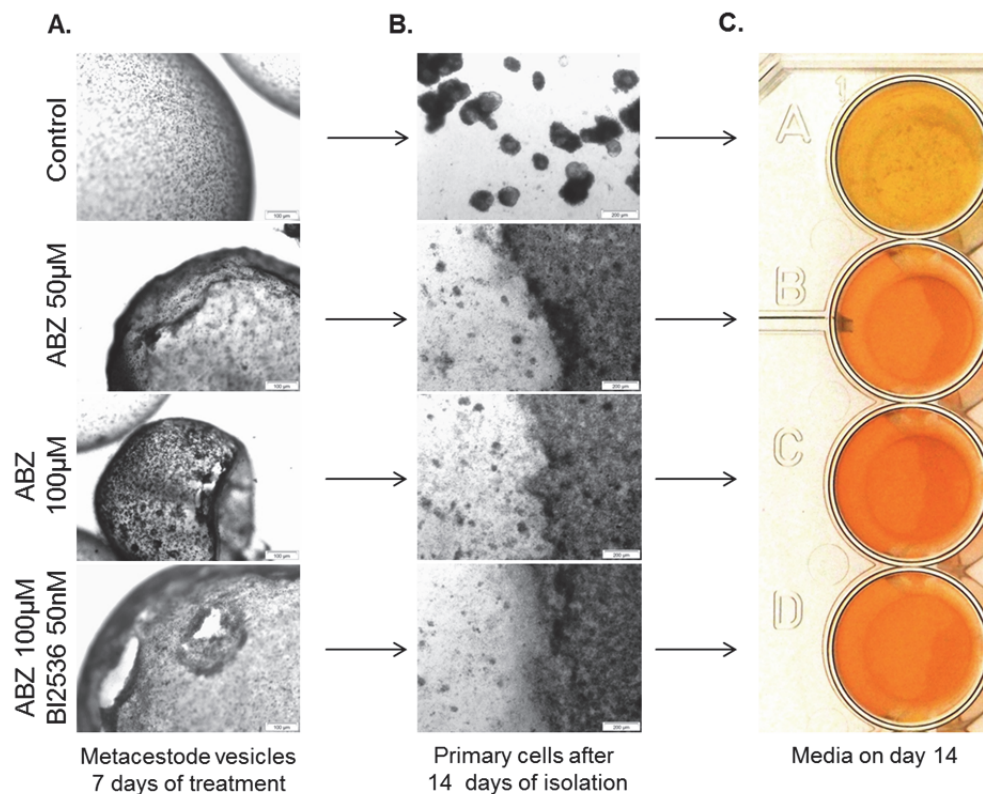


Figure 5.9.5 Inhibitor effects on the regeneration capacity of metacestode vesicles. Metacestode vesicles were treated with 50 μM and 100 μM of albendazole (ABZ) or in combination of 50 μM ABZ and 50 nM BI 2536 for one week under axenic conditions. (A) Primary cells were directly isolated from treated metacestode vesicles and 50 Units were co-cultivated for regeneration without any further treatment. (B) Pictures were taken after 14 days of the primary cell regeneration process. (C.) Colour change of the media was photographed as an indicator for active cellular metabolism. Sizes are indicated (white) at the bottom right corner (A) 100 μm (B) 200 μm .

In the case of the non-treated sample, aggregate formation and formation of metacestode vesicles could be observed as expected (Fig. 5.9.5 B, Control). However, independently of the concentration of ABZ or combinatory treatment, no formation of aggregates or mature vesicles was observed for the inhibitor-treated samples (Fig. 5.9.5 B). A cellular monolayer of cells covered the bottom of the 48-well plate in all treated samples. Metabolic activity was similar until 10 days after primary cell isolation. The first change in media (colour) was observed on day 14 (Fig. 5.9.5) and only occurred in samples deriving from non-treated metacestode vesicles. Taken together, these experiments indicated that treatment with high concentrations of albendazole is effective in eliminating the proliferation and regeneration capacity of metacestode vesicles.

6.0 Injection of isolated primary cells into metacestode vesicles treated with the Polo-like kinase 1 inhibitor BI 2536.

The experiments outlined above revealed that long-term BI 2536 treatment of metacestode vesicles leads to (largely) stem cell deprived vesicles that are otherwise structurally intact. This led to the interesting question whether stem cell deprived vesicles could be repopulated by stem cells upon introduction *via* injection. Such a system would prove highly valuable in tracking stem cell dynamics in their natural niche, e.g. by injecting fluorescently labelled stem cells. Furthermore, once transgenic techniques for stem cells are established, these could not only be used for vesicle generation in the primary culture system but for vesicle ‘transformation’ in the metacestode culture system.

This new method is in my opinion a promising new technique that can be utilised to study genetically manipulated primary cells in our *in vitro* cell culture system and might also be useful for further experiments. The present situation of a technique to genetically manipulate primary cells of *E. multilocularis* is still not given today, although efforts have been undertaken. The usage of the current *in vitro* cell culture technique for primary cells is not trivial and has to be improved for working with genetically manipulated primary cells. Independent of the outcome of the preliminary experiments, a technique that will finally be able to generate transgenic cells of *E. multilocularis* needs a method to further *in vitro* cultivate these cells. Primary cells of *E. multilocularis* are not adherent, which goes along with problems in the basic cell culture technique in direct comparison to several human cell lines. Furthermore, to protect these “stressed cells” from the environment and cultivate them in an optimal natural condition, the idea was to inject these cells were into a “physical intact metacestode vesicle” in our *in vitro* cultivation system. This new method is supported by the fact that the metacestode vesicle mimics the most natural environment for the transformed primary cells, while this method offers us a much easier handling of the non-adherent cell type; moreover, the influence of stress by change of the media is reduced. I suppose that the survival chance of genetically manipulated parasite stem cells is even higher in a “natural environment” compare with the current primary cell culture method. To this end, metacestode vesicles (isolate H95) were first deprived of stem cells by BI 2536 treatment for 21 days, followed by injection of stem cells from primary cells (isolate H95) as outlined in Fig. 6.0.1.

According to the experimental approach described in Fig 6.0.1, metacestode vesicles (H95) were selected by size (>0,5cm) and vesicle integrity (microscope), followed by treatment with BI 2536 for 21 days (Fig. 6.0.1 A-B). After five days of recovery without inhibitor treatment, fresh isolated primary cells (H95) were injected (Fig. 6.0.1 B-C- D). The injection process and handling of the metacestode vesicles were carried out carefully, resulting in ~25% of the injected vesicles surviving the approach. A picture of metacestode vesicles after the injection process is given in Fig 6.0.1 F. The picture shows metacestode vesicles before EdU staining and some metacestode vesicles that were seriously damaged during the injection process, as indicated by a change of the colour in the hydatid fluid (Fig. 6.0.1.F). Damaged metacestode vesicles were removed and EdU staining of the remaining metacestode vesicles followed. The EdU staining was carried out as before and described in Koziol *et al.* (2014) [32].

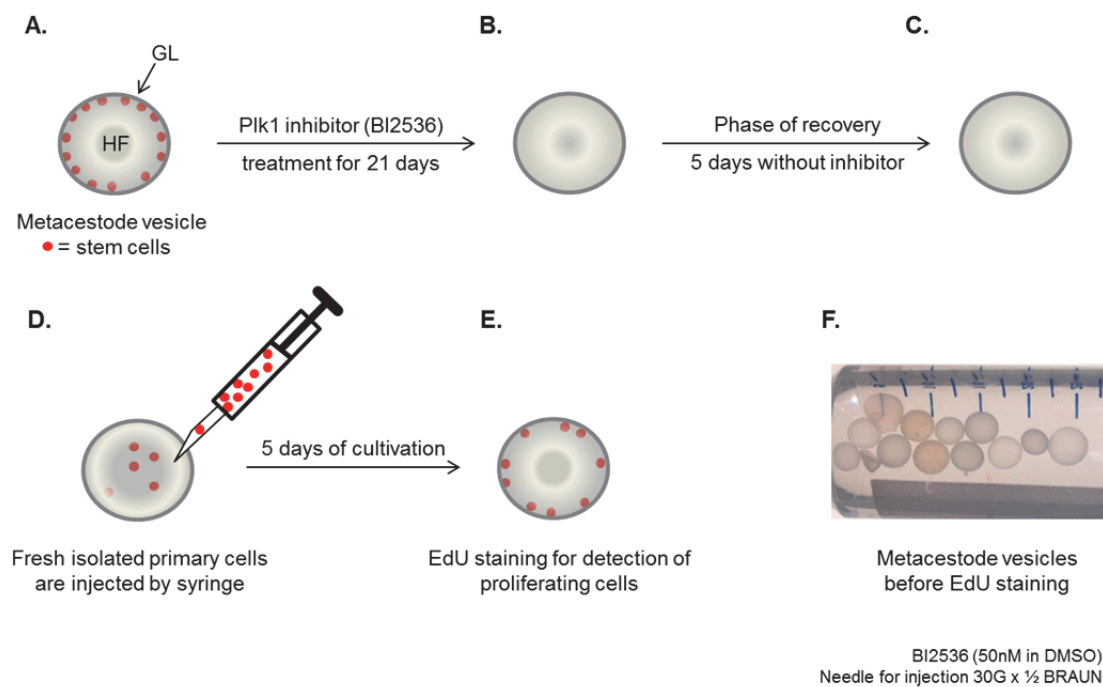


Figure 6.0.1 Schematic representation of an experimental approach to repopulate stem cell depleted metacystode vesicles. (A.-B.) Metacystode vesicles (>0.75 cm) were treated over 21 days with 50 nM BI 2536. (D.) Primary cells in A4-Media suspension were injected by syringe into intact BI 2536 treated metacystode vesicles. (E.) EdU staining for the detection of proliferating and integrated stem cells was carried out. (F.) Injected metacystode vesicles before EdU staining [32].

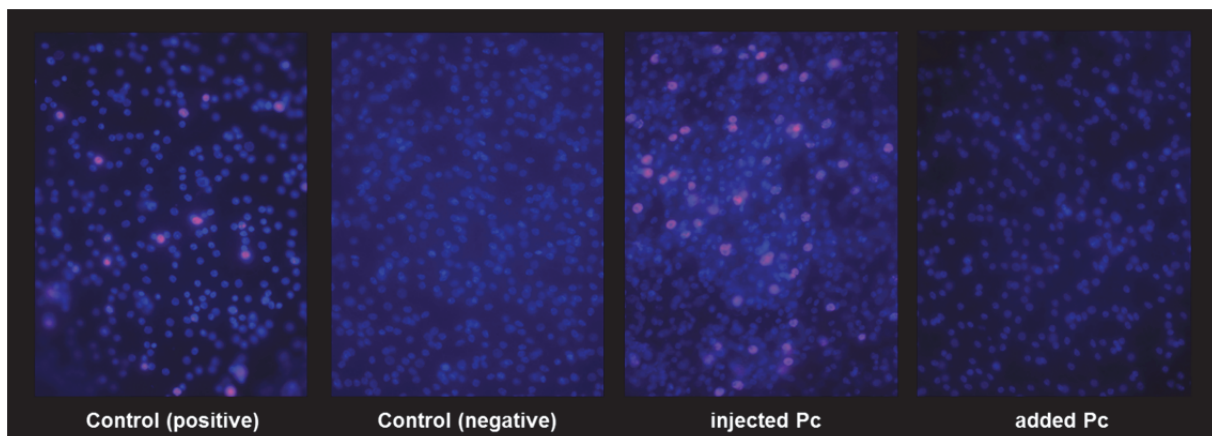


Figure 6.0.2 Repopulation of stem cell deprived metacystode vesicles with primary cells. Metacystode vesicles were treated over 21 days with BI 2536 (50 nM) followed by five days of recovery without treatment. Freshly isolated primary cells of non-treated metacystode vesicles were used for injection into stem cell depleted metacystode vesicles. 'Control (positive)' is non-treated metacystode vesicles; 'Control (negative)' is treated vesicles without injection of primary cells. Primary cells were injected in the sample 'injected Pc' whereas in the sample 'added Pc' the primary cells are simply added to the A4-media for co-culture. EdU (50 μ M) staining was carried out for 5 hours, 5 days after injection. Proliferating cells are labelled red. DAPI staining (blue) was used for labelling of nuclear DNA.

As can be seen in Fig. 6.0.2., BI 2536 treatment for 21 days was effective in eliminating proliferating stem cells in metacystode vesicles. After injection of primary cells (stem cells) and an incubation time for 5 days, the GL appeared completely repopulated by proliferating cells (Fig. 6.0.2). To exclude that the injection process itself led to an activation of 'dormant' stem cells, vesicles were also injected with A4 medium alone (Fig. 6.0.2. Control neg.). When the stem cells were only added (from outside) to the vesicles, no repopulation occurred (Fig. 6.0.2 added Pc). However, like in the negative control (Fig. 6.0.2) no positive signals were obtained for vesicles how have only been punctuated by a needle (mechanical stimulation, data not shown). Taken together, these experiments indicated that it is indeed possible to successfully repopulate stem cell deprived metacystode vesicles using the injection technique.

In addition to the repopulation of stem cell depleted metacystode vesicles with isolated primary cells of the same genetic background (Isolate H95; i.e. same parasite isolate), injection experiments with primary cells of other parasite isolates were performed (isolate GH09, Ingrid, J2012). To this end, metacystode vesicles of the isolate H95 were stem cell depleted and repopulated with primary cells of isolates GH09, J2012 or Ingrid. In all cases, the stem cells integrated into the stem cell depleted germinal layer of the metacystode vesicle and underwent proliferation (data not shown).

6.1 Additional inhibitor studies on *E. multilocularis*

Several other approaches on potential target proteins of *E. multilocularis* have been tested. All of the listed inhibitors have been tested for one week on metacystode vesicles and primary cells in A4-media under axenic conditions. All inhibitors have been used in a first trial in the following concentrations of 50 μ M, 25 μ M, 10 μ M and 1 μ M.

Name	CAS number	Protein target	Metacystode vesicles	Primary cells
Artemisinin	63968-64-9	target is not yet identified	neg.	neg.
BA-6; BA-3-35; BA-3-29; BA 3-61; BA 103; BA 3-45	University of Siena (Marco Radi)	DDX3, a DEAD-(Asp-Glu-Aal-Asp)-box RNA helicase [136]	neg.	neg.
BIRB 796 (Doramapimod)	285983-48-4	p38alpha MAPK (human)	neg.	neg.
Lufenuron	103055-07-8	chitin production and influences the exoskeleton production in many insects	neg.	neg.
2-Methoxyestradiol (2-MeOE2)	362-07-2	Cellular microtubule depolymerisation [137]	It was shown in a former study on <i>E. multilocularis</i> that metacystode vesicles treated with 2-ME2 (2–10 μ M) showed an adverse effect in the viability on the parasite [138]. These results could not be validated in my experiments, also for primary cells.	
Mycophenolic acid	24280-93-1	5'-Inosine monophosphate dehydrogenase (human)	neg.	neg.
Oridonin	28957-04-2	AML1-ETO (AE) fusion protein	neg.	neg.
Phenytoin, Zentropil® from Sandoz Pharmaceuticals GmbH	57-41-0	Blocking of voltage-dependent and voltage-gated sodium channels (human)	neg.	neg.
TAK-715	303162-79-0	p38alpha MAPK (human)	neg.	neg.

6.2 Characterisation and cloning of a Venus flytrap kinase receptor gene (*emvkr*) of *E. multilocularis*

The first member of the invertebrate-specific family of VKR was identified in the blood-dwelling fluke *Schistosoma mansoni* in 2003 [103]. Features of this new family of Tyrosine kinases receptor (RTKs) are the presence of an extracellular VFTM with homologies to similar modules in GABA_B receptors, which is connected via a single transmembrane domain to an intracellular TKD that is related to the TKD of Insulin receptors (IR-TKD). This kind of RTKs have only been described in invertebrates to date, with the feature that the extracellular insulin receptor domain (IR) are more distantly related to human IR-TKD than the TKD of invertebrates. This fact opens up the possibility to study the function of those RTKs and their potential role as a new protein targets for the development of drugs.

In *S. mansoni*, two VKR are already described (SmVKR1 (SmRTK1) and SmVKR2) [103, 109] and the published protein sequences (SmRTK1 Smp_019790 (previously known as Sm00.scaff00045.0290) supercontig Schisto_mansoni.SC_0136: 209761-238744) were used in this work to identify VKRs in *E. multilocularis*. *In silico* analysis, BLASTP genome sequence mining of the available genome data of *E. multilocularis* (<http://www.genedb.org/Homepage/Emultilocularis>) using the full-length amino acid sequence of the *S. mansoni* SmVKR1 (SmRTK1; AAL67949 (EMBL) Q8WSM2 (UniProtKB)) identified a single orthologous gene (EmuJ_000619800.1; supercontig pathogen_EMU_scaffold_007728: 4664450-4691242) encoding the protein EmVKR, with highest homologies to SmVKR1 (e-value 4.5e-256). A second hit by BLASTP analysis identified the ortholog of the insulin growth factor 1 receptor beta (EmuJ_000981300, supercontig pathogen_EMU_scaffold_007780: 4236535-4260814) of *E. multilocularis* (e-value of $1.8e^{-34}$ to SmVKR1), which was recently characterised and designated EmIR2 [33]. Hence, in contrast to the situation in *S. mansoni*, where two VKR-encoding paralogs are present, *E. multilocularis* only appears to encode one ortholog of the VKR family.

The EmVKR-encoding gene, *emvkr*, spans a genomic region of 26.792 bp. Analysis of the exon-intron structure of the gene *emvkr* structure identified 17 exons and 16 introns that displayed the canonical GT-AG dinucleotide sequence motifs at the splice donor and acceptor sites, respectively (Figure 6.2.1A). *Trans*-splicing and alternative splicing of this gene was not observed in analyses of the RNA-deep sequencing transcriptome data (data not shown). Further analysis of the RNA-deep sequencing transcriptome data represents the expression values of *emvkr* in all larval stages (Fig. 6.2.1 B) No significant differences between the larval stages are observed. The gene *emvkr* shows a similar expression profile in all larval stages also in the semi-qualitative RT-PCR approach (Fig. 6.2.1 C). The *emvkr* cDNA was cloned from total RNA isolated from metacystode vesicles (isolate H95) using RT-PCR. The total length of the open reading frame of *emvkr* was 5.112 kb (excluding poly-A tail), encoding a protein of 1703 amino acids and a calculated molecular mass of 190.5 kDa. Analysis of the protein sequence by SMART software (<http://smart.embl-heidelberg.de/>) identified an N-terminal ANF-receptor domain (aa 386-722), described as an extracellular ligand-binding domain present in many bacterial amino acid binding proteins and of a wide range of receptors as well as GABA_B receptor [139]. The identified amino acid sequence showed similarities to VFT-Motifs. Furthermore, a transmembrane helix region (aa 928-950) was identified, followed by a C-terminal TKD (aa 982-1256).

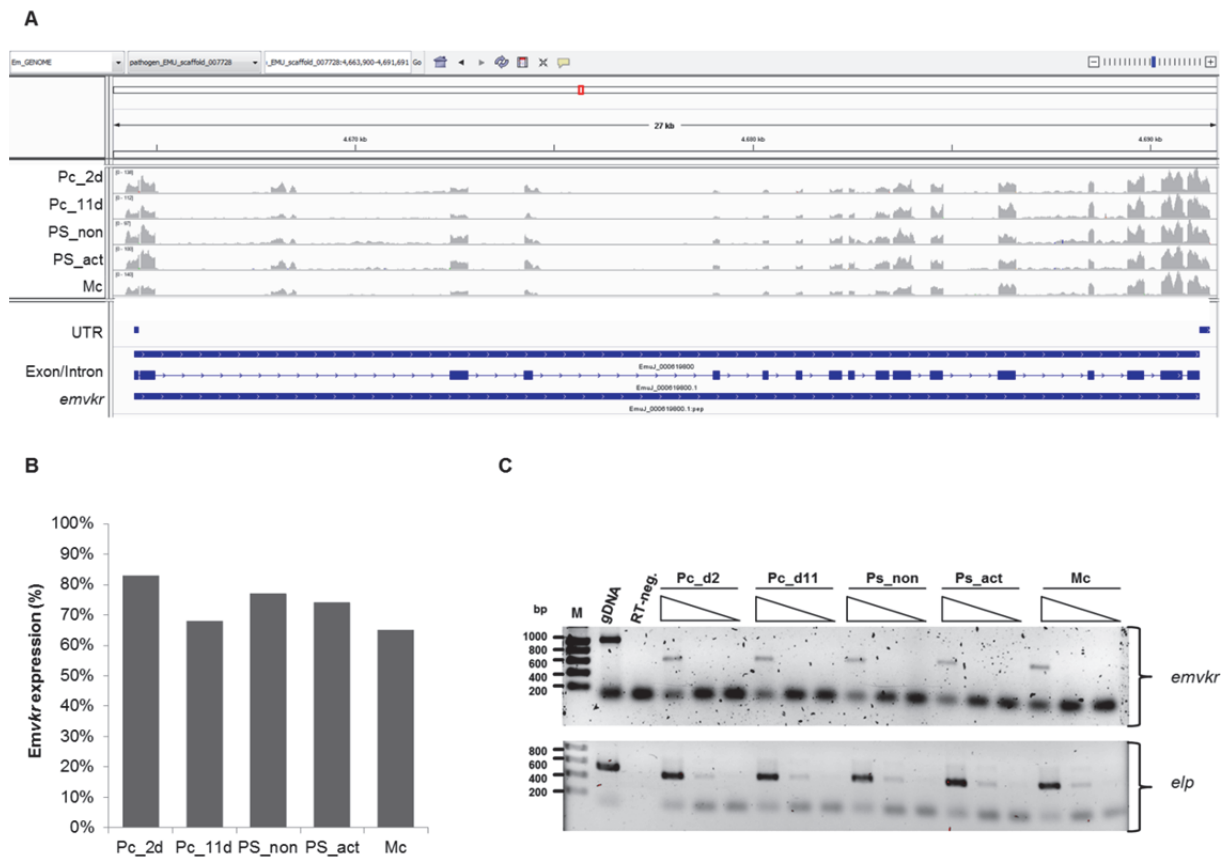
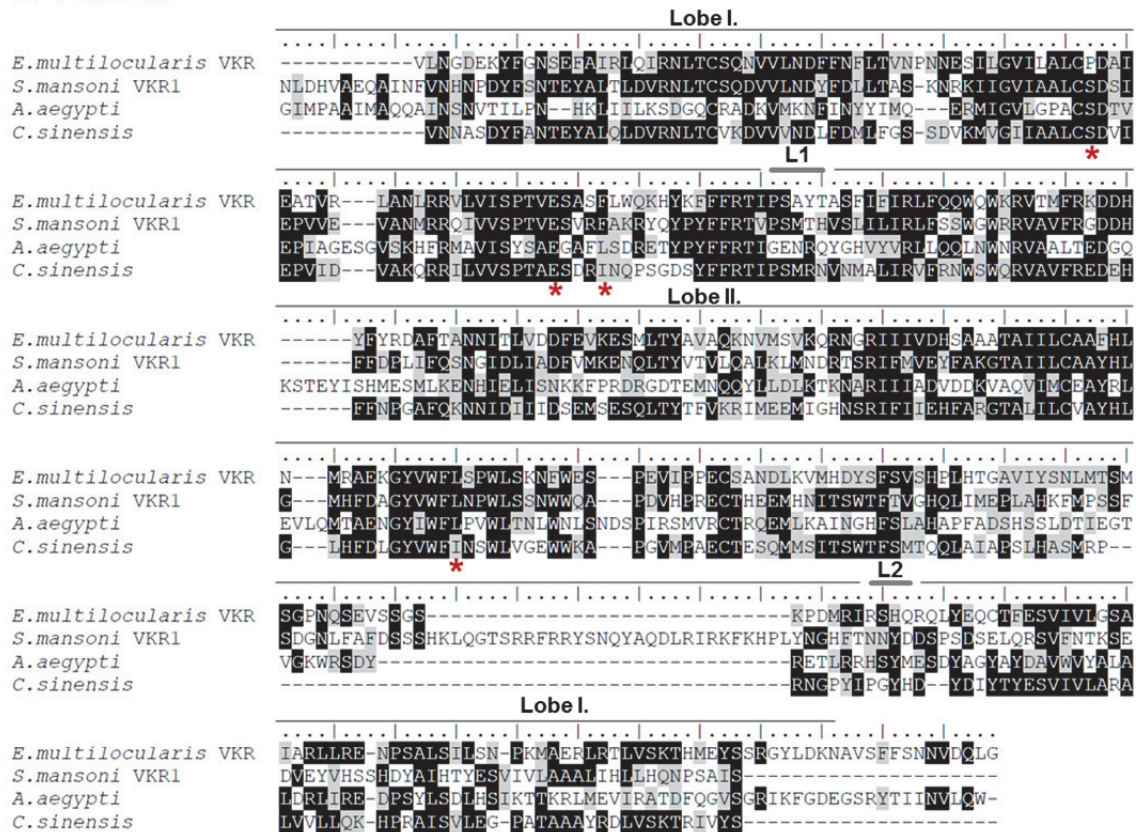


Figure 6.2.1 Transcriptome expression pattern of *emvkr* in *E. multilocularis* larval stages. (A) RNA-deep sequencing transcriptome data represents the expression values of *emvkr* in all larval stages from primary cell cultures (Pc) from day 2, and 11 (d2, d11), dormant (Ps_non), and activated protoscoleces (Ps_act), as well as *in vitro* cultivated metacystode vesicles (Mc). Untranslated regions (UTR) in the 5' and 3' end are highlighted by blue boxes, like the exon-intron structure (boxes and lines) of the gene *emvkr* spanning over a genomic region of 26792bp. (B) *emvkr* expression profile in parasite larvae was given in a graphical view by expression pattern in percent based upon fpkm (fragments per kilobase of exon per million fragments mapped; merge of all libraries analysed). (C) RT-PCR analysis of *emvkr* expression in parasite larvae. Total RNA was isolated from larval stages as indicated for (A). Equal amounts of isolated RNA were reverse transcribed to cDNA and subjected to gene-specific (RT)-PCR for *emvkr*. The house keeping gene *elg* was used for normalisation. The cDNA was diluted 10-fold in 1, 1:10 and 1:100 for PCR. Genomic DNA (gDNA) served as a positive control and purity of DNA contamination during RNA isolation. Non-reverse transcribed RNA was used as a purity control for DNA contamination during RNA isolation. Marker sizes are indicated on the left. (1% Agarose; EtBr stained). Note Illumina sequencing were only performed only once for each sample.

VFT-module



Tyrosin kinase domain

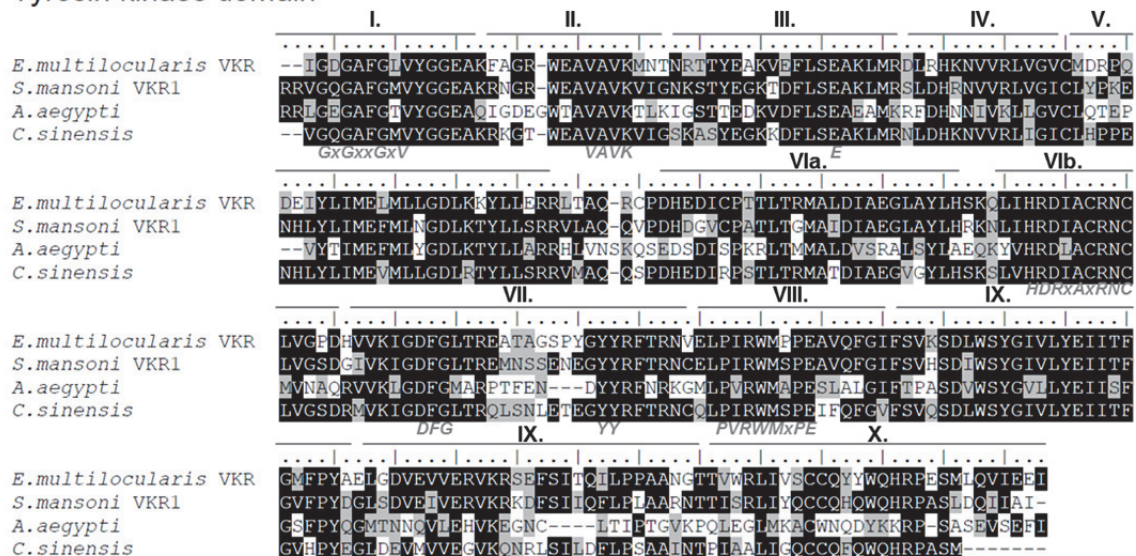


Figure 6.2.2 Amino acid sequence comparisons for EmVKR VFT- and TKD-domains. Multiple sequence alignment of two highly conserved regions in the VKR, the VFTM (VFT-module) and the TKDs from VKR of different taxa. Orthologous proteins of the Venus flytrap receptor were identified by BLASTP in *E. multilocularis* (EmuJ_000619800.1), *S. mansoni* (AAL67949.1), *Aedes aegypti* (DAA06509.1) and *C. sinensis* (GAA27163.2). Amino acid sequence was analysed by the SMART programme and orthologous regions containing the VFT-module and the Tyrosine kinases were extracted and aligned by ClustaW. Identical amino acid residues are shown in white on black background. Similar amino acid residues are shown in black on grey

background. The two Lobes of the extracellular VFT-module are indicated (I. & II.), interrupted by three flexible regions (L1, L2, L3). Asterisk (red) in the alignment indicate residues important for substrate binding in known GABA_B receptors [103, 140, 141]. The intracellular TKD includes the 11 sub-domains of the kinases as defined by Hanks and Hunter (I-XI) [66]. Relevant residues in the amino acid sequence for ATP binding domain (GxGxxGxV) and its stabilisation (VaV_kX₁₆E), the catalytic loop for the phosphor transfer (HRDXARN), the Mg²⁺-binding side (DFG) and the consensus sequence for tyrosine kinases (PVRWMXPE) and the present juxtaposed autophosphorylation site (YY) is subscribed in the alignment by grey bold letters.

Orthologous proteins of the Venus flytrap receptors from *E. multilocularis* (EmuJ_000619800.1), *S. mansoni* (AAL67949.1), *A. aegypti* (DAA06509.1) and *C. sinensis* (GAA27163.2) were identified by BLASTP search using *S. mansoni* as the initial amino acid sequence [108]. In all orthologous proteins, the N-terminal region of the receptor VFT-module (ANF-receptor, 386-722 aa), with similarities to the extracellular human GABA_B receptor was identified. This external domain is linked by a single transmembrane region to an intracellular tyrosine kinase that showed similarities to the tyrosine kinases of human IRs. The originally described and characterised Venus flytrap kinase receptor of *S. mansoni* (SmVKR1) showed an overall identity of 33.9% when compared to the full amino acid sequence of EmVKR. Analysis of the two major conserved protein regions gave an identity of 32.9% for the extracellular VFT-module (Similarities: 0.4822335 Similarity Matrix: BLOSUM62) and an identity 69.7% for the intracellular Tyrosine kinases domain (Similarities: 0.7970480 Similarity Matrix: BLOSUM62) between EmVKR and SmVKR1. Further analysis of the sequence of the two major conserved domains, containing the extracellular VFT-module and the intracellular TKD have been used for a multiple sequence alignment to identify identical and similar aa residues. As indicated in the aligned sequence of the VFT-module important regions (Lobe I. & Lobe II.) of the extracellular domain were identified and residues known to be essential for the substrate binding for GABA_B receptors were identified in EmVKR (indicated by asterisk in Figure 6.2.2).

The TKD of EmVKR contains all 11 sub-domains (I-XI) representative for RTK as described by Hanks and Hunter in 1995 [66]. Strong indicators for a RTK domain are particularly the amino acid sequence of H₁₁₁₅RDXARN₁₁₂₃ and P₁₁₆₀VRWMXPE₁₁₆₇, present in sub-domains VIb and VIII. A third important motif in the kinases domain is the canonical G₉₈₉xGxxGxV₉₉₆ motif, necessary for ATP binding and the stabilisation residues for ATP binding (V₁₀₁₀aV_kX₁₆E₁₀₃₀). In addition, the existence of the D₁₁₃₅FG₁₁₃₇-motif involved in the Mg²⁺-binding is an essential factor that is also present in the kinases subdomain VII flanked by two hydrophobic amino acids G₁₁₃₄ and L₁₁₃₈. Furthermore, in some RTK, an additional motif was characterised that was also described for IR tyrosine kinases domains, the juxtaposed autophosphorylation site (Y₁₁₅₀ Y₁₁₅₁).

The Venus flytrap kinase of *E. multilocularis* have been previously mentioned by Vanderstraete *et al.* (2013), in a genome wide screen for identifying orthologs of this receptor type in other organisms [107]. Within this study, I have been able to show that the Venus flytrap kinase showed all essential aa residues belonging to this new RTK family [103, 107]. In future experiments, it should be investigated whether EmVKR is suitable to be expressed in *Xenopus* oocytes and can be activated by amino acids like L-arginine and blocked by the previously-described inhibitor AG1024 [108, 110].

6.3. AG1024 (Tyrphostin), a potential Venus flytrap kinase inhibitor

Insulin-like growth factor receptors are cellular membrane receptors that dimerise after binding of external stimulating factors (such as insulin or IGF). Dimerisation of the intracellular Tyrosine kinase receptor leads to a so-called ligand-stimulated receptor autophosphorylation and activation of the kinase domain. Due to this activation, binding sites are formed for intracellular adaptor proteins that transduce the extracellular signal downstream in the cascade and often promote cell survival and cell proliferation. Suppressing the activation steps for autophosphorylation is a common drug target strategy and used in many cancer studies [142]. The synthetic protein tyrosine kinase inhibitor AG1024 (Tyrphostin) was initially identified to block the autophosphorylation of the insulin-like growth factor 1 (IGF-1) receptor [143]. In several studies, AG1024 inhibited the proliferation of the cell cycle and induced apoptosis in a human breast cancer cell line MCF-7 in a time-dependent manner [144]. In addition to the inhibitory action of AG1024 on IGF-1R, blocking of IR was also noticed [110].

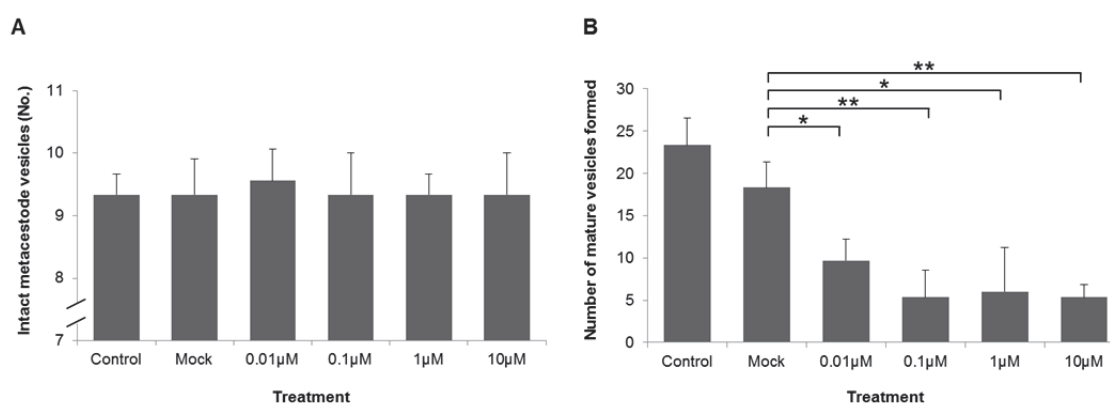


Figure 6.3.1 AG1024 does not affect the integrity of metacastode vesicles but inhibits the formation of metacastode vesicles from primary cell cultures. (A) Metacastode vesicles were co-cultivated over 10 days in the absence Control, Mock and in the presences of increasing concentrations of the inhibitor AG1024 (0.01 μM, 0.1 μM, 1 μM, 10 μM). Metacastode vesicle integrity was inspected by light microscope. (B) Primary cell cultures were established from intact metacastode vesicles and incubated under ideal growth conditions (A4 medium) treated with different concentrations (0.01 μM, 0.1 μM, 1 μM, 10 μM) of AG1024 or non-treated Control and Mock indicating cultures with DMSO (without inhibitor). Formation of new metacastode vesicles was observed by light microscope and counted on day 14. (A, B) All conditions were assessed in three different biological replicates with at least three technical replicates. *(p,0.05); **(p = 0.001–0.01) (Student's t-test). (A, B) 'Mock' indicating cultures with DMSO (without inhibitor).

In both organisms *S. mansoni* and *E. multilocularis* two types of IRs have already been described [105] [33]. In addition to presences of the family of IRs, the discovery of the uncommon VKR (SmVKR1 and SmVKR2) with the containing intracellular tyrosine kinase (TK) domain similar to that of IRs represents a new class of RTK. In *E. multilocularis* one of the VKR (*emvkr*) could be identified as part of this work. This class of RTK are interesting candidates for the development of novel drugs, based upon the conserved intracellular TKD and the availability of chemical compounds acting on IR-TKD. In a previous study by Vanderstraete *et al.* (2013), several inhibitors for the TKD of IRs like

AG1024 and HNMPA(AM) 3 were tested for their ability to inhibit the enzymatic activity of *S. mansoni* SmIR1, SmIR2, SmVKR1 and SmVKR2 using the *Xenopus* oocyte expression system [110]. These authors were able to show that AG1024 and HNMPA(AM)3 are able to inhibit GVBD in low micromolar concentrations (<10 μ M). Furthermore, treatment with AG1024 induced apoptosis in schistosomula and impairing of adult worms as well as a decrease of egg laying in a dose and time-dependent manner [110]. Within this study they were also able to show that AG1024 acts upon the IRs (SmIR1 or SmIR2) and the VKRs (SmVKR1 or SmvKR2), with slight differences in the number of oocytes that underwent GVBD [110]. Moreover, the study observed a similar inhibitory effect with another inhibitor HNMPA(AM) 3, which was tested in parallel in *E. multilocularis* [33]. It was assumed, that this inhibitor is acting on the two present IRs (EmIR1 and EmIR2) in *E. multilocularis*, but other inhibitory effects could not be excluded within this study.

To investigate possible anti-*Echinococcus* effects of AG 1024, the compound was tested on metacestode vesicles and primary cells. As shown in Figure 6.3.1 AG-1024 does not show lethal effect on metacestode vesicles under axenic condition within 10 days of treatment (Fig. 6.3.1A). However, in case of the primary cell culture system, treatment with AG1024 showed a statistical significant inhibition in the formation of metacestode vesicles at nanomolar concentrations (10 nM and 100 nM) (Fig. 6.3.1B). In summary, an inhibitor effect of AG1024 could be observed in the formation of metacestode vesicles. If AG1024 is active against the IRs or the Venus flytrap kinase receptor could not be addressed by this experiment, but likely, since it also affects both types of receptors in *Schistosoma* [110].

6.4 Further work on VKR

The full coding sequence of the VKR (EmuJ_000619800.1; 5112bp) was sub-cloned into the storage plasmid pJET1.2/blunt Cloning Vector (Fermentas) (ASP-054) and the expression vector pSecTag2/HygroA (Invitrogen) (ASP-055). The latter vector can be used for expression of the fusion protein in mammalian cells like human embryonic kidney 293 (HEK 293) cells for purification and detection. In a previous study by Ahier *et al.* (2009) focusing on analysing the functions of the Venus flytrap kinase receptor of *Apis mellifera* (AmVKR; ACF34409.1), the VKR was expressed in mammalian cells (immunoprecipitated from detergent lysates of HEK293) and *Xenopus* oocytes (TKD). Through this method, we want to ascertain what is the stimulating factor of EmVKR according to the previous experiments by Ahier *et al.* (2009) [108]. Newest experimental data suggest that EmVKR does not bind to the amino acid Arginine, as was shown for Venus flytrap kinase of the *S. mansoni*. It seems very likely that EmVKR utilises another ligand, perhaps specific to *Echinococcus*.

7. Discussion

7.1 Overview

In the past decades, cellular signalling cascades have been studied intensely in metazoan organisms. Findings arising from these studies influenced medical applications and helped to understand some basic aspects of cellular biology [65, 69, 145, 146]. Metazoan cells are frequently influenced by extracellular signals that bind to their surface, followed by either an activation or inhibition of responsive signalling cascades. A variety of respective cell signalling pathways are highly conserved across all metazoan taxa and several of these pathways have been identified in parasitic helminths [33, 105, 126, 147-153]. For example, in the past ten years, cell signalling pathways of the Mitogen-activated protein kinase (MAPK) cascade, as well as Transforming Growth Factor TGF- β , Fibroblast growth factor (FGF), Epidermal growth factor (EGF) and Insulin signalling have been identified in the tapeworm *E. multilocularis* [33, 70, 126, 149].

Many signal transduction processes are carried out by protein kinases, which are responsible for the transfer of a phosphate to the downstream substrate. In mammalian cells, there are approximately 518 protein kinases (1.7% of the human genome) present in different cell types and most of them have an influence on signal transduction pathways. In particular, cell proliferation and differentiation are mechanisms that crucially involve protein kinases [154-156]. Thus, many studies have shown that kinase signalling mechanisms are affected in cancer cells, often resulting in a constitutive activation or inactivation of the pathway, while it has been further observed that such signalling processes can be blocked by small-molecule inhibitors [157, 158]. The first respective inhibitors were derived from natural sources such as bis-indoylmaleimide staurosporine, which acts upon protein kinase C (PKC) [142]. Further investigations showed that staurosporine is not acting specifically on one single protein kinase but rather has a broad inhibitory effect on >90% of all kinases [142]. This lack of specificity prompted further investigations on the molecular action of staurosporine. It thus emerged that staurosporine acts as an ATP competitive inhibitor by out-competing the high cellular concentration of ATP from the highly conserved ATP binding pocket of the protein kinase. Today, most kinase inhibitors are designed with a greater specificity for binding in the kinase pocket with remarkable results on cancer therapy [65]. Based upon the plethora of inhibitors generated in human cancer research, it was possible to show in several studies with ATP competitive inhibitors that these drugs have an inhibitory effect on the orthologous proteins of the tapeworm *E. multilocularis* [33, 70, 123]. These studies suggest that inhibitors against human proteins, or modifications thereof, could be a viable strategy for searching for new chemotherapeutic options against AE.

7.2 Limitations of the current chemotherapy against alveolar echinococcosis

The human parasitic infection AE is linked to an asymptomatic incubation period of 5–15 years until the first symptoms appear. AE development of the primary tumour-like lesions is driven by the asexual growth of the larval stage, the metacystode, which in most cases affects the liver of the

patient [30, 159]. The current treatment options in AE chemotherapy rely on benzimidazole derivatives, such as Albendazol (ABZ) and Mebendazol (MZ) [30, 49]. Despite intense research into alternative anti-parasitic drugs, no reliable alternatives to ABZ and MZ are currently available [55, 73]. Furthermore, the chemotherapeutic treatment by Albendazol and Mebendazol in patients is difficult to evaluate given that no methods exist to determine whether all parasite cells are killed during the treatment. The urgent need for alternative chemotherapy is underscored by the fact that ABZ chemotherapy is associated with adverse side-effects, is parasitostatic, associated with high recurrence rates and often has to be given lifelong [49, 55, 57, 159]. The main reason for adverse side-effects of the drug is the high conservation of the protein targets, the β -tubulins, between host and parasite (>80%) [58, 59]. The high similarities of parasite and host β -tubulin are the reason why ABZ, can only be applied in parasitostatic doses to the patient. In addition, the drug – which is orally-administered in most cases – shows a low bioavailability, based upon the fact that it is poorly resorbed. A consequence of the low doses of ABZ is an ineffective AE chemotherapy, which only reaches parasitostatic concentrations [55, 127].

In mammalian tissues, multipotent stem cells are responsible for the development of different tissue-specific differentiated cells. In cestodes, a population of pluripotent stem cells (also called germinative cells or undifferentiated cells) are responsible for the development of all differentiated cell types and for infiltrative growth and metastasis formation of *Echinococcus* larvae within the host organs [40, 41, 44]. A recent publication by Koziol *et al.* (2014) showed that the primary cell culture contains up to 80% of stem cells of the parasite [32]. Moreover, these authors showed that the germinative cells exhibit a typical stem cell character by expressing several genes from the *argonaute* and *nanos* family [32]. Indeed, the expression of these genes is a typical component of the germline multipotency programme (GMP) of metazoan stem cells, but some of otherwise highly conserved GMP components, such as *vasa*, are absent or highly modified in parasitic flatworms [60].

In *in vitro* studies for the development of novel anti-parasitic drugs, the chemical lead compounds are often tested on protoscoleces, metacestode vesicles and in primary cell culture [33, 70, 120, 123, 160]. It was observed that the current anti-AE chemotherapy is ineffective in eliminating the stem cell population of the parasite, which leads to remission of parasite growth as soon as therapy is discontinued. Unpublished data showed that these stem cells are almost unaffected at high concentrations of ABZ in a cell-killing assay in the first days after primary cell isolation (Sarah Hemer – Doctoral thesis, 2012). ABZ did not affect the cellular integrity of primary cells when treated over a short time (48 hours) in our primary cell culture system, which is a model system for the early development of metacestode vesicles.

The limited activity of benzimidazoles on the parasite stem cells have also been indirectly observed in previous *in vitro* studies by Ingold *et al.* (1999) and Stettler *et al.* (2003) [57, 161]. In addition to the *in vitro* studies by Ingold and Stettler a recent publication by Küster *et al.* (2013) also supports the low bioavailability of ABZ of orally treated mice *in vivo*, which underlines the assumption of a primary cell insensitivity to ABZ, where ABZ has low effects on stem cells and ABZ plasma concentrations are low [162]. They showed with a new *in vivo* approach that the growth of a secondary subcutaneous infection with AE can be suppressed with ABZ (parasitostatic effect) but a complete cure of AE was not

observed, which indicates the low *in vivo* activity of ABZ on the parasite's stem cells [162]. Thus, these results are in line with the results of the *in vitro* primary cell culture and indicate that the growth of metacystode vesicles *in vivo* is suppressed but simultaneously the survival of stem cells during the treatment by ABZ is not affected. Long-term experiments within this new *in vivo* mice model system have not been carried out [162]. It would be interesting to observe whether the parasitostatic effect of ABZ is abolished after the interruption of the treatment and if recurrence of metacystode vesicle growth is generated by surviving stem cells, which remained relatively unaffected.

We now want to address the question derived from this experimental approach as to what is causing the insensitivity of parasite stem cells to benzimidazoles. Phenotypes of benzimidazole resistance have been previously observed in other parasites, such as *Haemonchus contortus*, although the reason for the resistance in this parasite is based upon a genetic mutation of a β -tubulin gene [163]. Suggestions for a benzimidazole insensitivity of stem cells of *E. multilocularis* base on a specific expression of a β -tubulin isoform (*tub-2*). Brehm *et al.* (2000) verified by a genomic and transcriptomic analysis that three isoforms of β -tubulins are present (Tub-1 (EmuJ_000202600), Tub-2 (EmuJ_000672200) and Tub-3 (EmuJ_000202500)) [58, 127]. All three β -tubulin genes have 99% identical amino acids, as shown in Fig. 5.9.1. As indicated in Fig. 5.9.1 (red star), Tub-1 and Tub-3 contain the same amino acid motif at position 200 (Phenylalanine). In direct comparison, Tub-2 shows a Tyrosine at this position. It has previously been reported that this specific change at this amino acid position is most likely the reason for the insensitivity of Tub-2 to benzimidazoles [58, 59, 127, 132]. This suggestion is supported by the fact that a higher binding affinity of benzimidazoles to β -tubulins was observed by a Phenylalanine at this position [59, 127]. At present, the binding site on β -tubulins to benzimidazoles is not known. Could this natural change in the amino acid sequence of β -tubulins be the reason for the infectivity of primary cells (e.g. stem cells) to high concentrations of benzimidazoles, further causing regeneration of the parasite tissue in patients?

Further *in silico* analyses indicate the presence of ten β -tubulin genes in *E. multilocularis* (Fig 5.9.1). The ten β -tubulin genes include the three genes already characterised by Brehm *et al.* (2000), namely *tub-1*, *tub-2* and *tub-3*, which show a high expression profile in the larval stages (Tab. 5.9.1) [58]. The expression pattern of the β -tubulin genes in each larval stage was further analysed by RNA-Sequencing data, which showed that *tub-2* has a high expression in primary cell cultures at day 2 and day 11 (Fig. 5.9.2) [60], known to be enriched by parasite stem cells (80%) [32]. Overall, the semi-quantitative RT-PCR approach was not sufficiently sensitive to detect the finely regulated genetic expression between all larval stages, as identified in the RNA-Deep sequencing data (Fig. 5.9.3) [60].

As previously shown by Koziol *et al.* (2014) is it possible to deplete of stem cells from metacystode vesicles by treatment with Hydroxyurea (HU) [32]. A similar effect was observed with the PIK1 inhibitor BI 2536 acting on parasite stem cells, and will be discussed in a following paragraph; a long-term treatment over 21 days should eliminate stem cells from metacystode vesicles. If Tub-2 is specifically expressed in stem cells, we assume to observe an expression profile change in the RNA transcription pattern. We observed a salient contrast in metacystode vesicles, which were treated over 21 days with BI 2536 (50nM) (Fig. 5.9.4). The treatment with the inhibitor BI 2536 does not influence the presence of cells expressing *tub-1* and *tub-3*, although the expression of *tub-2* was suppressed (Fig. 5.9.4). We

assume that, in correlation to the staining of proliferating cells by an EdU pulse experiment, all stem cells have been depleted (Fig. 5.7.1). These results are confirmed by the RNA-Sequencing data of Uriel Koziol (unpublished, personal communication), in which stem cells were shown to have been depleted from metacestode vesicles by treatment with HU. While this experiment highlighted that the expression of *tub-2* is related to stem cells, it also provides evidence why stems cells with the described protein modification of the β -tubulin show benzimidazole insensitivity.

Finally, the identification of a new potential drug target against AE is a crucial issue and newly found inhibitors should target the parasite's stem cells, given their relevance for disease progression and resurgence [75, 127].

7.3 Targeting of parasitic stem cells by inhibition of the Polo-like kinase 1 (*emplk1*)

Aware of the importance of parasite stem cells and their decisive influence on growth and development of the parasite tissue, we focused within this work on a new druggable enzyme that plays a key function in the proliferation and differentiation of cells. Similar to extracellular signal transduction, the cell cycle is regulated by kinases that execute the transmission of molecular switches. One of the best-studied kinase families involved in the cell cycle is the Polo-like kinase family [72, 77, 80, 90, 156]. One sub-member of this family is the Polo-like kinase 1 (Plk1), which triggers the G2/M transition [79, 93, 164]. Several cancer studies showed that an increase of enzymatic activity by these kinase force the growth of cancer tissue by influencing the proliferation of cells [165]. Often this observation of a higher expression of *plk1* is secondary effect, caused by a higher proliferation rate of the tumour. Due to this central function, inhibitors have been designed to inactivate this kinase in several types of cancers tissues [71, 85, 96, 128, 134, 166]. By analysing the *E. multilocularis* genomic and high throughput RNA-Sequencing data, an ortholog of *plk1*, *emplk1* (EmuJ_000471700) was identified, showing a higher expression level in primary cells, which is likely to be correlated to the expression of Plk1 in proliferating cells (Fig. 5.3.1). This was confirmed by an RT-PCR showing a high expression of the gene in the primary cell culture at day 2, day 5 and day 11 (Fig. 5.3.2). In direct comparison to other parasite flatworms like the trematode *S. mansoni* the Plks have also been studied intensively [102, 167, 168]. *S. mansoni*, SmPlk1 showed considerable homologies to the mammalian Plk1 [102]. Long *et al.* (2010) demonstrate a high expression of the gene in female vitelline cells, oocytes and in male spermatocytes. These results indicate that SmPlk1 has a prominent role in the proliferation cells like neoblasts with a key role for schistosome mitosis and/or meiosis [102, 168]. In this context Koziol *et al.* (2014), was able to demonstrate that mitotically active parasite stem cells are distributed throughout the germinal layer, brood capsule, protoscolex buds and at the base of developing suckers [32]. These experiments have been carried out by an *in situ* hybridisation (WMISH) experiment that was recently established on metacestode vesicles and protoscoleces [32]. Furthermore, Koziol was able to show that the specific expression of *emplk1* in metacestode vesicles is obtained in regions of parasite larvae that typically contain large numbers of proliferating stem cells, such as germinal layer

cells, early brood capsules and developing protoscolecocytes [132]. In summary, these data strongly indicate that *emlplk1* is specifically expressed in parasite stem cells.

Regarding the analysis of amino acid structure of EmPlk1, all relevant amino acid residues that are typical for protein kinases and the Plks could be identified (Fig. 5.1.2) [66]. However, the presence of relevant amino acid residues in the sequence EmPlk1 alone does not confirm their activity in a cellular context. Based upon previously-described protein-interaction partners in humans that are involved in the activity of the Plk1, *in silico* analysis has been carried out to identify upstream interaction partners [79, 93]. One of these interacting proteins is the Aurora A kinase, which acts as an initial activation kinase for Plk1 [91, 93]. Together with a co-factor protein Bora A, the kinase Aurora A binds to the Plk1 and activates the kinase by phosphorylation on T210 (T179 in *E. multilocularis*; Fig. 5.1.2) [91]. In *E. multilocularis*, Aurora A (EmuJ_001059700) and Bora A (EmuJ_000804300) have been identified by a BLASTP search. Furthermore, the presence of upstream activating proteins for EmPlk1, such as the cyclin B-bound cyclin-dependent kinases 1 (CDK1; EmuJ_001070150), was identified [77, 80]. These proteins are important downstream factors published as M-phase inducer phosphatase (Cdc25c; EmuJ_001174300) and act as a phosphorylating substrate for EmPlk1. We conclude from the *in silico* analysis of the genome data that a similar regulatory pathway of ortholog proteins in *E. multilocularis* exist.

The second gene identified during the BLASTP search was EmPlk4 (EmuJ_000104700; *emlplk4*), which is also expressed in primary cells, but this protein does not have such a high importance within this study based upon the fact that an effective inhibitor for Plk4 is missing. In a previous study by Long *et al.* (2010) it was already described that a similar set of Plks, SmPlk1 and SmPlk4 (SmSAK) exists in the closely related invertebrate *S. mansoni* [102]. Moreover, these authors showed in a second study a co-expression of both kinases SmPlk1 and SmPlk4 in female ovary and vitellarium and were able to validate a protein-interaction by *in vivo* and *in vitro* experiments, indicating a synergistic effect during meiosis of *S. mansoni* [168]. However, an inhibition of SmPlk4 was not observed by currently available Plk-inhibitors [102, 168]. In addition, a detailed study of the function of EmPlk4 at this time seems irrelevant for the development of novel drug targets against AE. The clinical manifestation of schistosomiasis depends on sexual reproduction in comparison to the infiltrative asexual growth by metacystode vesicles in case of AE.

Our structural analysis of EmPlk1 indicate that all protein domains and catalytic residues are present at the corresponding positions and typical for the Plk1-like subfamily, but they do not demonstrate the *in vitro* activity of the kinase. By heterologous expression in *Xenopus* oocytes, we were able to show by *in vitro* data that an active version of EmPlk1 in *Xenopus* oocytes is able to induce meiosis and GVBD (Tab. 5.4.1). This system was also used to validate whether BI 2536 is able to bind and inhibit EmPlk1, as it was previously shown for SmPlk1 in *S. mansoni* [102].

One of the best-studied ATP competitive inhibitors of Plk1 is BI 2536, which acts at low nanomolar concentrations [128, 169, 170]. In several studies of clinical phase I and phase II, this inhibitor was well tolerated by patients [99, 169, 171]. The inhibitor BI 2536 was tested on several cancer cells *in vitro* with IC₅₀ ranges of 5 to 175 nM [128, 169, 172]. These concentrations are in the same order of magnitude as the measured plasma concentrations of cancer patients ranging from 20 to 200 nM after

48 hours of orally given doses [99, 169, 171]. Based upon the amino acid sequence and the presence of all eight amino acid residues involved in the binding of the inhibitor, we assumed that BI 2536 and the second generation BI 6727 are able to bind to EmPlk1 (Fig. 5.2.1) [95, 97, 98].

In combinatory experiments with the active version of EmPlk1^{T179D} and with increasing concentrations of the inhibitor BI 2536, we observed an inhibitory effect at concentrations of 20 nM (Tab. 5.4.1). This ATP competitive inhibition was concentration dependent and, at higher concentrations of 50 nM and 100 nM, EmPlk1 was no longer able to induce GVBD (Tab. 5.4.1). Taking into account that all necessary amino acid binding residues involved in the inhibitor binding are present, we assume that BI 2536 acts against the orthologous protein EmPlk1 in a similar way as against *S. mansoni* SmPlk1 [102].

Having shown that BI 2536 is suitable to inhibit the activity of EmPlk1, inhibitor effects on primary cells and metacestode vesicles have been analysed by the following experiments. In the case of the primary cell culture, a clear inhibitory effect in the formation of metacestode vesicles was observed (Fig. 5.5.1; Fig. 5.5.2). Even at concentrations as low as 25 nM BI 2536 (a concentration in the same range as the plasma concentrations of patients after 48 hours of oral treatment [99]) the regeneration of metacestode vesicles from primary cells was affected. At higher concentrations of 50 nM and 100 nM, only a few metacestode vesicles were formed within 14 days (Fig. 5.5.2). This data suggest that BI2536 has profound effects on *Echinococcus* stem cells. Regarding the effects of BI 2536 on metacestode vesicles, direct killing was not observed within a week of treatment as compared to other inhibitors like ML3403 or Imatinib (Fig. 5.6.1) [70, 123]. However, long-time treatment over 21 days showed that metacestode vesicles were unable to grow in size (Fig. 5.6.1). To analyse whether the observed reduced growth of metacestode vesicles depends on the inhibition of proliferating stem cells, an EdU pulse approach was carried out according to Koziol *et al.* (2014) [32]. EdU labelling investigates how many proliferating stem cells remain in the tissues of the metacestode vesicle. Metacestode vesicles were treated for 21 days with concentrations of 50nM and 100nM of BI 2536. After five days without treatment, the proliferating cells – stem cells – in the intact metacestode vesicle were stained using an EdU pulse approach (Fig. 5.7.1). Upon further cultivation, these treated metacestode vesicles did not resume growth and their GL was no repopulated by residual (surviving) stem cells. In addition, primary cell cultures isolated from inhibitor-treated vesicles did not develop into metacestode vesicles. A short-term treatment of metacestode vesicles with BI 2536 at 50 nM and 100 nM was also performed (Fig. 5.7.2). After 24 hours of treatment followed by one day of regeneration, we observed that the proliferation rate is significantly reduced within such a short time of inhibitor administration. However, we assume that a short-time treatment even at high concentration of 50nM and 100nM is not sufficiently effective and that proliferating cells were simply blocked and kept probably in mitotic arrest until dissociation of the inhibitor. An experimental approach of isolating primary cells from these short-time treated metacestode vesicles to demonstrate the hypothesised formation of regeneration has not been carried out to date. These results are in line with existing studies; indeed, as previously mentioned, SmPlk1 shows a high expression rate in reproducing organs and morphological changes in testes and ovaries with significant effects on oogenesis and spermatogenesis in adult worms by inhibition of SmPlk1 with 100 nM of BI2536 [102]. The inhibitory

action of the Plk1 inhibitor BI 2536 has been originally observed in several cancer tissue cell lines at low nanomolar (2–25 nM) concentration (EC_{50}) values [100, 128]. Based upon the observation of cancer cell lines, Long *et al.* (2010) already discussed that BI 2536 led to a mitotic arrest in gonads of *S. mansoni* and cells are forced into apoptosis [102, 128]. Similar effects have been observed in cancer cell lines that have been treated with the second generations of this inhibitor class BI6727 [128, 169]. We conclude that BI 2536 is able to arrest the proliferating cells in the mitosis or cause killing by mitotic arrest followed by apoptosis of parasite stem cells but the metacystode vesicles can apparently survive for longer periods without much cell renewal.

Inhibitory effects in the parasite cell culture have also been observed with two other Plk1 inhibitors in preliminary experiments. In addition to the inhibitor BI 2536, we tested the second generation of this kind of inhibitor class, BI 6727, which also acts at nanomolar concentrations, as well as a third ATP competitive inhibitor, GW843682X (ATP competitive), which acts at micro-molar concentrations. Similar to the previously tested inhibitors, metacystode vesicles do not show a phenotypic effect over a short time of treatment (GW843682X Fig. 5.6.2; BI 6727 data not shown). The formation of metacystode vesicles from primary cells was suppressed, but the inhibitor concentrations have been up to 1000-fold higher, which depends on the fact that this inhibitor belongs to another inhibitor class (GW843682X Fig. 5.5.3; BI 6727 data not shown). The reason for a lower binding affinity of GW843682X to EmPlk1 could not be analysed, potential side changes residues of the drug are responsible for the less binding activity. The inhibitor was previously tested on 18 cancer cell lines showing an inhibitory effect at concentrations ranges from 0.02 to 11.7 μ M [173]. An effect at nanomolar concentrations could not be observed on *Echinococcus* cell lines. Further experiments with the inhibitor GW843682X are currently not planned.

Regarding the further development of anti-echinococcosis drug, we intend to increase the specificity of derivatives of BI 2536 for its parasitic protein target EmPlk1. In comparison to the second-generation inhibitor BI 6727 for Plk1, we observed 50% less activity at the same nanomolar concentration, concerning the formation of metacystode vesicles from primary cells and GVBD in *Xenopus* oocytes experiments (data not shown). Concerning all three tested inhibitors acting on Plk1 it has to be mentioned that side-effects by these drugs cannot be excluded due to the strong similarities between the human and parasite protein target.

Therefore, we are currently in the process of crystallising the protein structure of EmPlk1 in combination with both inhibitors BI 2536 and BI 6727 (Chapter 5.8). Having the crystal structure with the bound inhibitor would allow us to identify other chemical lead compounds or estimate which chemical modifications can be made to optimise the chemical structure of BI 2536 or BI6727 for binding to EmPlk1. Overall, it must be possible to specify the inhibitors BI 2536 or BI 6727 for the EmPlk1 enzyme based upon the fact that the amino acid identity to the human Plk1 is only 62%. Compared to the current treatment with benzimidazoles this is a great advantage, because the β -tubulin of humans and parasites share more than 80% identity.

Having shown that the Plk1 inhibitor BI2536 is acting on the parasite stem cells we want to validate the previous data (Sarah Hemer – Doctoral thesis) and show that parasite stem cells are insensitive to benzimidazoles. A further question that we investigated was whether a combinatory treatment *in vitro*

of metacystode vesicles with benzimidazole (ABZ) and BI 2536 would be sufficient to inhibit the regeneration process after primary cell isolation (Fig. 5.9.5). During the regeneration time, formation of new metacystode vesicles in treated samples was not observed but metabolic activity was detected by colour change of the culture media (Fig. 5.9.5C). The formation of intact metacystode vesicles could not be observed after seven days of primary cells isolation (Fig. 5.9.5B). Moreover, a suppression of aggregate formation during the regeneration process was also not seen, as visible in the control samples and previously-described studies [33, 70, 118, 123]. Therefore, it can be concluded that primary cells are able to survive a short time (2 days, Sarah Hemer – Doctoral thesis) of high concentration of ABZ, owing to differences in the expression pattern of Tub-2 as undifferentiated cells. However, we assumed that the regeneration process is also related to differentiated cells, such as muscle and nerve cells, which might have an influence on the regeneration process (personal communication Uriel Koziol). We propose that differentiated cells are unable to proliferate but instead trigger stem cell proliferation as described for other free-living flatworms [174-176]. Finally, the actual function of the differentiated cells in the regeneration process is unknown and should be further analysed regarding the signal cross communication of cells [32].

Taken together, we herein present a new inhibitor BI 2536 acting on EmPlk1 and directly affect the stem cells of *E. multilocularis*. The inhibitor is orally-administered and acts at a nanomolecular concentration in range of the measured plasma concentration of cancer patients. Although the human and the parasite kinases have a high homology of 62%, they are more divergent than the current drug for AE treatment. In conclusion, BI 2536 should act as a lead compound and the structural differences of the amino acid can further be used to optimise the chemical structure for a parasite specific drug.

7.4 Injection of primary cells into metacystode vesicles

The current cell culture of metacystode vesicles is carried out with several isolates of *E. multilocularis* showing different phenotypes during their “life in co-culture”. For example, some of the isolates that have been kept in co-culture over several years, such as the isolate H95, show fast growth of metacystode vesicles but does not produce any protoscoleces. Younger isolates such as GHO9, J2012 or DPZ grow slower but remain able to form brood capsules. The question arises as to what triggers the formation of protoscoleces at a certain point in the metacystode vesicle development and whether isolates like H95 have been genetically handicapped by mutations over the decades of co-culture.

With the herein presented new method of injection of primary cells into stem cell depleted metacystode vesicles and further co-cultivation, I propose that some of the questions can begin to be answered. Furthermore, with further experiments, it might be possible to gain information of the genomic stability (e.g. epigenetic modifications) and influencing factors of stem cells, like regulation protein factors. Does this mean that the possible “regulating protein factor” for the formation of protoscoleces is generated by differentiated cells types such as nervous cells, which are released in the stem cell depleted metacystode vesicle, or is the start point triggered by the parasite stem cell?

Through stem cell depletion of several isolates of *E. multilocularis* and cross-injection of isolate different primary cells, I propose addressing the initial questions concerning what the difference in stimulating the formation of protoscoleces in long-term *in vitro* cultivated metacestode vesicles might be, starting with first experiments on the method of injection of primary cells into stem cells depleted metacestode vesicles.

As previous studies have shown in other organisms such as free-living flatworms, a single stem cell can repopulate a whole organism by proliferation [177-180]. The organisms have previously been treated with ionising radiation, which eliminates all proliferating cells (mainly stem cells, such as neoblasts and germinate cells). In this thesis (Chapter 6), it has been shown that a similar principle in the metacestode vesicle is possible, leaving an intact shell of a metacestode vesicle without any further proliferating cells.

Generated data showing that a long-term treatment of metacestode vesicles with the inhibitor BI 2536 directly affects the survival of proliferating cells and suppresses the growth of metacestode vesicles gave rise to further questions. What happens with a metacestode vesicle, which is depleted from stem cells, when isolated primary cells are injected into the hydatid fluid? Are parasite stem cells able to integrate in to the stem cell depleted germinal layer? Is it possible to repopulate a stem cell depleted metacestode with stem cells of another isolate (e.g. H95 with GHO9) of *E. multilocularis*? In an experimental approach, I tried to generate some preliminary data to address some of the above-mentioned questions. Concerning the question of reintegration of stem cells into stem cell depleted metacestode vesicles I used a previously-described EdU pulse approach to stain proliferating cells (Fig 5.7.1). Primary cells were isolated as before from different isolates of *E. multilocularis*. Stem cell free metacestode vesicles were generated by treatment over 21 days with the inhibitor BI 2536 and primary cells were injected followed by an EdU pulse approach carried out five days later

Initial results showed that the injected primary cells were able to reintegrate and proliferate within the germinal layer of the metacestode vesicle (Fig. 6.0.2). In addition, I could observe that the integration was possible with stem cells of isolates of different genetic background. However, at this experimental point, we are unable to exclude that muscle or nerve cells were also able to reintegrate into the germinal layer, although we know that only proliferating cells such as the parasite stem cells are able to proliferate. Furthermore, we saw that the injection of primary cells had a local distribution at one side of the depleted vesicle. This observation could be caused by the fact that the primary cells were injected from the top of the metacestode vesicle and the sedimentation in the hydatid fluid was forced by gravity. According to the preliminary results, it can be concluded that firstly the reintegration of primary cells (stem cells) into stem cell depleted metacestode vesicles is possible, and secondly, the reintegration is independent from the specific isolate that was used. Nevertheless, this method has to be improved and it will be necessary to use a commercially available micro-injector for further experiments. In further experiments, this method might also be interesting because injecting transgenically manipulated primary cells into the hydatid fluid can reintegrate into the GL of the metacestode vesicle proliferately and form a genetic manipulated metacestode vesicle. I assume that even a single transgenic stem cell of *E. multilocularis* is able to repopulate a whole metacestode vesicle, as indicated by Koziol *et al.* (2014) after treatment with HU [32].

7.5 The Venus flytrap kinase receptor of *E. multilocularis*

The VKR represent a novel family of receptor tyrosine kinases (RTK) that are specific for invertebrates, as originally described in the parasitic platyhelminth *S. mansoni* [103]. The RTK superfamily is characterised as being involved in cellular and developmental processes, including cell-cell communications and tissue organisations in several metazoan organisms [181]. The growth of the parasite by cellular mitogenesis is dependent upon growth factor receptors and hormones, such as IRs, according to mammalian cells [103]. At present, it is already known that growth factors are stimulated by interacting the cellular surface and are relevant for the host-parasite and male and female communication, although less is known about ligands and receptors involved in this process in *S. mansoni* [103]. To date, no IR has been characterised in *S. mansoni* and efforts have been made to identify one of these essential receptors types [105]. Unexpectedly, Ahier *et al.* (2003) identified one uncharacterised membrane receptor that has an extracellular ligand-binding domain connected by a single membrane domain and one IR (previously named SmRTK-2) with an intracellular TKD (SmRTK-1) [103, 105]. This characteristic is typical for RTK showing an extracellular ligand-binding domain, linked to an integral single membrane protein domain to an cytoplasmic ligand-sensitive tyrosine kinases domain [181]. The biological function of SmRTK-1 (SmVKR1) remains unknown, although previous studies have observed that this receptor type is expressed in reproducing organs of parasites, like *S. mansoni* and other invertebrates, mainly insects [108]. A genome-wide analysis highlighted that no *vkr* gene was detectable in vertebrate genomes, which means that this receptor type is invertebrate-specific. In *S. mansoni*, two receptor types of this class have been characterised overall (SmVKR1, SmVKR2) and in Turbellaria genomes a putative truncated version of *vkr* in the planarian *Schmidtea mediterranea* (GenBank: AAWT01078636.1) has been detected [108]. Furthermore an existing gene of *vkr* in *E. multilocularis* was previous mentioned in a study by Vanderstraete *et al.* (2013) using the recently-published genome data of the four tapeworms by Tsai *et al.* (2013) [60, 107]. We now wanted to study the characteristics of this novel RTK in *E. multilocularis* to address the question of what might be the biological role and what are the activating ligands for this receptor. The study of this new receptor might essentially help to understand the development and differentiation of *Echinococcus* cells from larval stage to the adult worm, including the morphological changes necessary also to adapt to changes in the environment.

Analysis by BLASTP genome sequence identified one ortholog receptor type of the VKR (EmuJ_000619800.1; *emvkr*) in the genome of *E. multilocularis*. The gene *emvkr* is constitutively expressed over all larval stages as indicated by analysis of the RNA-Sequencing data (Fig 6.2.1B). Moreover, no unusual gene expression pattern caused by alternative splicing or *trans*-splicing was observed (Fig. 6.2.1A). Deeper analysis of the two domains (the extracellular VFTM (VFT-module) and the intracellular tyrosine kinase) was performed by a structural alignment of the amino acid sequences (Fig. 6.2.2). Furthermore, the amino acid homology of the VFT-module to SmVKR1 and EmVKR identified a similarity of 48%. Phylogenetic analysis identified that the extracellular domain has high homologies to GABA_B receptors (drug receptors) and the intracellular TKD confirmed similarities to IR catalytic domains [103, 139-141]. We were also able to identify previously-described amino acid residues involved in the binding of extracellular ligands from GABA_B receptors [139-141]. Overall, we

expected that the extracellular domain of the VKR might be involved in the binding of amino acids, such as L-arginine, as it was previously identified in the ortholog receptor of the honey bee [108]. However, first experiments by expressing EmVKR in *Xenopus* oocytes suggest that L-arginine is not the binding ligand and activation factor of this receptor (personal communication - Colette Dissous). In further experiments, efforts have to be made to identify the stimulating factor of EmVKR, whereby possibly another ligand - perhaps specific to *Echinococcus* - is used. To analyse this cell culture, supernatant and hydatid fluid has to be tested.

In case of the intracellular domain, we obtained homologies to the TKD (TDK) of the previously identified IRs in *E. multilocularis* [33]. This data was further validated by the amino acid alignment of the TKD in ortholog VKRs (Fig. 6.2.2). We were able to show that this kinases domain fruit fills all typical protein domains and catalytic residues for this enzyme family at the corresponding positions [66, 67]. In direct comparison to the tyrosine kinases domain of SmVKR1, a similarity of 80% was estimated. Moreover, all essential motifs for a dimerisation and autophosphorylation are present as previously describe of the VKR of *Apies mellifera* (AmVKR) [108].

In conclusion, we showed that the extra- and intracellular domain of the herein presented Venus flytrap kinases inhibitor of *E. multilocularis* are functional. Further studies in the activity and potential binding substances on the extracellular domain are under investigation. So far, a second gene of this receptors class that has previously been observed in invertebrates was not identified in *E. multilocularis* [108]. The question of why *S. mansoni* has two VKR and *E. multilocularis* only has one gene could not be answered and remains open; indeed, it might be an evolutionary question of “keep or loss” of gene in general in some species [107].

The characterisation of the unusual Venus flytrap kinase receptor, its specification to invertebrates and its role in the development of the parasite, suggests its ability as a potential new drug target [110]. The presence of a high similarity to the TKD of human IRs opens the possibility to test cancer drugs acting specifically in this domain of the receptor. In a recent study the IR inhibitor, Tyrphostin AG1024 (ATP competitive) was tested to inhibit the VKR. Vanderstraete *et al.* (2013) were able to show that this inhibitor was able to block the functions of the VKR at micro-molar concentrations [110]. Furthermore, they observed alterations of reproductive organs and apoptosis in a concentration dependent manner following treatment with AG1024. A disadvantage of this study is that they were unable to show that this inhibitor is only acting in the two VKR in *S. mansoni*. An inhibition of the two IRs in *S. mansoni* was also given [105, 110]. A second tested IR inhibitor in this study was HNMPA(AM) 3, which has previously been tested in *E. multilocularis* [33]. In *E. multilocularis* this inhibitor suppressed the formation of metacystode vesicles in the primary cells culture and decreased protoscolex viability [33]. A high potency in the killing of metacystode vesicles was not observed [33]. Independent from the chemotherapeutic studies of *S. mansoni* and the knowledge of the synergistic effect of AG1024 on IRs and the VKR, we tested AG1024 in our cell culture on primary cells and metacystode vesicles. Treatment over 10 days does not show any phenotypic effect on the integrity of metacystode vesicles (Fig. 6.3.1A). A concentration dependent inhibitory effect on the regeneration of metacystode formation from primary cells was observed (Fig. 6.3.1B).

Comparing the results from *S. mansoni* and the present experiments in *E. multilocularis*, it is unclear whether AG1024 and HNMPA(AM) 3 only target the IRs and VKRs. In *S. mansoni*, it was observed that AG1024 acts upon both receptors, which suggests that the inhibiting effect in the present study *E. multilocularis* is comparable [110]. The observed effects in the inhibition of the estimated protein targets could be generated by the IRs or the VKR. Unpublished results from RNA-Seq. data of stem cell depleted metacystode vesicles indicate that the VKR (*emvkr*) is not stem cell-specifically expressed (Personal communication – Uriel Koziol). These first observations from *E. multilocularis* are in line with the results from *S. mansoni* and show that an inhibition by AG1024 of the VKR affects the proliferating cells in the reproduction organs of the parasite [110].

The exclusive expression of the VKR in invertebrates makes this kind of receptor an interesting target for the development of novel drugs for AE. Moreover, resistances have also been observed in the current chemotherapy for the parasite *S. mansoni*. One reason for this is the mass-use of the single drug Praziquantel (PZQ) [182, 183]. Independent from the identification as VKR as new potential drug target, a more specific inhibitor of the AG1024 or HNMPA(AM) 3 compounds would help to study the biological role of this new type of receptor class in both parasites.

References:

1. Nakao, M., et al., *Phylogenetic systematics of the genus Echinococcus (Cestoda: Taeniidae)*. Int J Parasitol, 2013. **43**(12-13): p. 1017-29.
2. Gilbert, S.F., *Developmental biology*. Tenth edition. ed. 2014, Sunderland, MA, USA **2014.: Sinauer Associates, Inc. Publishers. xx, 719, G1-26, C1-2, A11-19, S11-50 pages.
3. McManus, D.P., *Current status of the genetics and molecular taxonomy of Echinococcus species*. Parasitology, 2013. **140**(13): p. 1617-23.
4. Kaletta, T. and M.O. Hengartner, *Finding function in novel targets: C. elegans as a model organism*. Nat Rev Drug Discov, 2006. **5**(5): p. 387-98.
5. Beckingham, K.M., et al., *Drosophila melanogaster--the model organism of choice for the complex biology of multi-cellular organisms*. Gravit Space Biol Bull, 2005. **18**(2): p. 17-29.
6. Eckert, J. and P. Deplazes, *Biological, epidemiological, and clinical aspects of echinococcosis, a zoonosis of increasing concern*. Clin Microbiol Rev, 2004. **17**(1): p. 107-35.
7. Torgerson, P.R., et al., *The global burden of alveolar echinococcosis*. PLoS Negl Trop Dis, 2010. **4**(6): p. e722.
8. Grosso, G., et al., *Worldwide epidemiology of liver hydatidosis including the Mediterranean area*. World J Gastroenterol, 2012. **18**(13): p. 1425-37.
9. Romig, T., A. Dinkel, and U. Mackenstedt, *The present situation of echinococcosis in Europe*. Parasitol Int, 2006. **55 Suppl**: p. S187-91.
10. Garippa, G. and M.T. Manfredi, *Cystic echinococcosis in Europe and in Italy*. Vet Res Commun, 2009. **33 Suppl 1**: p. 35-9.
11. Eckert, J. and P. Deplazes, *Biological, Epidemiological, and Clinical Aspects of Echinococcosis, a Zoonosis of Increasing Concern*. Clinical Microbiology Reviews, 2004. **17**(1): p. 107-135.
12. Vuitton, D.A., et al., *Epidemiology of alveolar echinococcosis with particular reference to China and Europe*. Parasitology, 2003. **127 Suppl**: p. S87-107.
13. Knapp, J., et al., *Echinococcus multilocularis in Svalbard, Norway: microsatellite genotyping to investigate the origin of a highly focal contamination*. Infect Genet Evol, 2012. **12**(6): p. 1270-4.
14. Craig, P.S. and C. Echinococcosis Working Group in, *Epidemiology of human alveolar echinococcosis in China*. Parasitol Int, 2006. **55 Suppl**: p. S221-5.
15. known, N., *Bucharest in Europe.png*. http://commons.wikimedia.org/wiki/File:Bucharest_in_Europe.png. **according to Creative Commons (CC)**.
16. Hegglin, D. and P. Deplazes, *Control of Echinococcus multilocularis: strategies, feasibility and cost-benefit analyses*. Int J Parasitol, 2013. **43**(5): p. 327-37.
17. Suld, K., et al., *An invasive vector of zoonotic disease sustained by anthropogenic resources: the raccoon dog in northern Europe*. PLoS One, 2014. **9**(5): p. e96358.
18. Deplazes, P., et al., *Wilderness in the city: the urbanization of Echinococcus multilocularis*. Trends Parasitol, 2004. **20**(2): p. 77-84.
19. Deplazes, P., *Ecology and epidemiology of Echinococcus multilocularis in Europe*. Parasitologia, 2006. **48**(1-2): p. 37-9.
20. Eckert, J., *[The "dangerous fox tapeworm" (Echinococcus multilocularis) and alveolar echinococcosis of humans in central Europe]*. Berl Munch Tierarztl Wochenschr, 1996. **109**(6-7): p. 202-10.
21. Pleydell, D.R., et al., *Modelling the spatial distribution of Echinococcus multilocularis infection in foxes*. Acta Trop, 2004. **91**(3): p. 253-65.
22. Moro, P. and P.M. Schantz, *Echinococcosis: a review*. Int J Infect Dis, 2009. **13**(2): p. 125-33.
23. Lewis, F.I., et al., *Dynamics of the force of infection: insights from Echinococcus multilocularis infection in foxes*. PLoS Negl Trop Dis, 2014. **8**(3): p. e2731.
24. Otero-Abad, B. and P.R. Torgerson, *A systematic review of the epidemiology of echinococcosis in domestic and wild animals*. PLoS Negl Trop Dis, 2013. **7**(6): p. e2249.

25. Tackmann, K., et al., *Spatial distribution patterns of Echinococcus multilocularis (Leuckart 1863) (Cestoda: Cyclophyllidea: Taeniidae) among red foxes in an endemic focus in Brandenburg, Germany*. *Epidemiol Infect*, 1998. **120**(1): p. 101-9.
26. Sreter, T., et al., *Echinococcus multilocularis: an emerging pathogen in Hungary and Central Eastern Europe?* *Emerg Infect Dis*, 2003. **9**(3): p. 384-6.
27. Kapel, C.M., et al., *Reproductive potential of Echinococcus multilocularis in experimentally infected foxes, dogs, raccoon dogs and cats*. *Int J Parasitol*, 2006. **36**(1): p. 79-86.
28. Thompson, R.C. and A.J. Lymbery, *Echinococcus: biology and strain variation*. *Int J Parasitol*, 1990. **20**(4): p. 457-70.
29. Martinek, K., et al., *Echinococcus multilocularis in European wolves (Canis lupus)*. *Parasitol Res*, 2001. **87**(10): p. 838-9.
30. Craig, P., *Echinococcus multilocularis*. *Curr Opin Infect Dis*, 2003. **16**(5): p. 437-44.
31. Gottstein, B. and A. Hemphill, *Immunopathology of echinococcosis*. *Chem Immunol*, 1997. **66**: p. 177-208.
32. Koziol, U., et al., *The unique stem cell system of the immortal larva of the human parasite Echinococcus multilocularis*. *Evodevo*, 2014. **5**(1): p. 10.
33. Hemer, S., et al., *Host insulin stimulates Echinococcus multilocularis insulin signalling pathways and larval development*. *BMC Biol*, 2014. **12**: p. 5.
34. Misbin, R.I., T.J. Merimee, and J.M. Lowenstein, *Insulin removal by isolated perfused rat liver*. *Am J Physiol*, 1976. **230**(1): p. 171-7.
35. Song, S.H., et al., *Direct measurement of pulsatile insulin secretion from the portal vein in human subjects*. *J Clin Endocrinol Metab*, 2000. **85**(12): p. 4491-9.
36. Thompson, R.C.A., *Biology and systematics of Echinococcus*, in *The Biology of Echinococcus and hydatid disease*, R.C.A. Thompson, Editor. 1986, George Allen & Unwin. p. 5-43.
37. Gottstein, B. and R. Felleisen, *Protective immune mechanisms against the metacestode of Echinococcus multilocularis*. *Parasitol Today*, 1995. **11**(9): p. 320-6.
38. Gottstein, B. and A. Hemphill, *Echinococcus multilocularis: the parasite-host interplay*. *Exp Parasitol*, 2008. **119**(4): p. 447-52.
39. Brehm, K., *Echinococcus multilocularis as an experimental model in stem cell research and molecular host-parasite interaction*. *Parasitology*, 2010. **137**(3): p. 537-55.
40. Eckert, J., R.C. Thompson, and H. Mehlhorn, *Proliferation and metastases formation of larval Echinococcus multilocularis. I. Animal model, macroscopical and histological findings*. *Z Parasitenkd*, 1983. **69**(6): p. 737-48.
41. Mehlhorn, H., J. Eckert, and R.C. Thompson, *Proliferation and metastases formation of larval Echinococcus multilocularis. II. Ultrastructural investigations*. *Z Parasitenkd*, 1983. **69**(6): p. 749-63.
42. Hildreth, M.B. and N.H. Granholm, *Effect of mouse strain variations and cortisone treatment on the establishment and growth of primary Echinococcus multilocularis hydatid cysts*. *J Parasitol*, 2003. **89**(3): p. 493-5.
43. Vuitton, D.A. and B. Gottstein, *Echinococcus multilocularis and its intermediate host: a model of parasite-host interplay*. *J Biomed Biotechnol*, 2010. **2010**: p. 923193.
44. Sakamoto, T. and M. Sugimura, *Studies on echinococcosis XXIII. Electron microscopical observations on histogenesis of larval Echinococcus multilocularis*. *Jap J vet Res*, 1970. **18**: p. 131-144.
45. Morseth, D.J., *Fine structure of the hydatid cyst and protoscolex of Echinococcus granulosus*. *J Parasitol*, 1967. **53**(2): p. 312-25.
46. Lascano, E.F., E.A. Coltorti, and V.M. Varela-Diaz, *Fine structure of the germinal membrane of Echinococcus granulosus cysts*. *J Parasitol*, 1975. **61**(5): p. 853-60.
47. Koziol, U., G. Krohne, and K. Brehm, *Anatomy and development of the larval nervous system in Echinococcus multilocularis*. *Front Zool*, 2013. **10**(1): p. 24.
48. Diaz, A., et al., *Understanding the laminated layer of larval Echinococcus I: structure*. *Trends Parasitol*, 2011. **27**(5): p. 204-13.

49. Brunetti, E., et al., *Expert consensus for the diagnosis and treatment of cystic and alveolar echinococcosis in humans*. Acta Trop, 2010. **114**(1): p. 1-16.
50. Kern, P., et al., *WHO classification of alveolar echinococcosis: principles and application*. Parasitol Int, 2006. **55 Suppl**: p. S283-7.
51. Horton, J., *Albendazole: a broad spectrum anthelmintic for treatment of individuals and populations*. Curr Opin Infect Dis, 2002. **15**(6): p. 599-608.
52. Brehm, K., et al., *Echinococcosis from every angle*. Parasitol Today, 1999. **15**(9): p. 351-2.
53. Mosimann, F., V. Bettschart, and R. Meuli, *Mediastinal recurrence of alveolar echinococcosis after liver transplantation*. Liver Transpl, 2003. **9**(1): p. 97-8.
54. Lopes, W.D., et al., *Historic of therapeutic efficacy of albendazol sulphoxide administered in different routes, dosages and treatment schemes, against Taenia saginata cysticercus in cattle experimentally infected*. Exp Parasitol, 2014. **137**: p. 14-20.
55. Hemphill, A., et al., *Innovative chemotherapeutical treatment options for alveolar and cystic echinococcosis*. Parasitology, 2007. **134**(Pt 12): p. 1657-70.
56. Jura, H., A. Bader, and M. Frosch, *In vitro activities of benzimidazoles against Echinococcus multilocularis metacestodes*. Antimicrob Agents Chemother, 1998. **42**(5): p. 1052-6.
57. Ingold, K., et al., *Efficacies of albendazole sulfoxide and albendazole sulfone against In vitro-cultivated Echinococcus multilocularis metacestodes*. Antimicrob Agents Chemother, 1999. **43**(5): p. 1052-61.
58. Brehm, K., et al., *Cloning and characterization of beta-tubulin genes from Echinococcus multilocularis*. Mol Biochem Parasitol, 2000. **107**(2): p. 297-302.
59. Olson, P.D., et al., *Cestode genomics - progress and prospects for advancing basic and applied aspects of flatworm biology*. Parasite Immunol, 2012. **34**(2-3): p. 130-50.
60. Tsai, I.J., et al., *The genomes of four tapeworm species reveal adaptations to parasitism*. Nature, 2013. **496**(7443): p. 57-63.
61. Maller, J.L., *On the importance of protein phosphorylation in cell cycle control*. Mol Cell Biochem, 1993. **127-128**: p. 267-81.
62. Cohen, P. and D.R. Alessi, *Kinase drug discovery--what's next in the field?* ACS Chem Biol, 2013. **8**(1): p. 96-104.
63. Melnikova, I. and J. Golden, *Targeting protein kinases*. Nat Rev Drug Discov, 2004. **3**(12): p. 993-4.
64. Strebhardt, K. and A. Ullrich, *Paul Ehrlich's magic bullet concept: 100 years of progress*. Nat Rev Cancer, 2008. **8**(6): p. 473-80.
65. Zhang, J., P.L. Yang, and N.S. Gray, *Targeting cancer with small molecule kinase inhibitors*. Nat Rev Cancer, 2009. **9**(1): p. 28-39.
66. Hanks, S.K. and T. Hunter, *Protein kinases 6. The eukaryotic protein kinase superfamily: kinase (catalytic) domain structure and classification*. FASEB J, 1995. **9**(8): p. 576-96.
67. Hanks, S.K., A.M. Quinn, and T. Hunter, *The protein kinase family: conserved features and deduced phylogeny of the catalytic domains*. Science, 1988. **241**(4861): p. 42-52.
68. Neveu, C., *The structure of the kinase domain of CaMKII rendered by pymol from PDB 2v70*. http://en.wikipedia.org/wiki/Ca2%2B/calmodulin-dependent_protein_kinase_II, 1 May 2005. **according to Creative Commons (CC)**.
69. Zhang, W. and H.T. Liu, *MAPK signal pathways in the regulation of cell proliferation in mammalian cells*. Cell Res, 2002. **12**(1): p. 9-18.
70. Gelmedin, V., R. Caballero-Gamiz, and K. Brehm, *Characterization and inhibition of a p38-like mitogen-activated protein kinase (MAPK) from Echinococcus multilocularis: antiparasitic activities of p38 MAPK inhibitors*. Biochem Pharmacol, 2008. **76**(9): p. 1068-81.
71. Strebhardt, K., *Multifaceted polo-like kinases: drug targets and antitargets for cancer therapy*. Nat Rev Drug Discov, 2010. **9**(8): p. 643-60.
72. Archambault, V. and D.M. Glover, *Polo-like kinases: conservation and divergence in their functions and regulation*. Nat Rev Mol Cell Biol, 2009. **10**(4): p. 265-75.

73. Hemphill, A., et al., *Echinococcus metacestodes as laboratory models for the screening of drugs against cestodes and trematodes*. Parasitology, 2010. **137**(3): p. 569-87.
74. Hemphill, A. and J. Muller, *Alveolar and cystic echinococcosis: towards novel chemotherapeutical treatment options*. J Helminthol, 2009. **83**(2): p. 99-111.
75. Hemphill, A., et al., *Treatment of echinococcosis: albendazole and mebendazole - what else?* Parasite, 2014. **21**: p. 70.
76. Sunkel, C.E. and D.M. Glover, *polo, a mitotic mutant of Drosophila displaying abnormal spindle poles*. J Cell Sci, 1988. **89 (Pt 1)**: p. 25-38.
77. de Cárcer, G., G. Manning, and M. Malumbres, *From Plk1 to Plk5: Functional evolution of polo-like kinases*. Cell Cycle, 2011. **10**(14): p. 2255-2262.
78. van Vugt, M.A. and R.H. Medema, *Getting in and out of mitosis with Polo-like kinase-1*. Oncogene, 2005. **24**(17): p. 2844-59.
79. Bruinsma, W., J.A. Raaijmakers, and R.H. Medema, *Switching Polo-like kinase-1 on and off in time and space*. Trends Biochem Sci, 2012. **37**(12): p. 534-42.
80. Lowery, D.M., D. Lim, and M.B. Yaffe, *Structure and function of Polo-like kinases*. Oncogene, 2005. **24**(2): p. 248-59.
81. Bibi, N., Z. Parveen, and S. Rashid, *Identification of potential Plk1 targets in a cell-cycle specific proteome through structural dynamics of kinase and Polo box-mediated interactions*. PLoS One, 2013. **8**(8): p. e70843.
82. Zitouni, S., et al., *Polo-like kinases: structural variations lead to multiple functions*. Nat Rev Mol Cell Biol, 2014. **15**(7): p. 433-52.
83. Degenhardt, Y. and T. Lampkin, *Targeting Polo-like kinase in cancer therapy*. Clin Cancer Res, 2010. **16**(2): p. 384-9.
84. Strebhardt, K. and A. Ullrich, *Targeting polo-like kinase 1 for cancer therapy*. Nat Rev Cancer, 2006. **6**(4): p. 321-30.
85. Weiss, L. and T. Efferth, *Polo-like kinase 1 as target for cancer therapy*. Exp Hematol Oncol, 2012. **1**(1): p. 38.
86. Taniguchi, E., F. Toyoshima-Morimoto, and E. Nishida, *Nuclear translocation of plk1 mediated by its bipartite nuclear localization signal*. J Biol Chem, 2002. **277**(50): p. 48884-8.
87. Wang, P., et al., *Cell cycle regulation of Greatwall kinase nuclear localization facilitates mitotic progression*. J Cell Biol, 2013. **202**(2): p. 277-93.
88. Teixeira, L.K. and S.I. Reed, *Ubiquitin ligases and cell cycle control*. Annu Rev Biochem, 2013. **82**: p. 387-414.
89. Archambault, V., et al., *Sequestration of Polo kinase to microtubules by phosphopriming-independent binding to Map205 is relieved by phosphorylation at a CDK site in mitosis*. Genes Dev, 2008. **22**(19): p. 2707-20.
90. Barr, F.A., H.H. Sillje, and E.A. Nigg, *Polo-like kinases and the orchestration of cell division*. Nat Rev Mol Cell Biol, 2004. **5**(6): p. 429-40.
91. Seki, A., et al., *Bora and the kinase Aurora a cooperatively activate the kinase Plk1 and control mitotic entry*. Science, 2008. **320**(5883): p. 1655-8.
92. Toyoshima-Morimoto, F., et al., *Polo-like kinase 1 phosphorylates cyclin B1 and targets it to the nucleus during prophase*. Nature, 2001. **410**(6825): p. 215-20.
93. Macurek, L., et al., *Polo-like kinase-1 is activated by aurora A to promote checkpoint recovery*. Nature, 2008. **455**(7209): p. 119-23.
94. Lindon, C. and J. Pines, *Ordered proteolysis in anaphase inactivates Plk1 to contribute to proper mitotic exit in human cells*. J Cell Biol, 2004. **164**(2): p. 233-41.
95. Kothe, M., et al., *Selectivity-determining residues in Plk1*. Chem Biol Drug Des, 2007. **70**(6): p. 540-6.
96. Medema, R.H., C.C. Lin, and J.C. Yang, *Polo-like kinase 1 inhibitors and their potential role in anticancer therapy, with a focus on NSCLC*. Clin Cancer Res, 2011. **17**(20): p. 6459-66.
97. Rudolph, D., et al., *BI 6727, a Polo-like kinase inhibitor with improved pharmacokinetic profile and broad antitumor activity*. Clin Cancer Res, 2009. **15**(9): p. 3094-102.

98. Schoffski, P., et al., *A phase I, dose-escalation study of the novel Polo-like kinase inhibitor volasertib (BI 6727) in patients with advanced solid tumours*. Eur J Cancer, 2012. **48**(2): p. 179-86.
99. Schoffski, P., et al., *Multicentric parallel phase II trial of the polo-like kinase 1 inhibitor BI 2536 in patients with advanced head and neck cancer, breast cancer, ovarian cancer, soft tissue sarcoma and melanoma. The first protocol of the European Organization for Research and Treatment of Cancer (EORTC) Network Of Core Institutes (NOCI)*. Eur J Cancer, 2010. **46**(12): p. 2206-15.
100. Schoffski, P., *Polo-like kinase (PLK) inhibitors in preclinical and early clinical development in oncology*. Oncologist, 2009. **14**(6): p. 559-70.
101. Soto, E., et al., *Semi-mechanistic population pharmacokinetic/pharmacodynamic model for neutropenia following therapy with the Plk-1 inhibitor BI 2536 and its application in clinical development*. Cancer Chemother Pharmacol, 2010. **66**(4): p. 785-95.
102. Long, T., et al., *Schistosoma mansoni Polo-like kinase 1: A mitotic kinase with key functions in parasite reproduction*. Int J Parasitol, 2010. **40**(9): p. 1075-86.
103. Vicogne, J., et al., *An unusual receptor tyrosine kinase of Schistosoma mansoni contains a Venus Flytrap module*. Mol Biochem Parasitol, 2003. **126**(1): p. 51-62.
104. Lee, J. and P.F. Pilch, *The insulin receptor: structure, function, and signaling*. Am J Physiol, 1994. **266**(2 Pt 1): p. C319-34.
105. Khayath, N., et al., *Diversification of the insulin receptor family in the helminth parasite Schistosoma mansoni*. FEBS J, 2007. **274**(3): p. 659-76.
106. O'Hara, P.J., et al., *The ligand-binding domain in metabotropic glutamate receptors is related to bacterial periplasmic binding proteins*. Neuron, 1993. **11**(1): p. 41-52.
107. Vanderstraete, M., et al., *The venus kinase receptor (VKR) family: structure and evolution*. BMC Genomics, 2013. **14**: p. 361.
108. Ahier, A., et al., *A new family of receptor tyrosine kinases with a venus flytrap binding domain in insects and other invertebrates activated by aminoacids*. PLoS One, 2009. **4**(5): p. e5651.
109. Vanderstraete, M., et al., *Venus kinase receptors control reproduction in the platyhelminth parasite Schistosoma mansoni*. PLoS Pathog, 2014. **10**(5): p. e1004138.
110. Vanderstraete, M., et al., *Dual targeting of insulin and venus kinase Receptors of Schistosoma mansoni for novel anti-schistosome therapy*. PLoS Negl Trop Dis, 2013. **7**(5): p. e2226.
111. Hemphill, A. and B. Gottstein, *Immunology and morphology studies on the proliferation of in vitro cultivated Echinococcus multilocularis metacestodes*. Parasitol Res, 1995. **81**(7): p. 605-14.
112. Jura, H., et al., *Hepatic tissue culture model for study of host-parasite interactions in alveolar echinococcosis*. Infect Immun, 1996. **64**(9): p. 3484-90.
113. Spiliotis, M., et al., *Long-term in vitro cultivation of Echinococcus multilocularis metacestodes under axenic conditions*. Parasitol Res, 2004. **92**(5): p. 430-2.
114. Fiori, P.L., et al., *Establishment of cell cultures from hydatid cysts of Echinococcus granulosus*. Int J Parasitol, 1988. **18**(3): p. 297-305.
115. Furuya, K., *An established cell line of larval Echinococcus multilocularis*. Int J Parasitol, 1991. **21**(2): p. 233-40.
116. Yamashita, K., et al., *Establishment of a primary culture of Echinococcus multilocularis germinal cells*. J Gastroenterol, 1997. **32**(3): p. 344-50.
117. Toledo, A., et al., *In vitro culture of Taenia crassiceps larval cells and cyst regeneration after injection into mice*. J Parasitol, 1997. **83**(2): p. 189-93.
118. Spiliotis, M., et al., *Transient transfection of Echinococcus multilocularis primary cells and complete in vitro regeneration of metacestode vesicles*. Int J Parasitol, 2008. **38**(8-9): p. 1025-39.
119. Spiliotis, M., et al., *Echinococcus multilocularis primary cells: improved isolation, small-scale cultivation and RNA interference*. Mol Biochem Parasitol, 2010. **174**(1): p. 83-7.

120. Brehm, K. and M. Spiliotis, *Recent advances in the in vitro cultivation and genetic manipulation of Echinococcus multilocularis metacestodes and germinal cells*. *Exp Parasitol*, 2008. **119**(4): p. 506-15.
121. Hemphill, A., et al., *Culture of Echinococcus multilocularis metacestodes: an alternative to animal use*. *Trends Parasitol*, 2002. **18**(10): p. 445-51.
122. Siles-Lucas, M. and A. Hemphill, *Cestode parasites: application of in vivo and in vitro models for studies on the host-parasite relationship*. *Adv Parasitol*, 2002. **51**: p. 133-230.
123. Hemer, S. and K. Brehm, *In vitro efficacy of the anticancer drug imatinib on Echinococcus multilocularis larvae*. *Int J Antimicrob Agents*, 2012. **40**(5): p. 458-62.
124. Nono, J.K., et al., *Excretory/secretory-products of Echinococcus multilocularis larvae induce apoptosis and tolerogenic properties in dendritic cells in vitro*. *PLoS Negl Trop Dis*, 2012. **6**(2): p. e1516.
125. Nono, J.K., M.B. Lutz, and K. Brehm, *EmTIP, a T-Cell immunomodulatory protein secreted by the tapeworm Echinococcus multilocularis is important for early metacestode development*. *PLoS Negl Trop Dis*, 2014. **8**(1): p. e2632.
126. Gelmedin, V., M. Spiliotis, and K. Brehm, *Molecular characterisation of MEK1/2- and MKK3/6-like mitogen-activated protein kinase kinases (MAPKK) from the fox tapeworm Echinococcus multilocularis*. *Int J Parasitol*, 2010. **40**(5): p. 555-67.
127. Brehm, K. and U. Koziol, *On the importance of targeting parasite stem cells in anti-echinococcosis drug development*. *Parasite*, 2014. **21**: p. 72.
128. Lenart, P., et al., *The small-molecule inhibitor BI 2536 reveals novel insights into mitotic roles of polo-like kinase 1*. *Curr Biol*, 2007. **17**(4): p. 304-15.
129. Faustino, N.A. and T.A. Cooper, *Pre-mRNA splicing and human disease*. *Genes Dev*, 2003. **17**(4): p. 419-37.
130. Dereeper, A., et al., *Phylogeny.fr: robust phylogenetic analysis for the non-specialist*. *Nucleic Acids Res*, 2008. **36**(Web Server issue): p. W465-9.
131. Dereeper, A., et al., *BLAST-EXPLORER helps you building datasets for phylogenetic analysis*. *BMC Evol Biol*, 2010. **10**: p. 8.
132. Schubert, A., et al., *Targeting Echinococcus multilocularis stem cells by inhibition of the Polo-like kinase EmPlk1*. *PLoS Negl Trop Dis*, 2014. **8**(6): p. e2870.
133. Brehm, K., et al., *Analysis of differential gene expression in Echinococcus multilocularis larval stages by means of spliced leader differential display*. *Int J Parasitol*, 2003. **33**(11): p. 1145-59.
134. Brassesco, M.S., et al., *In vitro targeting of Polo-like kinase 1 in bladder carcinoma: comparative effects of four potent inhibitors*. *Cancer Biol Ther*, 2013. **14**(7): p. 648-57.
135. Grabowski, M., et al., *Benefits of structural genomics for drug discovery research*. *Infect Disord Drug Targets*, 2009. **9**(5): p. 459-74.
136. Schroder, M., *Viruses and the human DEAD-box helicase DDX3: inhibition or exploitation?* *Biochem Soc Trans*, 2011. **39**(2): p. 679-83.
137. Rao, P.N., et al., *Synthesis and antimutotoxic activity of novel 2-methoxyestradiol analogs*. *Steroids*, 2002. **67**(13-14): p. 1079-89.
138. Spicher, M., et al., *In vitro and in vivo effects of 2-methoxyestradiol, either alone or combined with albendazole, against Echinococcus metacestodes*. *Exp Parasitol*, 2008. **119**(4): p. 475-82.
139. Kuryatov, A., et al., *Mutational analysis of the glycine-binding site of the NMDA receptor: structural similarity with bacterial amino acid-binding proteins*. *Neuron*, 1994. **12**(6): p. 1291-300.
140. Galvez, T., et al., *Mutagenesis and modeling of the GABAB receptor extracellular domain support a venus flytrap mechanism for ligand binding*. *J Biol Chem*, 1999. **274**(19): p. 13362-9.
141. Galvez, T., et al., *Mapping the agonist-binding site of GABAB type 1 subunit sheds light on the activation process of GABAB receptors*. *J Biol Chem*, 2000. **275**(52): p. 41166-74.
142. Dar, A.C. and K.M. Shokat, *The evolution of protein kinase inhibitors from antagonists to agonists of cellular signaling*. *Annu Rev Biochem*, 2011. **80**: p. 769-95.

143. Parrizas, M., et al., *Specific inhibition of insulin-like growth factor-1 and insulin receptor tyrosine kinase activity and biological function by tyrphostins*. *Endocrinology*, 1997. **138**(4): p. 1427-33.
144. Wen, B., et al., *Tyrphostin AG 1024 modulates radiosensitivity in human breast cancer cells*. *Br J Cancer*, 2001. **85**(12): p. 2017-21.
145. Assoian, R.K., *Common sense signalling*. *Nat Cell Biol*, 2002. **4**(8): p. E187-8.
146. Kholodenko, B.N., *Cell-signalling dynamics in time and space*. *Nat Rev Mol Cell Biol*, 2006. **7**(3): p. 165-76.
147. Brehm, K., *The role of evolutionarily conserved signalling systems in Echinococcus multilocularis development and host-parasite interaction*. *Med Microbiol Immunol*, 2010. **199**(3): p. 247-59.
148. Gelmedin, V., et al., *Echinococcus multilocularis: cloning and characterization of a member of the SNW/SKIP family of transcriptional coregulators*. *Exp Parasitol*, 2005. **111**(2): p. 115-20.
149. Spiliotis, M., et al., *Characterisation of EmMPK1, an ERK-like MAP kinase from Echinococcus multilocularis which is activated in response to human epidermal growth factor*. *Int J Parasitol*, 2006. **36**(10-11): p. 1097-112.
150. Spiliotis, M., et al., *Molecular cloning and characterization of Ras- and Raf-homologues from the fox-tapeworm Echinococcus multilocularis*. *Mol Biochem Parasitol*, 2005. **139**(2): p. 225-37.
151. You, H., et al., *Cloning and characterisation of Schistosoma japonicum insulin receptors*. *PLoS One*, 2010. **5**(3): p. e9868.
152. Zavala-Gongora, R., et al., *A member of the transforming growth factor-beta receptor family from Echinococcus multilocularis is activated by human bone morphogenetic protein 2*. *Mol Biochem Parasitol*, 2006. **146**(2): p. 265-71.
153. Zavala-Gongora, R., et al., *Identification and characterisation of two distinct Smad proteins from the fox-tapeworm Echinococcus multilocularis*. *Int J Parasitol*, 2003. **33**(14): p. 1665-77.
154. Hubbard, S.R. and W.T. Miller, *Receptor tyrosine kinases: mechanisms of activation and signaling*. *Curr Opin Cell Biol*, 2007. **19**(2): p. 117-23.
155. Lemmon, M.A. and J. Schlessinger, *Cell signaling by receptor tyrosine kinases*. *Cell*, 2010. **141**(7): p. 1117-34.
156. Taylor, S.S. and A.P. Kornev, *Protein kinases: evolution of dynamic regulatory proteins*. *Trends Biochem Sci*, 2011. **36**(2): p. 65-77.
157. Bianco, R., et al., *Key cancer cell signal transduction pathways as therapeutic targets*. *Eur J Cancer*, 2006. **42**(3): p. 290-4.
158. Lawrence, M.C., et al., *The roles of MAPKs in disease*. *Cell Res*, 2008. **18**(4): p. 436-42.
159. Kern, P., *Clinical features and treatment of alveolar echinococcosis*. *Curr Opin Infect Dis*, 2010. **23**(5): p. 505-12.
160. Spiliotis, M. and K. Brehm, *Axenic in vitro cultivation of Echinococcus multilocularis metacystode vesicles and the generation of primary cell cultures*. *Methods Mol Biol*, 2009. **470**: p. 245-62.
161. Stettler, M., et al., *In vitro parasitocidal effect of Nitazoxanide against Echinococcus multilocularis metacystodes*. *Antimicrob Agents Chemother*, 2003. **47**(2): p. 467-74.
162. Kuster, T., et al., *Subcutaneous infection model facilitates treatment assessment of secondary Alveolar echinococcosis in mice*. *PLoS Negl Trop Dis*, 2013. **7**(5): p. e2235.
163. Von Samson-Himmelstjerna, G., et al., *Single nucleotide polymorphism (SNP) markers for benzimidazole resistance in veterinary nematodes*. *Parasitology*, 2007. **134**(Pt 8): p. 1077-86.
164. Li, R., et al., *Involvement of polo-like kinase 1 (Plk1) in mitotic arrest by inhibition of mitogen-activated protein kinase-extracellular signal-regulated kinase-ribosomal S6 kinase 1 (MEK-ERK-RSK1) cascade*. *J Biol Chem*, 2012. **287**(19): p. 15923-34.
165. Luo, J. and X. Liu, *Polo-like kinase 1, on the rise from cell cycle regulation to prostate cancer development*. *Protein Cell*, 2012. **3**(3): p. 182-97.

166. Grinshtein, N., et al., *Small molecule kinase inhibitor screen identifies polo-like kinase 1 as a target for neuroblastoma tumor-initiating cells*. *Cancer Res*, 2011. **71**(4): p. 1385-95.
167. Dissous, C., C.G. Greveling, and T. Long, *Schistosoma mansoni Polo-like kinases and their function in control of mitosis and parasite reproduction*. *An Acad Bras Cienc*, 2011. **83**(2): p. 627-35.
168. Long, T., et al., *SmSak, the second Polo-like kinase of the helminth parasite Schistosoma mansoni: conserved and unexpected roles in meiosis*. *PLoS One*, 2012. **7**(6): p. e40045.
169. Frost, A., et al., *Phase I study of the Plk1 inhibitor BI 2536 administered intravenously on three consecutive days in advanced solid tumours*. *Curr Oncol*, 2012. **19**(1): p. e28-35.
170. Leinung, M., et al., *Small molecules in combination with conventional chemotherapeutic drugs: Light at the end of the tunnel?* *Oncol Lett*, 2012. **4**(5): p. 1043-1046.
171. Mross, K., et al., *A randomised phase II trial of the Polo-like kinase inhibitor BI 2536 in chemo-naïve patients with unresectable exocrine adenocarcinoma of the pancreas - a study within the Central European Society Anticancer Drug Research (CESAR) collaborative network*. *Br J Cancer*, 2012. **107**(2): p. 280-6.
172. Stewart, H.J., et al., *The polo-like kinase inhibitor BI 2536 exhibits potent activity against malignant plasma cells and represents a novel therapy in multiple myeloma*. *Exp Hematol*, 2011. **39**(3): p. 330-8.
173. Spaniol, K., J. Boos, and C. Lanvers-Kaminsky, *An in-vitro evaluation of the polo-like kinase inhibitor GW843682X against paediatric malignancies*. *Anticancer Drugs*, 2011. **22**(6): p. 531-42.
174. Witchley, J.N., et al., *Muscle cells provide instructions for planarian regeneration*. *Cell Rep*, 2013. **4**(4): p. 633-41.
175. Rossi, L., P. Iacopetti, and A. Salvetti, *Stem cells and neural signalling: the case of neoblast recruitment and plasticity in low dose X-ray treated planarians*. *Int J Dev Biol*, 2012. **56**(1-3): p. 135-42.
176. Reuter, M. and M. Gustafsson, *Neuronal signal substances in asexual multiplication and development in flatworms*. *Cell Mol Neurobiol*, 1996. **16**(5): p. 591-616.
177. Collins, J.J., 3rd, et al., *Adult somatic stem cells in the human parasite Schistosoma mansoni*. *Nature*, 2013. **494**(7438): p. 476-9.
178. Sikes, J.M. and P.A. Newmark, *Restoration of anterior regeneration in a planarian with limited regenerative ability*. *Nature*, 2013. **500**(7460): p. 77-80.
179. Forsthoefel, D.J., A.E. Park, and P.A. Newmark, *Stem cell-based growth, regeneration, and remodeling of the planarian intestine*. *Dev Biol*, 2011. **356**(2): p. 445-59.
180. Newmark, P.A. and A. Sanchez Alvarado, *Bromodeoxyuridine specifically labels the regenerative stem cells of planarians*. *Dev Biol*, 2000. **220**(2): p. 142-53.
181. Hunter, T., et al., *Receptor protein tyrosine kinases and phosphatases*. *Cold Spring Harb Symp Quant Biol*, 1992. **57**: p. 25-41.
182. Doenhoff, M.J., et al., *Resistance of Schistosoma mansoni to praziquantel: is there a problem?* *Trans R Soc Trop Med Hyg*, 2002. **96**(5): p. 465-9.
183. Coeli, R., et al., *Praziquantel treatment decreases Schistosoma mansoni genetic diversity in experimental infections*. *PLoS Negl Trop Dis*, 2013. **7**(12): p. e2596.

Doctoral thesis

Sarah Hemer Molecular characterization of evolutionarily conserved signaling systems of *Echinococcus multilocularis* and their utilization for the development of novel drugs against Echinococcosis, 2012 (urn:nbn:de:bvb:20-opus-74007).

Supplement Material

A Sequences

Start-, stopcodons are highlighted in grey.

EmPlk1 CDS (EmuJ_000471700; supercontig pathogen_EMU_scaffold_007614 : 4512575-4515749)

```

1  ATGGATAAGT CAAAAGCGAA GGAGGTTCCT GCTATTGTGC ATGACAAGTC AAACGGTAAA ACGTATGTGA GAGGGAGGTT
81  TCTTGAAAAA GGAGGCTTCG CTCGCTGTTG GGAGTTGAGT GACCAAGACA CCGGTGTAAA GTATGCGGGA AAGTTGTTG
161  CAAAATGCGA TATCCTCAAG CCCTCCCAGC GTCAGAAGAT GCAGCAAGAA ATTACAATTC ATGCTTCATT GAAGCACGAA
241  AATATTGTCG GTTTTCACAG GTCTTTTGTG GATGAAGCCA ACATATACAT ACTGCTCGAG CTGTGCCCAA GCGGACTCT
321  CATGGAAGTC CATAAGAGAC GTCGACAAGT TACTGAGCCA GAAGCCCGGT ACTTTATTAG GCAAATCGTC ACCGGATGTC
401  AATATCTGCA CCTAATAAAC ATAATTCATC GCGATCTTAA ACTGGCCAAT CTGTTTTTAA ATGATGACAT GATTGTAAAG
481  ATCGGGGATT TTGGTTTGGC CTCTAGAATT ACTAAAGAAG GTGAAATGAA GAAGACATTA TGTGGGACGC CAAACTATAT
561  TGCTCCTGAG ATTCTCTGCA AACATGGCCA CAGCTTTGAG GTAGATTCGT GGTCCGTGGG TTGCATTTTG TACTACTCTC
641  TTGTGGGTCG TCCGCCTTTC GAAACGTCGA GTTTGCATGA CACATATGAA AAAATAAAGA AGAACGATTA CCTCGTTCCT
721  GGTAACATCA GCATAGCAGC CACAAACTTG ATTCGCGCCT TTCTTAACTC TGATCCACAA AAGCGGCCGA GCATGTTGAG
801  TGTGATGGAC CACAGTTTCT TTAAGGATT TACTCCCACC GGTCTCCCTG TCAGTGCAC TACCACCTGT CCCCATTTCG
881  ACAATCTTGC TCGCAATCCC TCCGACAGAC GACCACTCTC TGTTATTGAT GCTAATCTAA ATGATGTATC AACAGTCAGT
961  ACAGAGGCGA ATAAAGATTA CACTACAGAC GATTGCTGGC TTACAGTTTT GTTTGAGAAG TTAGGAGAAC TACTACATGC
1041  ACCCGTACTG CAAGCAACCT CCATAACCGC AATGGAAGAG AGCGAAGATC CAGCATGTGT TCCCATTAT TGGGTCTCTA
1121  AGTGGGTGGA TTATTCGGAC AAGTATGGCA TTGGTTATCA TCTGTGTGAT TTCTCGAAGC GTGTCTTTT TAATGATGAT
1201  ACACGCTTAA TCTTCACTGC GAACAAAGAG AACCTCCAAT ATATTGAAAG TGGTGGCAA GAGCACTTGT ATACCAAGAA
1281  TGACTACCCC GCTACACTCA AAAAGAAAGT AACATTACTT ACTTGCTTCA CTAGTTACAT GCAGGAAAAT CTGCTTCATG
1361  CCGGAGAGAA CATTGTGCGT CGGGAATCAG ATAGCATGGC CAGACTTCCC TTCCTCCGAA GCTGGTGTG AAGCCGCGTC
1441  GCAATCGTGC TTCATCTCAG CAATGGAACA TTGCAACTCA ATTTCTTCGA CGATCACTCC AAAATCATCC TCTGCCCTTT
1521  GATGGAGGCT GTTACTTTTA TTGACCCGAG TCGTAATTC AAAACCTTTC GTTCAATTT GCTCAGGAAA TATGGCATTA
1601  CTGATGACTT AATAAGCGA TTGAAGTACG CCTACGATAT GATAGATCGC AAGCTCTTGC AACGGCAGTC TGAATCCCAC
1681  GCGCGTTGCA CTGGCGCAA GAATAAAAAA GGTTCGAG AGGCAGTTC ACATCCAGCC ATTGCTCCAA TGAAGAAGA
1761  AGATCCTGTT AGTGCAGCCG TTGGCGCAAG GAAGCAAGAC GCTCCAAGG TTGATGTTCT GAAACACAAA TAA

```

EmPlk1 Protein sequence

```

1  MDKSKAKEVP AIVHDKSNGK TYVRGRFLGK GGFARCWELS DQDTGVKYAG KVVAKCDILK PSQRQKMQQE ITIHASLKHE
81  NIVGFHRSFE DEANIYILLE LCPRTLMEL HKRRRQVTEP EARYFIRQIV TGCQYLHLNN IIHRDLKLAN LFLNDDMIVK
161  IGDFGLASRI TKEGEMKKTLL CGTPNYIAPE ILCKHGSFE VDSWSVGCIL YTLVGRPPF ETSSLHDTYE KIKKNDYLPV
241  GNISIAATNL IRAFLNSDPQ KRPSMFSVMD HSFFKGFTPT GLPVSALTTT PRFDNLARNP SDRRPLSVID ANLNDVSTVS
321  TEANKDYTTD DCWLTVLFEK LGELLHAPVL QATSITAMEE SEDPACVPIY WWSKWVDYSD KYGIGYHLCD FSNGVLFNDD
401  TRLIFTANKE NLQYIESGGK EHLTKNDYP ATLKKKVTL TCFYSYMQEN LLHAGENIVR RESDSMARLP FLRSWCRTVR
481  AIVLHLSNGT LQLNFFDDHS KIILCPLMEA VTFIDPSRNF KTFRFNLLRK YGITDDLIKR LKYAYDMIDR KLLQRQSESH
561  ARCTGAKNKK GSREAVPHPA IAPMKEEDPV SAAVGARKQD APKVDVLKHK *

```

EmPlk4 CDS (EmuJ_000104700; contig pathogen_EMU_contig_62145 : 542458-548585)

1 ATGTACGTTC AACCAAACCT AAAGGGGTTA GGGTCCTCAA AGGATGATTT TCAGGTTTTT GAACTCCTCG GCCGTGGGGG
81 CTTTGCACAA GTATATAGAG CCAAGTCGGT CATCACTGGT CAGGAGGTTG CAATCAAAAT GATTGATAAA AAATATATGC
161 ATCAACATGG CCTCACTCAT CGCGTTCAAC GAGAGGTCGA AATCCACAGT CGTTTGAAGC ATCCTGCGGT TCTCGAGTTA
241 TACACATGCT TTGAAGATGC AAACACTCGTT TACTTGGTCC TCGAATTTTG TGACAATGGG GAGCTACAGG CTTACATTCCG
321 GCAGAACGGA TCTGTTTCGG AGGACATGGC TCGTCACTAT ATGAAGCAA TCATCAGTGG CTTGCTCTAC CTTCATTAC
401 ACAACATCCT TCACAGGGAT CTCACCTTGG CTAACCTTCT GCTGACAAAG GACATGAAAG TGAAAATTGC TGACTTCGGC
481 CTCGCGACCA AAATTGAGCC TGGTGAAGAT CACACCACCA TGTGTGGCAC ACCTAATTAC ATCTCACCTG AGGTGGCAAG
561 TCGAGGTAC CAGGTTCTGG AGACGGACGT TTGGTCTCTT GGTTCATGC TCTACACCCT AGTGGTGGGT CATCCTCCAT
641 TTGATACGCG CGAGGTGAGA AGTACCCTGA GTCGAGTAAT CGCCGGGGAT TATGAAATGC CTGAACATCT CTCTCCCGAT
721 TGCTCTGATC TCATTGCCAA ACTCCTGCGG AAGCAACCGC AGGATCGTAT CAAACTCTCC GATATGATCA GACATCCCTT
801 TATCACTAGG AGCACAACAC CTCGACGTAA AATGGAGCAC TCCAGAGACA GTGGGATCGA TTCGATGTCG CGTACACCCA
881 CCATTGGAAT GCAGTCAAAC TCACTCACTG CAACAACAAC CACTACAGCT GCCACTGCAA ACAGTCGTCA CTCCTGCCT
961 TACCGACCGG GTGCGAGCAT TCTGCCTCCA CGTGCAGCCT CCCGCTGTC AGTGGATATG CATCGTTTCA CGCAGAACCA
1041 GCAATCTGGT CACCAGACGC CTCTGACCCC CTTTCGATTCT AGAGGTCACC AACCGCCAAC TTCTGCCACG CGACTGCGTG
1121 GTGGCTCTCT ACAACACCTT CTTCTCCTT CAAAGAGTAT GTCAGGCCA TCTCTTGCGA CCTCATCGCC TTCTCCTTGT
1201 CGTTCCGCT CAGTGGGAAA TCTTCAGCGC ACCTCACATC AGCCGAGCCT CTCACCTCTC TGTACCTGTC GCCTGCGCCC
1281 AATGCGCACA GTCACACGGA TGGCAGTGAT CAACATTCTC CCTGATGAGT CGGTTTGTTF GGAGTTTTTT GACCCGCAGG
1361 TGAATCAACA GAAGCTCGTC GTTGAAGTGA TGGGCATCTC GGCTGATGGA CAGGAGGTGA TTATCTATCA TCCTAATGGA
1441 GGACGTGGAG TGCCCTCAAA TACGAACAGC CCGGTAGCAG CCCGCTCTGG CGATACGTAT GGAGTATATA GACTTGCTCA
1521 GCTCCCTGAG AAGTACTGGA AGAAGTATCA GTTTGTGTCC AAATTCATAA ATATGGCCAA GGCTCATAA CCCAAAGTGA
1601 CGTGATACAC ATCGCGAGCA AAGTGTATTC TAATGGAGAA GGTGGAGCCT CAGGCGGACT TTGAGATGGA GGTGCTTACA
1681 GACGGTAGTC GGGTTATCTG TCTCGGTGGT GAGGCAGCCG GAACGGTGCA GGTATTACA CAGACCAACG GCACCGTTAC
1761 TGTTGATCGC AAACAGCCTT TGGACAATCT GCCAACTGCC ACCCGGGAAC TCATTTCCCTA CGCAGAAAGA TGCCGACGTC
1841 GCTGTCTGGA GGTGAAAGT TCACTGGAGA AGTTTAAATGT TGCCCTATCT CCGCTGGATG CAGAAGTTTC CTCGCCTTTC
1921 CCCGTAATAA TTGGTCGTCG ATCTTGCGCC GCTTCTAAAA CCTCGTCCAA AGGCCCGTC TCATCCGCAT GCCTCTCTCA
2001 GCTCGTGGCT AGCTGCGGTA CCTCGGTCAG CGATAGTCAG CCGCGCTCTT TCTCGCGCCA CTACGATCCT GTATTTGTTC
2081 CCTCCGTGG GTGGGTCTCA CAGTCCTCTC CGGAGGAGTT GCAAGTTCAA TTCACGACG GCGCCGACT TGAGTTGTT
2161 TACTCCACAG CGACAGTCCA CAGCATCCGC TACCATCCAC CGGCAATAGC TGGAGAGGAG GAAGAGGAGC AGGTCTACTC
2241 GACTGCATCA TCGTCCACAC CTCTGCCAGC CGAAGTGGG AGCCGTTTGG AGGTCATTCC AAAAGTTGTT AAATGTCTCC
2321 GTTCGAGGTC TAAAACCTCA CCCTGA

EmPlk4 Protein sequence

1 MYVQPNLKGL GSSKDDFQVF ELLGRGGFAQ VYRAKSVITG QEVAIKMIDK KYMHQHGLTH RVQREVEIHS RLKHPAVLEL
 81 YTCFEDANYV YLVLEFCDNG ELQAYIRQNG SVSEDMARHY MKQIISGLLY LSHSNILHRD LTLANLLLT KDMVKIADFG
 161 LATKIEPGED HTTMCCTPNY ISPEVASRQH QVLETDVWSL GCMLYTLVVG HPPFDTREVR STLSRVIAGD YEMPEHLSPD
 241 CSDLIAKLLR KQPQDRIKLS DMIRHPFITR STTPRRKMEH SRDSGIDSMS RTPTIGMQSN SLTATTTTTA ATANSRHSLEP
 321 YRPGASILPP RAASRLSVDH HRSTQNQQSG HQTPLTPFDS RGHQPPTSAT RLRGGSLLQHL LPPSKSMSGL SLATSSPSPC
 401 RSASVGNLQR TSHQPSLSPL CTCRLRPMRT VTRMAVINIL PDESVCLEFF DPQVNQQKLV VEVMGISADG QEVIIYHPNG
 481 GRGVPNTNS PVAARSGDTY GYVRLAQLPE KYWKYQFVS KFINMAKAHT PKVTLYTSRA KCILMEKVEP QADFEMEVLV
 561 DGSRVICLGG EAAGTVQVIT QTNGTVTVDR KQPLDNLPTA TRELISYAER CRRRCLEVES SLEKFNVALS PLDAEVSSPF
 641 PVIIGRRSCA ASKTSSKGPV SSACLSQLVA SCGTSVSDSQ PRSFSRHYDP VVFPVSGWVS QSSPEELQVQ FNDGARLVVV
 721 YSTATVHSIR YHPPAIAGEE EEEQVYSTAS SSTPLPAEVR SRLEVIPKV KCLRSRSTP P*

Emvkr CDS (EmuJ_000619800; supercontig pathogen_EMU_scaffold_007728 : 4664450-4691242)

1 ATGAATGCAA TGGTGGCGTT TGTTCACTTG ACATTTCTAC TATGTACTGT GTCTTTGTGC GTTCTTGCCA AACAAGGCCT
 81 TGATTTAAGC GAAAGTGTGC TTGCAGCTAA AGAAAAAGCA AAATGGATAA GAAGTCTTCA CTCAATAAT AAGTCTTTTT
 161 CCCTCAATGT TGAGGTGAAC GATAGGCCTT CCCACTGGAT CATAAACTAC ATATTTGAGA TACTTATTCG AGAGCGTTTT
 241 GGGTACAGAA ATATCAATTT TATCTACTACT CCATGGGATT CCTCTTCGAA TCGCATCAAT CGTCTCAAT GTGAAAAGTC
 321 CAATGATTGT TCTTGCCCC CGCCCATTC TGTTAATCTG GAATTATGGC TTCGCACTGG AGAGCAAGCT TCGGATTATG
 401 CACCGCCACA TCGTGTAAAC ATGAACGGAC CGCTTGGTCC GATAACCGA TGGGGCCTCT ATACCAATGA GGAATTAGTA
 481 GGTCGTCAGG CTCCACAGCT TAGTACTGAC CCGAGGATCT CCCAGGATGT TCACCCAAGC CAGTCTTTG GCGAAGGTGT
 561 ACTCTTTTAC GACCGCCAT CTATGTGAA GGCCTACAAG ACCCTCCTCT CGGAGGATGG CATGTCAATG GAGATGCATG
 641 TAGAGCAGCG TCCAACCCAG TTCCTGTGGA ACCTTACCAC ACAGCCCCA CGCTTCCCCA TCCTCCTTAA TTGGTACCCC
 721 AATACTCTGA CGCTCAAGTC ACGACTGGTA CGCCTTGGTG TGCCCGACTG TGTGCTCTC CGTGCCCGCA CTCCCGTGA
 801 CTCCTCCGTC GACTCCACTT GCGCTTTCGA GGTCAATCAA CTAGTAAAG TCTCCTGGGC CGGCCTCGCG GAGGCAGCTC
 881 CTCTTGTCAC CCAGCTAATT AATCGATTC ATATCAAGCA GACTGACTAC ATTCAACTCC TCCGCCGTGT TAGCCCCAAC
 961 CTCCTAAACT ACACCGATGC AATCGAACGA GGCAGGAGA AGCAGTTTCG TGACGTTTT CGCGAAACGG CCTGTTGGTG
 1041 GCTGCGAATG CATCGATCGA GGTGGGAACA GTGGACTGAG GGATGGAACG TTAAGAAAGA GATCATCATT GGGGGCATGT
 1121 TCACCTTCGC GGGCACCGAG GAGTTCAAAG ATTTGGCTCC CAATGCCTTC CATGCAGTGG ACGTTCTGAA CGGTGACGAG
 1201 AAGTACTTTG GCAACTCGGA GTTTGCCATT CGTCTTCAA TTCGCAATCT TACTTGCTCT CAGAATGTAG TGCTCAACGA
 1281 TTTCTTCAAT TTCTCACCG TCAACCCTAA CAATGAAAGC ATCCTTGGCG TGATCCTTGC CCTTGCCCC GATGCCATTG
 1361 AGGCGACTGT GCGGTTGGCG AACCTACGTC GGGTGTGTT CATCTCGCCC ACTGTGGAGT CTGCTCCTT CCTGTGGCAG
 1441 AACATTACA AGTTCTTCT TCGCACCATT CCCTCCGCT AACTGCCAG CTTTATCTT ATCCGCCTGT TCCAGCAGTG
 1521 GCAGTGAAG CGGGTACGA TGTTCGGAA GGATGACCAC TATTTTTATC GCGATGCCTT CACCGCAAAT AACATTACCC
 1601 TGGTGGACGA CTTTGAAGTG AAGGAGTCTA TGCTCACCTA TGCTGTTGCT CAAAAGAAGC TCATGTCGGT GAAACAGCGC
 1681 AATGGACGAA TCATAATCGT GGATCATTCG GCTGCGGCAA CCGTATTAT CCTTTGCGCC GCTTTTCATC TGAACATGCG
 1761 CGCTGAGAAG GGTACGTGT GGTTCCTCAG CCCTTGCTC TCCAAGAAGT TCTGGGAGTC GCCGGAAGTG ATTCTCCCG
 1841 AGTGCAGTGC CAATGATCTC AAGGTCATGC ATGATTACTC CTTACGCTC TCACATCCCC TTCACACTGG TGCTGTCATT
 1921 TACTCCAATC TCATGACCTC CATGAGTGGA CCCAATCAAT CTGAGGTGTC CAGTGAAGC AAACCCGATA TGCGAATTGC

2001 CTCACATCAG CGCCAGCTAT ACGAGCAGTG TACTTTTGAA TCGGTGATCG TCCTCGGGAG TGCAATAGCT CGGCTTCTGC
 2081 GTGAAAATCC CTCCGCGCTG TCGATTTTGA GCAATCCCAA AATGGCTGAG CGTTACGGA CGTTGGTGTC GAAAACGCAC
 2161 ATGGAGTACT CGAGCAGAGG CTACCTGGAC AAGAATGCAG TCTCCTTTTT CAGTAACAAT GTGGACCAGT TGGGTGAGAC
 2241 CCTCGTCTAT CAATTCGGCG TCACTCCACC CTCACCACCT GTGCCGCCAC AGACTCCACC TCCTGCCTAT GACGAAGACC
 2321 CCCTTGCTAG CACCGTTCAT CAGCTTAGCT TTGATTCACA CAATGATCGT CTTCTGGAGG CGTGGCTGCT GAAACAAATC
 2401 CAAGATAAAA CGACTGTTCC CATCACCCTC TGGTCTTTCA GTGGACCTCT CCATGGAGAT GAGGATGGCG AGTCGACCCT
 2481 GTTGTCGAAA GATAGATTTT GGCTGCATTC CAGCAGCGGT TACTCATCAT CCTCCTCTCG AGGGGCGTGG GGTGGGGGCA
 2561 AGGAGAACGG AGAGGAGGGC GAGGAAAATG GGGCGGAGGA CAACCGGAAC GATGCGATCG CCTTCAAGAC TTTCTGTTGAC
 2641 AACCTCTTCG AGAAGCCCTA CGACAAACCG CGCTGGGGTG GCAGTGGCTC TCTGCGTCCC ACCGATGGCT CCATAACTGA
 2721 GGCCGATTGT GCCTTCAGT TCCTCTCACG CTGGTTTGGT GTCAGTTGTG TCGTTGGCAA CTGGATATTC GCCATGGGCG
 2801 TTCTTATCAT CATCGCTATA CCTGTGGTCG CTGTCTGTCT TGCTTACTTC CGGCGACGTC TGCAGAGGC AGAAAAATC
 2881 ACCCGGAAGC CCTATGAAGA ACTTTGCGCT CTTTTGGCTG ACGTCAATAT CCCACTAACT GACATCGTTA TCAATCGCCG
 2961 AATCGGTGAC GGTGCCTTTG GTTTGGTGTA CGGTGGAGAA GCCAAGTTG CGGGTCGTTG GGAAGCGGTG GCAGTGAAGA
 3041 TGAATACCAA CCGCACCACC TACGAGGCGA AGGTGGAGTT CCTCTCTGAG GCCAAGTTGA TGCGTGACCT GCGACACAAG
 3121 AATGTGGTAC GTCTCGTCGG TGTCTGCATG GATCGGCCG AGGATGAAAT CTATCTCATT ATGGAACTCA TGCTACTTGG
 3201 TGACCTCAA AAGTACCTCC TTGAACGCC TCTCACGCC CAGCGATGTC CGGACCACGA GGATATTTGT CCGACGACGC
 3281 TGACTCGGAT GCGGTTAGAC ATAGCCGAGG GGCTGGCGTA TCTGCACAGT AAACAGCTCA TTCATCGCGA TATCGCTTGT
 3361 CGTAACTGCC TGGTGGGCC GGACCAGTG GTGAAAATAG GCGACTTCGG ACTGACGCGC GAGGCTACTG CGGGCTCGCC
 3441 GTATGGCTAC TACCGCTTTA CGCGCAACGT CGAGCTGCCT ATCCGGTGA TGCCGCCCGA GCGGGTGAC TTCGGCATCT
 3521 TCTCGGTTAA GTCGGACCTC TGGTCCTATG GCATCGTTCT TTATGAGATT ATTACCTTCG GCATGTTTCC CTACGCTGAA
 3601 CTCGGCGACG TGGAAGTTGT TGAACGGGTC AAACGATCCG AGTTCTCGAT CACGCAGATT CTCCGCGCTG CTGCCAACGG
 3681 AACTACTGTG TGGCGTCTGA TCGTGAGCTG CTGTCACTAC TACTGGCAAC ACCGTCTTGA GTCAATGCTC CAGGTTATAG
 3761 AGGAGATACG GGCCAACGAG AACTGCATTC GACCTTACCT CACCGACGAA CCACCTACTC TAGAGACCAC GGGGATTCCT
 3841 TTCCTTCCTG GTCCGGGTGC GTGCATAATG CCGGAGCCGC CGCCGGTTC ACAGCCTGCC TTCTCGGCGC CGATGGGGGC
 3921 ACGTGCCTGG GTTGGCGGTG CACCCTTTAT GAACCCCTCG ATGCCCTTCA CGGAGCCCC CTCAGCGGGC GAGGGGCCCC
 4001 AACTCCATAC AGCCGCCAAC AGCAGCAGTG GTGGCTGCGG TGGTGGTGA GGATGTAGTC AGAAGGTCTA TTTCTCTCT
 4081 GCCAACTCTT CTTCCTCCTT TACATCCAAC TCCGCTCCT CCAGACGTCC CCACAATGCT GCTTTAAACA TCAGACAAAC
 4161 TCCGGTCAA CAAGCTCCAC CTCCCCTTC GGTCTATGCG CCGCCTGGAC ATCCTGGTTA CCAACCATCG GATGAATTGA
 4241 ATCCCCTTCT CAACCCCTCC AACCGATCGA TGTCTTGA GTTCTGCAA AAGTCAGACT TCCATCTCCA AACACTGCCG
 4321 TCGAGGAGAG CGAACGAAAT TGATGTCGAG GAAGAGTTAG AGAGAATCAG CGAGAGCGGG GACGTTGATC TTCGGCGTGA
 4401 GGTGGAGGAC GAGGAAGGTG AGGTGGATTT TCAAGTTCG AGAACCAAGC ACCAGCGTAC CTCACGTCCC CAAAAGCCCT
 4481 CTCTTTTGG TCGCAGCCCC TTCAGCGTCT CCGTGGATCC TAGTGGTGGG ACACGACGGC AACAGCAGCA CAGTGGTAAC
 4561 TTCTTTGCAC GCACATTTGC GGTTCGATTG GATCCGCGTG GCGGCGCCGG GAAGTCGCAC CCCCACGCC CGGTGGGACT
 4641 GGCCTCCTTT CTGCACAGCG ATCAGTCCTC CTCTATACGA ATGCGACTGC TGCCCTCTTT ACGCCATCAT AATCAACAAC
 4721 ACCACTTTCA TCAAACAGCC GCCGCTGTCG CTTTTTCCCC CCCATCTCC TCGCACAATG AACTTACTGC CAAGTCTCTT
 4801 CCTCAGGTGA GCGGTACCAA CTGTACACCC TCTACAGTAG TGTCGATGAC GAAAACGTCA CGGCGAGGCG CGTGCAGCTC
 4881 GGCAGGGGAC GCGCACTACC TTGCGCGACC ACGTCCACCC ACGACTGCGG CCTTCTCCAC CTCTGCCTCT CGTCTATCCT
 4961 CAGCAGCGGT GGCTGTGGGG TCGCCTCGGG GTCAGCGACC GCCCATAGTG ACGCAGAACG GCGCCGCGGG CCTGATTACC
 5041 TCCAGCGGGA GTAGTCCCAC CTTTTCTTAT CCATCCCAC CTCCTCTCC TCCGCACAAC TCCTTCGTCT AG

EmVKR Protein sequence

1 MNAMVAFVHL TFLLCVSLC VLAKQGLDLS ESCLAAEKA KWIRSLHFNN KSFSLNVEVN DRPSHWIINY IFEILIRERF
 81 GYRNINFIYT PWDSSSNAIN RLNCEKSNDK SCPPPIHVNL ELWLRTGEQA SDYAPPHRVN MNGPLGPITR WGLYTNEELV
 161 GRQAPQLSTD PRISQDVHPS QSFGEQVLFY DRPSMLKAYK TLLSEDMGSM EMHVEQRPTQ FLWNLTQAP RFPILLNWYP
 241 NTLTLKSRLV RLGVPDCVAL RARTPVDSSV DSTCAFEVNO LVKVSWAGLA EAAPLVTQLI NRFHIKQTDY IQLLRRVSPN
 321 LLNYTDAIER GEEKQFRARF RETACWWLRM HRSRWEQWTE GWNVKEIII GGMFTFAGTE EFKDLAPNAF HAVDVLNGDE
 401 KYFGNSEFAI RLQIRNLTCQ QNVVLNDFFN FLTVNPNNES ILGVILALCP DAIEATVRLA NLRRLVVISF TVESASFLWQ
 481 KHFKFFFTI PSAYTASFIF IRLFQQWQWK RVTMFRKDDH YFYRDAFTAN NITLVDDFEV KESMLTYAVA QKNVMSVKQR
 561 NGRIIIIVDHS AAATAIILCA AFHLNMRAEK GYVWFLSPWL SKNFWESPEV IPPECSANDL KVMHDYSFSV SHPLHTGAVI
 641 YSNLMTMSG PNQSEVSSGS KPDMRIRSHQ RQLYEQCTFE SVIVLGSIAA RLLRENPSAL SILSNPKMAE RLRTLVSKTH
 721 MEYSSRGYLD KNAVFFSNN VDQLGETLVY QFGVTPPSPP VPPQTPPPAY DEDPLASTVH QLSFDSHNDL LLEAWLLKQI
 801 QDKTTVPITL WSFSGPLHGD EDGESTLLSK DRFRLHSSSG YSSSSSRGAW GGGKENGEEG EENGAEDNRN DAIAFKTFVD
 881 NLFKPYDKP RWGGGSLRP TDGSITEADC AFSFLSRWFG VSCVGNWIF AMGVLIIIAI PVVAVVLAYF RRLREAEKL
 961 TRKPYEELCA LLADVNIPLT DIVINRRIGD GAFGLVYGG EAKFAGRWEAV AVKMNTNRTT YEAKVEFLSE AKLMRDLRHK
 1041 NVVRLVGVCN DRPQDEIYLI MELMLLGLDK KYLLERLTA QRCPDHEDIC PTTLTRMALD IAEGLAYLHS KQLIHRDIAC
 1121 RNCLVGPDPV VKIGDFGLTR EATAGSPYGY YRFTRNVELP IRWMPPEAVQ FGIFSVKSDL WSYGIVLYEI ITFGMFPYAE
 1201 LGDVEVVERV KRSEFSITQI LPPAANGTTV WRLIVSCCQY YWQHRPESML QVIEEIRANE NCIRPYLTDE PPTLETTAIP
 1281 FLPGPACIM PEPPVPQPA FSAPMGARAW VGGAPFMNPS MPFTEPPSAG EGPQLHTAAN SSSGGCGGGG GCSQKVYFSS
 1361 ANSSSSLTSN SASSRRPHNA ALNIRQTPVK QAPPPTSUYA PPGHPGYQPS DELNPLLNPS NRSMSLEFLQ KSDFHLQTLF
 1441 SRRANEIDVE EELERISESG DVDLRREVED EEEVDFQGR RTKHQRTSRP QKPSLLSRSP FSVSVDPSGG TRRQQHSGN
 1521 FFARTFAVAL DPRGGAGKSH PRRPVGLASF LHSQSSSIR MRLPLSLRHH NQQHFFHQTA AAVAFSPSS SHNELTAKSL
 1601 PQVSGTNCHT STVVSMTKTS RRGACSSAGD AHYLARPRPP TTAAFSTSAS RSSSAAVAVG SPRGQRPIV TQNGAAGLIT
 1681 SSGSSPTFSY PSPPPPPHN SFV*

B Table S1 Primer List

Name	Gene, Order and Date	Primer Sequence 5' - 3'
AKO-cDNA	sigma_08_10_2012	ATCTCTTGAAAGGATCCTGCAGGTTTTTT TTTTTTTTTTTTTTTTTTTTTTA
AKO-011	pBAD Forward	ATGCCATAGCATTTTTATCC
AKO-012	pBAD Reverse	GATTTAATCTGTATCAGG
T7-Primer	sequencing primer for several plasmids	TAATACGACTCACTATAGGG
AKO-024	Exon-2b_VFTK_Primer_fwd_21.03.2012_Sigma	GCTAGGCGAAGAAGGAAACGAAATC
AKO-025	Exon-2b_VFTK_Primer_rev_RC_21.03.2012_Sigma	GTGATAACTTTACCGCGCTTGGGG
AKO-026	5-UTR_VFTK_Primer_fwd_21.03.2012_Sigma	GAGTTATCTCCCGTAACTCATGTGCG
AKO-027	3-UTR_VFTK_Primer_rev_RC_21.03.2012_Sigma	GACGGACATTTCGCATACAGGGG
AKO-028	Exon-1_VFTK_Primer_fwd_21.03.2012_Sigma	ATGGTGGCGTTTGTTCACCTTTGTTCAC
AKO-029	Exon-2_VFTK_Primer_fwd_21.03.2012_Sigma	GGCCTTCCCACTGGATCATAAAC
AKO-030	Exon-3_VFTK_Primer_fwd_21.03.2012_Sigma	CTCTTTTACGACCGCCATCTATGC
AKO-031	Exon-3_VFTK_Primer_rev_RC_21.03.2012_Sigma	GTCGTGACTTGAGCGTCAGAG
AKO-032	Exon-9_VFTK_Primer_fwd_21.03.2012_Sigma	CACATCAGCGCCAGCTATACG
AKO-033	Exon-10_VFTK_Primer_fwd_21.03.2012_Sigma	GTGGACCAGTTGGGTGAGACCCCTCG
AKO-034	Exon-10_VFTK_Primer_rev_RC_21.03.2012_Sigma	CCAGAGGGTGATGGGAACAGTCG
AKO-035	Exon-17_VFTK_Primer_rev_RC_21.03.2012_Sigma	GGACTACTCCCGCTGGAGGTAATCAGG
AKO-036	EM10/15 (<i>elp</i> fwd)	AATAAGGTCAGGGTGACTAC
AKO-037	EM10/16 (<i>elp</i> rev)	TTGCTGGTAATCAGTCGATC
AKO-042	Exon-1_VFTK_Primer_fwd_03.05.2012_Sigma_second_primer	ATGGTGGCGTTTGTTCACCTTGAC
AKO-043	5-UTR_VFTK_Primer_fwd_04.05.2012_Sigma_second_primer	CTGAATCAAACCTTAGACAATGAATGC
AKO-044	3-UTR_VFTK_Primer_rev_04.05.2012_Sigma_second_primer	GGGGATTTGGGCTGCGTCCTAGACG
AKO-045	3-UTR_VFTK_Primer_rev_04.05.2012_Sigma_third_primer	CGTCCTAGACGAAGGAGTTGTGC
AKO-046	VFTK_Exon_1_PstI_fwd_Sigma_09.05.2012	TATCTGCAGATGAATGCAATGGTGGCGTT TG
AKO-047	VFTK_Exon_10_NheI_fwd_Sigma_09.05.2012	GTGGACCAGTTGGGTGAGAC
AKO-048	VFTK_Exon_10_NheI_fwd_Sigma_09.05.2012	ACTGTTCCCATCACCTCTG
AKO-049	VFTK_Exon_17_NotI_rev_Sigma_09.05.2012	TATGCGGCCGCTAGACGAAGGAGTTGT GC
AKO-050	VFTK_Exon_10_NheI_rev_Sigma_09.05.2012	CAGAGGGTGATGGGAACAGT
AKO-053	EmPLK-5'UTR_fwd_(dw)	GACTTCTGCCCGGGTATGGATA
AKO-054	EmPLK-3UTR_rev_(up)	GGAAGACGGCAAACATGTGAT
AKO-055	EmPLK-350_fwd_(dw)	CTCTCATGGAAGTGCATAAGAG
AKO-056	EmPLK-650_rev_(up)	CGGACCACGAATCTACCTC
AKO-057	EmPLK-830_fwd_(dw)	GAGCATGTTCAAGTGTGATGG
AKO-058	EmPLK-1150_rev_(up)	GCCATACTTGTCCGAATAATC
AKO-059	EmPLK-1350_fwd_(dw)	ACTTGCTTCACTAGTTACATGC
AKO-060	EmPLK-1650_rev_(up)	CGATCTATCATATCGTAGGGC
AKO-061	Em_eEF1A_fwd	CACAAGTCCGAGTGTCCG
AKO-065	EmPlk1_NcoI_fwd_pGBKT7-BD_sigma_09_07_2012	ATACCATGGATGGATAAGTCAAAGCGAA GG

AKO-066	EmPlk1_PstI_rev_pGBKT7-BD_sigma_09_07_2012	ATCTGCAGTTTGTGTTTCAGAACATCAAC C
AKO-067	EmPlk1_ATG_fwd_sigma_09_07_2012	ATGGATAAGTCAAAGCGAAGG
AKO-068	EmPLK_NO-STOP_rev_sigma_09_07_2012	TTTGTGTTTCAGAACATCAACCTTTGG
AKO-069	EmPlk1_EcoRI_fwd_pGBKT7-AD_sigma_09_07_2012	ATATGAATTCATGGATAAGTCAAAGCGA AGG
AKO-070	EmPlk1_SacI_rev_pGBKT7-AD_sigma_09_07_2012	TATGAATTCCTTTGTGTTTCAGAACATCAAC C
AKO-080	EmPlk1_Mutations_T182D_sigma_18_07_2012_fwd	GGTGAATGAAGAAGGACTTATGTGGGA CGCC
AKO-081	EmPlk1_Mutations_T182D_sigma_18_07_2012_rev	CCCACATAAGTCCTTCTTCATTTACCTT C
AKO-082	EmPlk1_Mutations_T182V_sigma_18_07_2012_fwd	GGTGAATGAAGAAGGTGTTATGTGGGA CGCC
AKO-083	EmPlk1_Mutations_T182V_sigma_18_07_2012_rev	CCCACATAACACCTTCTTCATTTACCTT C
AKO-084	Em_VFTK_Primer_EcoRI_fwd_1995bp_sigma_23_07_2012	CCATGAGTGGACCCAATCAATCTGAGGT
AKO-085	Em_VFTK_Primer_EcoRI_rev_1995bp_sigma_23_07_2012	GCTCGTATAGCTGGCGCTGATGTGAG
AKO-086	Em_VFTK_Primer_XbaI_fwd_3820bp_sigma_23_07_2012	CCAACGAGAAGTGCATTTCGACCCTACC
AKO-087	Em_VFTK_Primer_XbaI_rev_3820bp_sigma_23_07_2012	CACCCGGACCAGGAAGGAAAGGAATC
AKO-095	pJET 1.2 fwd_plasmid primer for sequencing	CGACTCACTATAGGGAGAGCGGC
AKO-096	pJET 1.2 rev_plasmid primer for sequencing	AAGAACATCGATTTTCCATGGCAG
AKO-106	EmPlk1 EcoRI	ATAGAATTCATAATGGATAAGTCAAAGC GAAGGAG
AKO-107	EmPlk1 NotI	TATGCGGCCGCTTGTGTTTCAGAACATCA ACC
AKO-109	EmVFTK_Exon_8_fwd	GATTCCTCCCGAGTGCAGTGCCAATG
AKO-110	EmVFTK_NotI_fwd_for_pSecTag2/Hygro A (<i>Xenopus</i> oocytes)	ATATATGCGGCCGCAATGAATGCAATGG TGGCGTTTG
AKO-111	EmVFTK_NotI_rev_for_pSecTag2/Hygro A (<i>Xenopus</i> oocytes)	ATATATGCGGCCGCGACGAAGGAGTTGT GCGGAGG
AKO-120	Primer_GPCR_VKR_5'UTR_fwd	GCTGTCCCTGATATGCTCTTCTTCC
AKO-121	Primer_GPCR-VKR_3'UTR_rev_short_NO-1_RC	ACTTCCTCCAAATCATCGGCCG
AKO-122	Primer_GPCR-VKR_middle_1st_fwd	CGGTTTTGAATAACTCCCGTGTCCG
AKO-123	Primer_GPCR-VKR_middle_1st_rev_RC	GCGACACGGGAGTTATTCAAACCG
AKO-124	Primer_GPCR_middle_2nd_fwd	CGGCTTTGACCCGCCGTCAACTCGCG
AKO-125	Primer_GPCR_middle_2nd_rev_RC	CGCGAGTTGACGGCGGGTCAAAGCCG
AKO-126	Primer_GPCR-VKR_3'UTR_No-2_rev_NO-2_RC	CATATTCTAAAGATTCCTATACGGAGC
AKO-132	EmVKR_Primer_5'-end_fwd_31012013	CGCACAAAGACACAGTACATAGTAGAAAT GTCAAGTGAACAAACGCCACCATTGCATT CAT
AKO-133	EmVKR_Primer_5'-end_rev_31012013	CACTTGACATTTCTACTATGTAAGTGTGTC TTTGTGCGTTCTTGCCAAACAAGCCTTG ATTTAAGCG
AKO-134	EmVKR_Primer_3'-end_fwd_31012013	GGCCTGATTACCTCCAGCGGGAGTAGTC CCACCTTTTCTTATCCATCCCCACCTCCT CCTCCTCCGCACAACCTCTTCGTCTAG
AKO-135	EmVKR_Primer_3'-end_rev_31012013	GGACTACTCCCGCTGGAGGTAATCAGGC CCGCGGCGCCGTTCTGCGTCACTATGGG
AKO-136	EmVKR_Primer_3'-end_NotI_fwd_31012013	GGCCTGATTACCTCCAGCGGGAGTAGTC CCACCTTTTCTTATCCATCCCCACCTCCT CCTCCTCCGCACAACCTCTTCGTCCGG CCGCATATAT
AKO-137	EmVKR_Primer_5'-end_NotI_fwd_31012013	CGCACAAAGACACAGTACATAGTAGAAAT GTCAAGTGAACAAACGCCACCATTGCATT CATTGCGGCCGCATATAT
AKO-138	EmPlk1 T179D_rev (mutations for <i>Xenopus</i> oocytes)	GGTGAATGAAGAAGGACTTATGTGGGA CGCCAAACTATATTGCTCC
AKO-139	EmPlk1 T179D_fwd (mutations for <i>Xenopus</i> oocytes)	CCACATAAGTCTTCTTCATTTACCTTCT TTAGTAATTCTAG

AKO-140	EmPlk1 T179V_fwd (mutations for <i>Xenopus</i> oocytes)	GGTGAAATGAAGAAGGTATTATGTGGGA CGCCAAACTATATTGCTCC
AKO-141	EmPlk1 T179V_rev (mutations for <i>Xenopus</i> oocytes)	CCACATAATACCTTCTTCATTTACCTTCT TTAGTAATTCTAG
AKO-142	EmPlk1_D163NA165_fwd (mutations for <i>Xenopus</i> oocytes)	GATCGGGGATAATGCTTTGGCCTCTAGA ATTACTAAAGAAGG
AKO-143	EmPlk1_D163NA165_rev (mutations for <i>Xenopus</i> oocytes)	CTAGAGGCCAAAGCATTATCCCCGATCTT TACAATC
AKO-144	EmVKR_Start_fwd	ATGAATGCAATGGTGGCGTTTGTTCACCTT GACATTTCTAC
AKO-145	EmVKR_Ende_rev	CTAGACGAAGGAGTTGTGCGGAGGAGGA GGAGGTGGGGATG
AKO-146	EmPlk1_D163SV165_fwd (mutations for <i>Xenopus</i> oocytes)	GACATGATTGTAAAGATCGGGGATTCCGG TGTTGGCCTCTAGAATTACTAAAGAAGG
AKO-147	EmPlk1_D163SV165_rev (mutations for <i>Xenopus</i> oocytes)	GTAATTCTAGAGGCCAACACCGAATCCC CGATCTTTACAATCATGTCATCTTTAAAA ACAGATTGGC
AKO-148	EmVKR_3'ende_TAG_rev	CTAGACGAAGGAGTTGTGCGGAGGAGGA GGAGGTGGGGATGGATAAGAAAAGGTG GGACTACTCCCGCTGGAG
AKO-149	EmVKR_5'NotI_+70bp_fwd_sigma_22042013	TATATGCGGCCGCCAAACAAGGCCCTTGA TTTAAGCGAAAGTTGTCTTGC
AKO-150	EmVKR_3'NotI_+5065bp_rev_sigma_22042013	TATATGCGGCCGCCAAAGGTGGGACTACT CCCCTGGAGGTAATCAGG
ASO-151	EmPLK4_forward_ATG_sigma_18092013 (full transcript)	ATGTACGTTCAACCAAACCTAAAGGGGTT AGG
ASO-152	EmPLK4_reverse_TAG_sigma_18092013 (full transcript)	TCAGGGTGGAGTTTGTAGCTCGAACGG AGAC
ASO-159	EmPlk1_reverse_kinases domain	AGTGCCTGACAGGGAGACCGGTG
ASO-160	EmPlk1_reverse_kinases domain_II	TGCACTGACAGGGAGACCGGT
ASO-161	EmVKR_fwd	ATGAATGCAATGGTGGCGTTTGTTCACCTT GACATTTCTACTATGTACTGTGTCTTTGT GCG
ASO-162	EmVKR_rev	CTAGACGAAGGAGTTGTGCGGAGGAGGA GGAGGTGGGGATGGATAAGAAAAGGTG GGACTACTCCCGCTGGAGGTAATCAGGC C
ASO-163	EmPlk1_fwd_NcoI	ATATATCCATGGTATGTGAGAGGGAGGTT TCTTGGAAAAGGAGGCTTCGC
ASO-164	EmPlk1_rev_BamHI	ATATATGGATCCGTCATCACACTGAACA TGCTCGGCCGCTTTTGTG
ASO-165	EmPlk1_fwd_NcoI	ATATATCCATGGTGTATGTGAGAGGGAG GTTTCTTGGAAAAGGAGGCTTCGC
ASO-166	EmPlk1_rev_BamHI	ATATATATGGATCCCTAAGTGTGGTCCAT CACACTGAACATGCTCGGCCGCTTTTGT G
ASO-167	EmVKR_fwd_+NotI 69bp cut	GTAATGTGTCTTTGTGCGTTCTTGGCGCC GCCAAACAAGGCCTTGATTTAAGCG
ASO-168	EmVKR_rev_+NotI 5073 cut	GGGAGTAGTCCCACCTTTGCGGCCGCTC TTATCCATCCCACCTCCTCCTCCTCCGC
ASO-169	TB1-5 (beta tubulin 1 fwd; full transcript; Brehm 2000)	CAGGCTACCGCAGGCTACCG
ASO-170	TB1-3 (beta tubulin 1 rev; full transcript; Brehm 2000)	AGAATGCAAGGAAGAAATAGCTA
ASO-171	TB2-5 (beta tubulin 2 fwd; full transcript; Brehm 2000)	TTTGGATTTGGATTCGCTTG
ASO-172	TB2-3 (beta tubulin 2 rev; full transcript; Brehm 2000)	GAAATTTTATTGATAAAGCACATG
ASO-173	TB3-5 (beta tubulin 3 fwd; full transcript; Brehm 2000)	ATTCTCCAACATGCGTGAGC
ASO-174	TB3-3 (beta tubulin 3 rev; full transcript; Brehm 2000)	ATCTAATCCCAAGATAATTTGTTG
ASO-175	EmVKR	CCTCCCACTTCGGTCTATGC
ASO-176	EmVKR	TACCGCTCACCTGAGGAAGA
ASO-177	EmVKR	CTCCCACTTCGGTCTATGCG
ASO-178	EmVKR	ATCGCTGTGCAGAAAGGAGG
ASO-179	beta tubulin-1 5' (RT-PCR)	TGCAACCATGTCAGGTGTGA
ASO-180	beta tubulin-1 3' (RT-PCR)	ACCGACATCTTGTAGTCCACG

ASO-181	beta tubulin-2 5' (RT-PCR)	AACCAGTCGTGGTAGTCAGC
ASO-182	beta tubulin-2 3' (RT-PCR)	AACAGCTCTTGATGGCGGT
ASO-183	beta tubulin-3 5' (RT-PCR)	TGGTCCCTTTCCACGTCTG
ASO-184	beta tubulin-3 3' (RT-PCR)	ACTCCGCTCCGAAACTCC
ASO-185	EmVKR fwd VFT-Modul (<i>in situ</i> probe version A)	TCCAATGCCTTCCATGCAG
ASO-186	EmVKR rev VFT-Modul (<i>in situ</i> probe version A)	GTTTTCGACACCAACGTCCG
ASO-187	EmVKR fwd VFT-Modul (<i>in situ</i> probe version B)	GGCACCGAGGAGTTCAAAGAT
ASO-188	EmVKR rev VFT-Modul (<i>in situ</i> probe version B)	GCTCAGCCATTTGGGATTGC
ASO-189	EmVKR fwd TK-Domain (<i>in situ</i> probe version A)	CTTTGCGCTCTTTGGCTGA
ASO-190	EmVKR rev TK-Domain (<i>in situ</i> probe version A)	AGTTCTCGTTGGCCGTATC
ASO-191	EmVKR fwd TK-Domain (<i>in situ</i> probe version B)	TGGCTGACGTCAATATCCCAC
ASO-192	EmVKR rev TK-Domain (<i>in situ</i> probe version B)	AGTACTGACAGCAGCTCAGG

C List of Abbreviations

aa	Amino acids
ABZ	Albendazole
ABZSO	Albendazole Sulfoxide
ABZSN	Albendazole Sulfone
AE	Alveolar Echinococcosis
AKO	Andreas Kalbfleisch Oligo (Primer)
AKS	Andreas Schubert Oligo (Primer)
AKP	Andreas Kalbfleisch Plasmid
ASP	Andreas Schubert Plasmid
AKS	Andreas Kalbfleisch Strain (Bacterial stain, DMSO-Stock)
ASS	Andreas Schubert Strain (Bacterial stain, DMSO-Stock)
bp	Base pairs
BI 2536/6727	Boehringer Ingelheim 2536/6727
<i>C. elegans</i>	<i>Caenorhabditis elegans</i>
CML	chronic myelogenous leukemia
Ctrl	Control
<i>D. melanogaster</i>	<i>Drosophila melanogaster</i>
<i>E. multilocularis</i>	<i>Echinococcus multilocularis</i>
EmPlk1	<i>Echinococcus multilocularis</i> Polo-like kinase 1
EmPlk4	<i>Echinococcus multilocularis</i> Polo-like kinase
EmVKR	<i>Echinococcus multilocularis</i> Venus kinase receptor
EmVRTK	<i>Echinococcus multilocularis</i> Venus kinase receptor
<i>H. microstoma</i>	<i>Hymenolepis microstoma</i>
IGF	Insulin like growth factor
LBD	Ligand binding domain
Mc	Metacystode vesicles
MAP	Mitogen-activated protein
MAPK	Mitogen activated protein kinase
Na ₃ VO ₄	Sodium orthovanadate
nt	Nucleotides
ORF	Open reading frame
Pc	Primary cells
PS+	Activated protoscoleces
Ps-	Nonactivated protoscoleces
<i>S. japonicum</i>	<i>Schistosoma japonicum</i>
<i>S. mansoni</i>	<i>Schistosoma mansoni</i>
<i>T. crassiceps</i>	<i>Taenia crassiceps</i>
<i>T. solium</i>	<i>Taenia solium</i>

D List of Publications**Scientific Publications**

Schubert A., Koziol U., Cailliau K., Vanderstraete M., Dissous C., Brehm K. (2014); Targeting *Echinococcus multilocularis* stem cells by inhibition of the Polo-like kinase EmPlk1. PLoS Negl Trop Dis. 2014 Jun 5;8(6).

Harrison N.* , **Kalbfleisch A.***, Connolly B., Pettitt J. and Müller B. (2010); SL2-like spliced leader RNAs in the basal nematode *Prionchulus punctatus*: New insight into the evolution of nematode SL2 RNAs. RNA, 16: 1500-1507.

* **equal contribution.**

Voss B., Hölscher M., Baumgarth B., **Kalbfleisch A.**, Kaya C., Hess W.R., Becker A., Evgueniev-Hackenberg E., (2009); Expression of small RNAs in Rhizobiales and protection of small RNA and its degradation product by Hfq in *Sinorhizobium meliloti*. Biochemical and Biophysical Research Communications, 390(2):331-6.

E Conference Contributions

Gesellschaft für Biochemie und Molekularbiologie (GBM): Participation on several conferences of Mosbacher Kolloquium 56th, 58th, 59th, sowie der Herbsttagung Berlin 2005.

American Society for Microbiology (ASM) Conference: ASM conference on Regulating with RNA in Bacteria in San Juan, Poster Presentation (Puerto Rico, 7-11. March 2011).

Internationale Symposien der Graduate School of Life Science: Poster Presentation at the 6th (Bio Bang, 2011), 7th (EPOS, 2012, Organisation-Team) and 8th (Scientific Crosstalk, 2013) International Symposium of the Graduate School of Life Science.

Drug Design and Development Seminar: Organisation-Team (Abstract book) and participation at the 14th Drug and Development Seminar in Würzburg (11-13. April 2013).

Sonderforschungsbereich (SFB) 630 Universität Würzburg: Poster Presentation at the 3th International Symposium of the SFB 630, "Novel Agents against Infectious Diseases – An Interdisciplinary Approach" (20-22. November 2013)